

## Supporting information for:

### Design of substrate transmembrane mimetics as structural probes for $\gamma$ -secretase

Sanjay Bhattarai<sup>1</sup>, Sujan Devkota<sup>1</sup>, Kathleen M. Meneely<sup>1</sup>, Minli Xing<sup>2</sup>, Justin T. Douglas<sup>2</sup> and Michael S. Wolfe<sup>1\*</sup>

<sup>1</sup>Department of Medicinal Chemistry and <sup>2</sup>Biomolecular NMR Laboratory, University of Kansas, Lawrence, KS, USA

#### Table of Contents

<b>Synthetic Materials and Methods</b>	<b>S2-10</b>
<b>Scheme S1:</b> Synthesis of tripeptidomimetic building block	S3
<b>Scheme S2:</b> Solid-phase synthesis of <i>N</i> -Boc, C-amide peptidomimetics	S8
<b>Scheme S3:</b> Solid-phase synthesis of <i>N</i> -acetylated, C-amide peptidomimetics	S8
<b>Scheme S4:</b> Solid-phase synthesis of <i>N</i> -Boc, C-methyl ester peptidomimetics	S9
<b>Table S1:</b> Calc'd mass, HPLC retention time and LC-MS purity of tested peptides	S10
<b>Table S2. Inhibition of <math>\gamma</math>-secretase by helical peptide/transition-state analogue conjugates: P2' = Ala</b>	<b>S11</b>
<b>LC-MS/MS analysis of proteolysis of control peptides</b>	<b>S12-13</b>
<b>Figure S1:</b> LC/MS/MS analysis of peptide <b>8</b> cleavage product	12
<b>Figure S2:</b> LC/MS/MS analysis of peptide <b>12</b> cleavage product	13
<b>Conformational analysis of compounds <b>6</b> and <b>9</b> by 2D NMR</b>	<b>S14-17</b>
<b>Tables S3 and S4:</b> NMR chemical shift assignment for <b>6</b> and <b>9</b>	S14-15
<b>Figures S3 and S4:</b> ROESY spectra for <b>6</b> and <b>9</b>	S16-17
<b>Protein expression/purification, <math>\gamma</math>-secretase assays, cross-competition kinetics</b>	<b>S18-20</b>
<b>Figures S5 and S6:</b> Noncompetitive inhibition by HPI-TSAs <b>6</b> and <b>16</b>	S19
<b>Figure S7:</b> Noncompetitive inhibition with HPI <b>2</b> and TSA <b>17</b>	S20
<b>Photoaffinity labeling</b>	<b>S21</b>
<b>Table S5:</b> Inhibition of $\gamma$ -secretase by photoprobes	S21
<b>Figure S8:</b> Dose response for HPI-TSA <b>6</b> against photoprobes	S21
<b>NMR-based low-energy structural calculations</b>	<b>S22-23</b>
<b>Table S6:</b> Statistics for the 10 lowest-energy structures	S22
<b>Figure S9:</b> Summary of 10 lowest energy structures	S23
<b>Figure S10:</b> Summary of restraints on structure	S23
<b>Spectra for compounds and intermediates</b>	<b>S24-94</b>
<b>References</b>	<b>S95</b>

## I. Synthesis

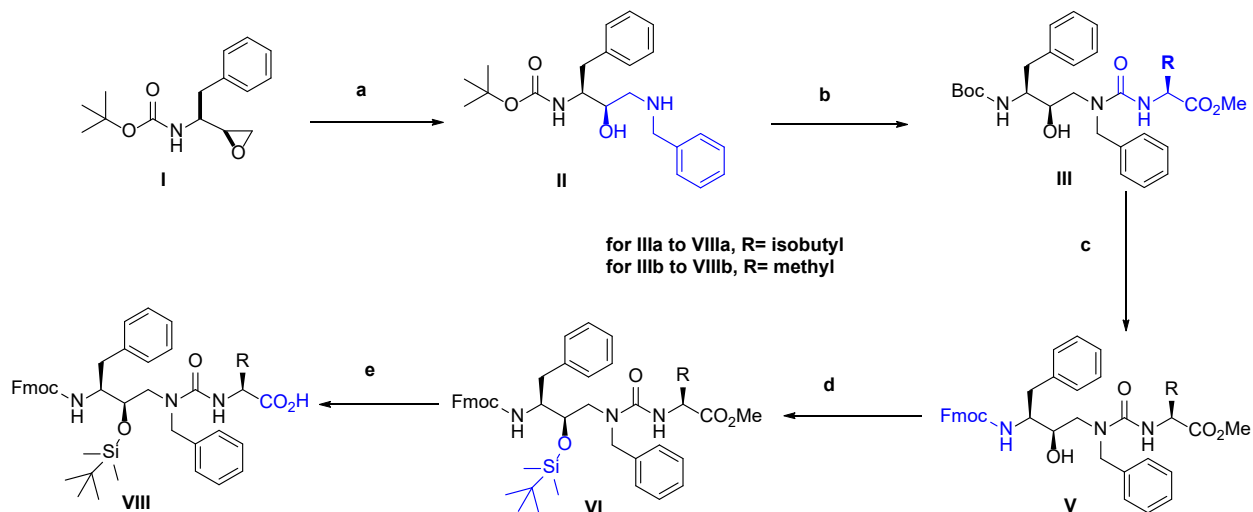
### General

All reagents used for synthesis were commercially obtained from various producers (Acros, TCI America, Sigma-Aldrich, Chem-Impex International) as noted and used without further purification. The purity of all reagents and final products was greater than 95%. Reactions were monitored by thin layer chromatography (TLC) using aluminum sheets with silica gel 60 F<sub>254</sub> (Merck). Solid phase synthesis of peptides were carried out using standard Fmoc-Chemistry using an Aapptec Focus XC peptide synthesizer. Column chromatography was carried out with silica gel 0.060-0.200 mm, pore diameter ca. 6 nm. Mass spectra were recorded on a LCT Premier mass spectrometer (Micromass Ltd., Manchester, UK), a quadrupole and time of flight tandem mass analyzer with an electrospray ion source. For LC-MS analysis, samples were prepared by dissolving 1 mg/mL of compound in H<sub>2</sub>O/MeOH (1:1), 10  $\mu$ L was injected into a Waters Analytical System-Acquity HPLC, eluting with a gradient of water/methanol: 2-propanol (1: 1) (containing 0.02% formic acid) from 60:40 to 0:100 or with a gradient of water/acetonitrile (containing 0.05% trifluoroacetic acid) from 50:40 to 0:100 for 15 min at a flow rate of 250  $\mu$ L/min. UV absorption was detected using an Acquity diode array detector. <sup>1</sup>H- and <sup>13</sup>C-NMR spectra were performed on a Bruker AVIIIHD 400 MHz and AVIII 500 MHz spectrometer. Melting points were determined on a Mel-Temp Digital Melting Point Apparatus and are reported without correction. Lyophilization was carried out using a FreeZone 4.5 Liter Benchtop Freeze Dry Systems from Labconco. For peptide purification, a preparative HPLC purification system (2545 Quaternary Gradient Module) from Waters was used with XBridge Peptide BEH C18, 300Å Column.

### Synthesis of tripeptidomimetic building blocks

For the preparation of the tripeptidomimetics building blocks **VIIIa/b** (**Scheme S1**), commercially available epoxide (**I**) was opened by benzylamine to hydroxyethylamine **II** as previously reported.<sup>1</sup> The isocyanates of *L*-leucine methyl ester and *L*-alanine methyl ester were made separately by stirring the commercially available HCl salt of the amino acid ester and triphosgene in an ice-cooled 1:1 biphasic mixture of CH<sub>2</sub>Cl<sub>2</sub> and NaHCO<sub>3</sub>.<sup>2</sup> Product was extracted with CH<sub>2</sub>Cl<sub>2</sub>, and solvent was removed under reduced pressure. Solvent removal was carried out with extra care for the preparation of isocyanate of *L*-alanine methyl ester, because its boiling point is close to that of CH<sub>2</sub>Cl<sub>2</sub>. Hydroxyethylamine **II** was then coupled with the isocyanate methyl esters as we previously reported to obtain hydroxyethylureas **III**.<sup>1</sup> The Boc protecting group of **III** was removed using trifluoroacetic acid (TFA). For Fmoc protection, several conditions were tried, using 1.2 eq. of Fmoc chloride and various bases and solvents, and the best yield of **V** was obtained with 2.0 eq. of DIPEA in DCM. Although we have previously used hydroxyethylureas such as **V** for solution-phase synthesis of small peptidomimetic inhibitors of  $\gamma$ -secretase, the free hydroxyl group might interfere in the solid-phase synthesis of larger TMD mimetics by generating impurities that could be too tedious to purify. To overcome this problem, we sought to block this hydroxyl group with a suitable protecting group, specifically one stable under basic conditions but readily removed under mild orthogonal conditions. Installation of various protecting groups for the sterically hindered hydroxyl functionality of **V** were attempted: *t*-butyl ether, *t*-butyl ester, *O*-benzyl ethers, and TBDMS using basic conditions. Protection with 2 eq. TBDMS chloride and 1.2 eq. DMAP provided the maximum yields (75-82%). Use in solid-phase synthesis requires hydrolysis of the methyl ester functionality with LiOH (0.5 M), which also resulted in removal of the Fmoc group. Fmoc was therefore reinstalled with 1.2 eq. Fmoc chloride, 2.0 eq. of DIPEA and DCM to provide **VIIIa** and **VIIIb** in 55-60% yield.

**Scheme S1.** Synthesis of tripeptidomimetic building blocks <sup>a</sup>



<sup>a</sup>Reagents and conditions: (a) 20 eq. benzylamine, 2-propanol, reflux, overnight (97%); (b) (S)-(-)-2-isocyanato-4-methylvaleric acid methyl ester or methyl (S)-(-)-2-isocyanatopropionate 1 eq., CH<sub>2</sub>Cl<sub>2</sub>, 0 °C to r.t., 4-5 h (92-94%); (c) *i.* TFA: CH<sub>2</sub>Cl<sub>2</sub> 3:7, r.t., 15 min; *ii.* 1.2 eq. Fmoc chloride, 2 eq. DIPEA, CH<sub>2</sub>Cl<sub>2</sub>, r.t., overnight (90-92%); (d) 2 eq. TBDMS chloride, 1.2 eq. DMAP, DMF, 36 h (75-82%); (e) *i.* 0.5 M LiOH in THF, r.t., 3 h; *ii.* 1.2 eq. Fmoc chloride, 2 eq. DIPEA, CH<sub>2</sub>Cl<sub>2</sub>, r.t., overnight (55-60%).

**tert-Butyl ((2S,3R)-4-(benzylamino)-3-hydroxy-1-phenylbutan-2-yl)carbamate (II).** To a 5.0 M solution of oxirane I (1 eq.) in 2-propanol (5 mL) was added 20 eq. of benzylamine, and the reaction was refluxed under dry N<sub>2</sub> for 20 h. The reaction mixture was allowed to cool to room temperature, diluted with ethyl acetate and washed consecutively with water, aqueous 1 N HCl and saturated NaHCO<sub>3</sub> solution. The organic phase was dried over anhydrous MgSO<sub>4</sub>, concentrated, and pure II was obtained by precipitation with hexane, filtration and drying.

**(S)-(-)-2-isocyanato-4-methylvaleric acid methyl ester or Methyl (S)-(-)-2-isocyanatopropionic acid methyl ester.** The isocyanates of L-leucine and L-alanine methyl ester were obtained by stirring the HCl salt of the corresponding amino ester (20 mmol) in a mixture of CH<sub>2</sub>Cl<sub>2</sub> (10 mL) and saturated NaHCO<sub>3</sub> solution (10 mL) for 20 min in a three-necked flask followed by addition of triphosgene (20 mmol) in a single portion. After being stirred for 1 h, the reaction mixture was poured into a beaker containing ice and stirred for 20 min. The mixture was then extracted with 3 X 50 mL CH<sub>2</sub>Cl<sub>2</sub>. The combined organic fraction was dried over MgSO<sub>4</sub>, filtered, and evaporated to a colorless oil. Then the colourless oil was purified using flash chromatography (Methanol: CH<sub>2</sub>Cl<sub>2</sub> 1:50) and a trituration with ethyl acetate and hexane provided a white solid.

**General procedure for synthesis of hydroxyethylureas (IIIa, IIIb).** To a solution of hydroxyethylamine II (2.0 g, 15.4 mmol) in CH<sub>2</sub>Cl<sub>2</sub> (3 mL) was added (S)-(-)-2-isocyanato-4-methylvaleric acid methyl ester or methyl (S)-(-)-2 isocyanatopropionic acid methyl ester (1 eq.)

in CH<sub>2</sub>Cl<sub>2</sub> (3 mL) at 0 °C for 30 min. After being stirred at room temperature for 6 h, the reaction mixture was concentrated, and the hydroxyethylurea **III** was purified using flash chromatography (Methanol:CH<sub>2</sub>Cl<sub>2</sub> 1:49).

**Methyl (benzyl((2R,3S)-3-((tert-butoxycarbonyl)amino)-2-hydroxy-4-phenylbutyl)carbamoyl)-L-leucinate (IIIa).** Hydroxyethylamine **II** (2.0 g, 5.40 mmol) and (S)-(-)-2-isocyanato-4-methylvaleric acid methyl ester (935 mg, 5.46 mmol) were combined in dry CH<sub>2</sub>Cl<sub>2</sub> (3 mL) according to the general procedure to provide **IIIa** as a white solid (2.7 g, 93% yield). <sup>1</sup>H NMR (400 MHz, CDCl<sub>3</sub>) δ 7.28 – 7.10 (m, 10H), 5.41 (s, 1H), 4.75 (s, 1H), 4.51 (dd, *J* = 12.4 Hz, 2H), 4.36 (m, 2H), 3.68 (m, 1H), 3.65 (s, 3H), 3.64 (m, 1H), 3.52 (m, 1H), 3.15 (m, 1H), 2.88 (m, 2H), 1.49 (m, 2H), 1.39 (m, 1H), 1.21 (s, 9H), 0.82 (m, 6H). <sup>13</sup>C NMR (125 MHz, CDCl<sub>3</sub>) δ 175.13, 159.37, 155.82, 137.28, 137.06, 129.48, 128.89, 128.42, 127.64, 127.11, 126.39, 73.64, 54.55, 53.82, 52.66, 52.24, 42.09, 35.87, 28.24, 24.87, 22.89, 21.81. LC-MS (*m/z*): negative mode 540 [M-H]<sup>-</sup>, positive mode 542 [M+H]<sup>+</sup>. Purity by HPLC-UV (214 nm)-ESI-MS: 98.60%. mp 175-177 °C.

**Methyl(benzyl((2R,3S)-3-((tert-butoxycarbonyl)amino)-2-hydroxy-4-phenylbutyl)carbamoyl)-L-alaninate (IIIb).** Hydroxyethylamine **II** (2.0 g, 15.40 mmol), and methyl (S)-(-)-2-isocyanatopropionate (980 mg, 7.60 mmol) were combined in dry CH<sub>2</sub>Cl<sub>2</sub> (3 mL) according to the general procedure to provide **IIIb** as a white solid (2.5 g, 94%). <sup>1</sup>H NMR (400 MHz, CDCl<sub>3</sub>) δ 7.37 – 7.19 (m, 10H), 5.58 (s, 1H), 4.88 (s, 1H), 4.61 (m, 2H), 4.47 (m, 1H), 4.38 (d, *J* = 16.5 Hz, 1H), 3.77 (m, 1H), 3.75 (s, 3H), 3.59 (m, 1H), 3.24 (m, 1H), 2.94 (m, 1H), 2.85 (m, 1H), 1.37 (d, *J* = 7.3 Hz, 3H), 1.33 (s, 9H). <sup>13</sup>C NMR (125 MHz, CDCl<sub>3</sub>) δ 177.05, 159.66, 155.83, 137.74, 136.99, 129.51, 128.87, 128.42, 127.63, 127.13, 126.39, 79.60, 73.53, 54.52, 52.40, 51.55, 49.68, 48.74, 35.64, 28.05, 18.58. LC-MS (*m/z*): negative mode 498 [M-H]<sup>-</sup>, positive mode 500 [M+H]<sup>+</sup>. Purity by HPLC-UV (214 nm)-ESI-MS: 99.00%. mp 171-173 °C.

**General procedure for synthesis of hydroxyethylureas (IVa, IVb).** To a solution of hydroxyethylurea **III** (2.0 g) in CH<sub>2</sub>Cl<sub>2</sub> (7 mL) was added trifluoroacetic acid (3 mL). After being stirred at r.t. for 2 h, the reaction mixture was quenched by adjusting to pH 7 with saturated aq. sodium bicarbonate. Extraction with CH<sub>2</sub>Cl<sub>2</sub> (2 X 50 mL) was followed by washing with water and additional extraction with CH<sub>2</sub>Cl<sub>2</sub> (2 X 50 mL). All organic fractions were pooled, dried over anhydrous MgSO<sub>4</sub> and concentrated to obtain pure product.

**Methyl (((2R,3S)-3-amino-2-hydroxy-4-phenylbutyl)(benzyl)carbamoyl)-L-leucinate (IVa).** Hydroxyethylurea **IIIa** (2.0 g, 3.69 mmol) according to the general procedure provided 1.58 g (97%). <sup>1</sup>H NMR (400 MHz, CDCl<sub>3</sub>) δ 7.38 – 7.17 (m, 10H), 4.75 (d, 1H), 4.44 (m, 2H), 3.72 (d, 1H), 3.70 (s, 3H), 3.67 (m, 2H), 3.34 (m, 1H), 3.05 (m, 1H), 2.95 (m, 1H), 2.51 (m, 1H), 1.66 – 1.42 (m, 3H), 0.92 (d, 3H), 0.91 (d, 3H). <sup>13</sup>C NMR (125 MHz, CDCl<sub>3</sub>) δ 175.27, 159.94, 138.60, 137.67, 135.35, 128.82, 128.63, 127.50, 127.31, 126.50, 74.44, 55.35, 52.60, 52.12, 51.69, 50.91, 41.29, 39.04, 24.94, 22.91, 21.85. LC-MS (*m/z*): negative mode 440 [M-H]<sup>-</sup>, positive mode 442 [M+H]<sup>+</sup>. Purity by HPLC-UV (214 nm)-ESI-MS: 99.00%. mp 158–160 °C.

**Methyl (((2R,3S)-3-amino-2-hydroxy-4-phenylbutyl)(benzyl)carbamoyl)-L-alaninate (IVb).** Hydroxyethylurea **IIIb** (2.0 g, 4 mmol) according to the general procedure provided 1.50 g (97%). <sup>1</sup>H NMR (400 MHz, CDCl<sub>3</sub>) δ 7.29 – 7.08 (m, 10H), 4.66 (d, *J* = 16.3 Hz, 1H), 4.41 – 4.27 (m, 2H), 3.63 (m, 1H), 3.62 (s, 3H), 3.61 (d, *J* = 13.8 Hz, 1H), 3.23 (d, *J* = 13.2 Hz, 1H), 2.97 (m, 1H), 2.93 – 2.79 (m, 1H), 1.27 (d, *J* = 7.3 Hz, 3H). <sup>13</sup>C NMR (125 MHz, CDCl<sub>3</sub>) δ 175.44, 159.67, 138.44, 137.53, 129.34, 128.81, 128.65, 127.51, 127.30, 126.55, 74.13, 55.43, 52.27, 51.52, 50.40, 49.70, 49.73, 38.80, 18.32. LC-MS (*m/z*): negative mode 398 [M-H]<sup>-</sup>, positive mode 400 [M+H]<sup>+</sup>. Purity by HPLC-UV (214 nm)-ESI-MS: 99.50%. mp 159–160 °C.

**General procedure for the synthesis of *N*-Fmoc-protected hydroxyethylureas (**Va**, **Vb**).** To a solution of **IVa** or **IVb** in CH<sub>2</sub>Cl<sub>2</sub> (5 mL) under dry N<sub>2</sub>, was added 1.2 eq. of Fmoc chloride and 2 eq. of DIPEA. The reaction mixture was stirred overnight at r.t. and concentrated *in vacuo*. Silica gel chromatography (0 to 5% MeOH in CH<sub>2</sub>Cl<sub>2</sub>) provided **Va** and **Vb** as white powders.

**Methyl(((2*R*,3*S*)-3-(((9*H*-fluoren-9-yl)methoxy)carbonyl)amino)-2-hydroxy-4-phenylbutyl)-(benzyl)carbamoyl)-*L*-leucinate (**Va**).** Hydroxyethylurea **IVa** (1.0 g, 2.27 mmol) according to the general procedure resulted in 1.5 g of **Va** (91%). <sup>1</sup>H NMR (400 MHz, CDCl<sub>3</sub>) δ 7.78 (d, *J* = 7.6 Hz, 2H), 7.50 (dd, *J* = 7.5 Hz, 2H), 7.45 – 7.38 (m, 2H), 7.34 – 7.20 (m, 10H), 7.16 (d, *J* = 7.4 Hz, 2H), 4.79 (d, *J* = 9.0 Hz, 2H), 4.55 (m, 3H), 4.43 (m, 1H), 4.27 (dd, *J* = 10.7 Hz, 1H), 4.13 (m, 1H), 3.84 (m, 1H), 3.75 (s, 3H), 3.66 (m, 1H), 3.22 (d, *J* = 14.9 Hz, 1H), 2.98 – 2.84 (m, 2H), 1.56 (m, 2H), 1.45 (m, 1H), 0.92 (d, 3H), 0.90 (d, 3H). <sup>13</sup>C NMR (125 MHz, CDCl<sub>3</sub>) δ 175.07, 159.89, 156.14, 143.89, 141.34, 137.43, 129.50, 128.95, 128.50, 127.70, 127.04, 126.53, 124.98, 119.96, 73.30, 66.52, 54.98, 52.55, 52.29, 53.98, 51.97, 47.23, 41.32, 35.48, 31.60, 24.87, 22.89, 21.79. LC-MS (*m/z*): negative mode 662 [M-H]<sup>-</sup>, positive mode 664 [M+H]<sup>+</sup>. Purity by HPLC-UV (214 nm)-ESI-MS: 99.60%. mp 183-185 °C.

**Methyl(((2*R*,3*S*)-3-(((9*H*-fluoren-9-yl)methoxy)carbonyl)amino)-2-hydroxy-4-phenylbutyl)-(benzyl)carbamoyl)-*L*-alaninate (**Vb**).** Hydroxyethylurea **IVb** (1.0 g, 2.50 mmol) according to the general procedure resulted in 1.4 g of **Vb** (91%). <sup>1</sup>H NMR (400 MHz, CDCl<sub>3</sub>) δ 7.78 (d, *J* = 7.5 Hz, 2H), 7.50 (dd, *J* = 7.9 Hz, 2H), 7.45 – 7.37 (m, 2H), 7.33 – 7.20 (m, 10H), 7.16 (d, *J* = 7.4 Hz, 2H), 4.80 (d, *J* = 9.1 Hz, 2H), 4.57 (m, 1H), 4.49 (m, 1H), 4.46 – 4.41 (m, 1H), 4.40 – 4.35 (m, 1H), 4.27 (m, 1H), 4.18 – 4.08 (m, 1H), 3.86 (m, 1H), 3.75 (s, 3H), 3.65 (m, 1H), 3.21 (m, 1H), 2.92 (m, 2H), 1.37 (d, *J* = 7.3 Hz, 3H). <sup>13</sup>C NMR (125 MHz, CDCl<sub>3</sub>) δ 174.91, 159.63, 156.14, 143.78, 141.34, 137.41, 136.70, 129.52, 128.93, 128.50, 127.75, 73.23, 66.51, 54.97, 52.42, 52.04, 51.81, 49.67, 47.23, 35.49, 18.42. LC-MS (*m/z*): negative mode 620 [M-H]<sup>-</sup>, positive mode 622 [M+H]<sup>+</sup>. Purity by HPLC-UV (214 nm)-ESI-MS: 99%. mp 185-187 °C.

**General method for the synthesis of *O*-TBDMS-protected, *N*-Fmoc-protected hydroxyethylureas (**Via**, **Vib**).** To a stirred solution of **Va** or **Vb** (1.0 g) in DMF (3 mL) under dry N<sub>2</sub> at r.t. was added 2 eq. of TBDMS chloride and 1.2 eq. DMAP. After 36 h, the reaction mixture was quenched with water, extracted with 3 X 100 mL of ethyl acetate, dried under anhydrous MgSO<sub>4</sub> and concentrated *in vacuo*. The resultant oil was purified by silica gel chromatography (0 to 2 % MeOH in CH<sub>2</sub>Cl<sub>2</sub>) to obtain **Via** and **Vib** as white powders.

**Methyl(((2*R*,3*S*)-3-(((9*H*-fluoren-9-yl)methoxy)carbonyl)amino)-2-((tert-butyl)dimethylsilyloxy)-4-phenylbutyl)-(benzyl)carbamoyl)-*L*-leucinate (**Via**).** Fmoc-protected hydroxyethylurea **Va** (1.0 g, 1.50 mmol) according to the general procedure resulted in 880 mg of **Via** (75% yield). <sup>1</sup>H NMR (400 MHz, CDCl<sub>3</sub>) δ 7.73 (d, *J* = 7.7 Hz, 2H), 7.45 (dd, *J* = 7.6 Hz, 2H), 7.36 (m, 2H), 7.30 – 7.20 (m, 10H), 7.16 (d, *J* = 7.4 Hz, 2H), 4.71 (m, 1H), 4.45 (m, 3H), 4.03 (m, 1H), 3.67 (m, 3H), 3.58 (s, 3H), 3.48 (m, 1H), 3.26 – 3.12 (m, 1H), 2.99 (m, 1H), 2.85 (m, 1H), 1.41 (m, 1H), 1.23 (m, 2H), 0.89 (s, 9H), 0.86 (s, 3H), 0.83 (s, 3H), 0.03 (s, 3H), 0.00 (s, 3H). <sup>13</sup>C NMR (125 MHz, CDCl<sub>3</sub>) δ 174.72, 159.89, 158.65, 141.34, 139.26, 135.99, 129.50, 129.16, 128.68, 127.38, 126.47, 119.96, 74.92, 66.52, 55.93, 55.31, 52.56, 52.27, 51.94, 49.99, 47.24, 41.47, 31.60, 25.94, 22.84, 21.96, 17.98, -4.25, -4.87. LC-MS (*m/z*): negative mode 777 [M-H]<sup>-</sup>, positive mode 779 [M+H]<sup>+</sup>. Purity by HPLC-UV (214 nm)-ESI-MS: 99%. mp 193-195 °C.

**Methyl(((2*R*,3*S*)-3-(((9*H*-fluoren-9-yl)methoxy)carbonyl)amino)-2-((tert-butyl)dimethylsilyloxy)-4-phenylbutyl)-(benzyl)carbamoyl)-*L*-alaninate (**Vib**).** Fmoc-(hydroxyethyl)urea **Vb** (1.0 g, 1.61 mmol) according to the general procedure resulted in 948 mg of **Vib** (80%). <sup>1</sup>H NMR (400

MHz, CDCl<sub>3</sub>)  $\delta$  7.76 – 7.69 (m, 2H), 7.45 (m, 2H), 7.38 – 7.31 (m, 4H), 7.24 (m, 8H), 7.18 (m, 2H), 5.10 (d,  $J$  = 16.5 Hz, 2H), 4.54 (d,  $J$  = 4.7 Hz, 1H), 4.45 (m, 1H), 4.18 (m, 3H), 3.89 (dd,  $J$  = 4.9 Hz, 1H), 3.68 (m, 1H), 3.66 (s, 3H), 3.26 (m, 1H), 3.06 (m, 1H), 2.75 (m, 1H), 1.42 (d,  $J$  = 7.2 Hz, 3H), 0.90 (s, 9H), 0.03 (s, 6H), 0.00 (s, 3H). <sup>13</sup>C NMR (125 MHz, CDCl<sub>3</sub>)  $\delta$  174.32, 157.86, 155.85, 143.89, 141.25, 138.38, 136.02, 129.22, 128.91, 128.51, 127.64 – 127.61, 127.01 – 126.98, 126.44, 125.22, 125.10, 119.96, 66.69, 52.30, 51.37, 49.74, 49.68, 47.12, 25.93, 18.71, 18.03, -4.44, -4.75. LC-MS ( $m/z$ ): negative mode 735 [M-H]<sup>-</sup>, positive mode 737 [M+H]<sup>+</sup>. Purity by HPLC-UV (214 nm)-ESI-MS: 99.00%. mp 189-191 °C.

**General procedure for the deprotection of methyl ester (VIIa, VIIb).** To a solution of **Vla** or **Vlb** (500 mg) in THF (5 mL) was added 5 mL of 1.0 M aqueous LiOH and the reaction was stirred for 4 h. After addition of brine (20 mL), the aqueous solution was extracted with 3 X 100 mL of ethyl acetate, dried over anhydrous MgSO<sub>4</sub> and concentrated to give **VIIa** and **VIIb** as white solids.

**(((2R,3S)-3-amino-2-((tert-butyldimethylsilyl)oxy)-4-phenylbutyl)(benzyl)carbamoyl)-L-leucine (VIIa).** *N*-Fmoc-hydroxyethylurea **Vla** (1.0 g, 1.28 mmol) according to the general procedure provided 580 mg of **VIIa** (85%). <sup>1</sup>H NMR (400 MHz, CDCl<sub>3</sub>)  $\delta$  7.31 – 7.15 (m, 10H), 4.70 (d,  $J$  = 7.5 Hz, 1H), 4.45 – 4.34 (m, 1H), 4.09 (m, 1H), 3.70 (m, 1H), 3.50 (m, 2H), 3.18 (m, 1H), 2.99 (m, 1H), 2.32 (m, 1H), 1.84 (m, 1H), 1.70 (m, 1H), 0.94 (d,  $J$  = 6.6 Hz, 3H), 0.89 (m, 12H), 0.03 (s, 3H), 0.00 (s, 3H), 1.02 (s, 3H). <sup>13</sup>C NMR (125 MHz, CDCl<sub>3</sub>)  $\delta$  174.19, 155.77, 139.26, 138.07, 129.15, 128.67, 128.56, 127.40, 127.13, 126.40, 74.59, 55.84, 52.55, 51.83, 48.98, 41.47, 34.67, 31.60, 25.90, 22.62, 14.12, -4.26, -4.88. LC-MS ( $m/z$ ): negative mode 540 [M-H]<sup>-</sup>, positive mode 542 [M+H]<sup>+</sup>. Purity by HPLC-UV (214 nm)-ESI-MS: 99.00%.

**(((2R,3S)-3-amino-2-((tert-butyldimethylsilyl)oxy)-4-phenylbutyl)(benzyl)carbamoyl)-L-alanine (VIIb).** *N*-Fmoc-hydroxyethylurea **Vlb** (1.0 g, 1.35 mmol) according to the general procedure provided 558 mg of **VIIb** (80%). <sup>1</sup>H NMR (400 MHz, CDCl<sub>3</sub>)  $\delta$  7.51 – 7.34 (m, 10H), 4.91 (d,  $J$  = 16.7 Hz, 1H), 4.46 (d,  $J$  = 16.6 Hz, 1H), 4.26 (m, 2H), 3.78 (m, 1H), 3.33 (m, 1H), 3.10 (m, 2H), 2.94 (m, 1H), 1.42 (d,  $J$  = 7.3 Hz, 3H), 0.96 (s, 9H), 0.03 (s, 3H), -0.00 (s, 3H). <sup>13</sup>C NMR (125 MHz, CDCl<sub>3</sub>)  $\delta$  174.33, 155.96, 141.25, 138.38, 136.45, 129.22, 128.91, 127.61, 127.01, 126.44, 66.70, 52.25, 51.36, 49.60, 47.15, 41.67, 25.94, 18.71, 18.08, -4.53, -4.73. LC-MS ( $m/z$ ): negative mode 498 [M-H]<sup>-</sup>, positive mode 500 [M+H]<sup>+</sup>. Purity by HPLC-UV (214 nm)-ESI-MS: 96.50%.

**General procedure for Fmoc protection (VIIIa, VIIIb).** To a solution of **VIIa** or **VIIb** (0.5 g) in CH<sub>2</sub>Cl<sub>2</sub> (5 mL) under dry N<sub>2</sub> was added 1.2 eq. of Fmoc chloride and 2 eq. of DIPEA, and the reaction mixture was stirred overnight at room temperature. After being concentrated *in vacuo*, the mixture was eluted through silica gel using 0 to 5 % MeOH in CH<sub>2</sub>Cl<sub>2</sub> to give title compounds as white powders.

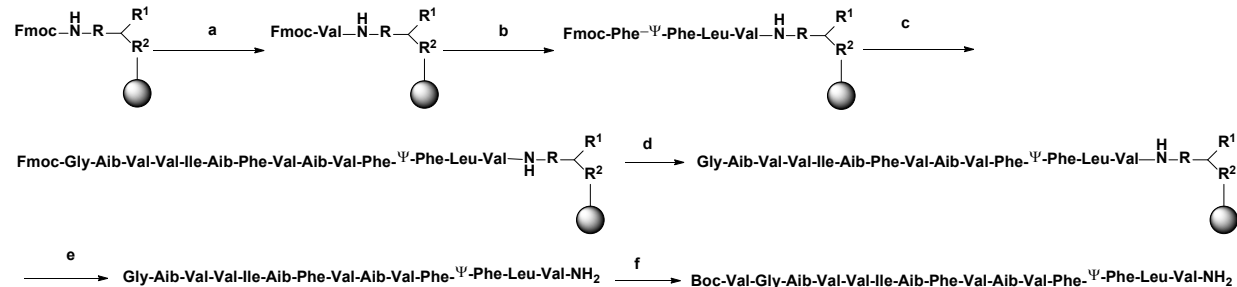
**(((2R,3S)-3-(((9H-fluoren-9-yl)methoxy)carbonyl)amino)-2-((tert-butyldimethylsilyl)oxy)-4-phenylbutyl)(benzyl)carbamoyl)-L-leucin (VIIIa).** Hydroxyethylurea **VIIa** (500 mg, 0.92 mmol) according to the general procedure yielded 423 mg of **VIIIa** (60%). <sup>1</sup>H NMR (400 MHz, CDCl<sub>3</sub>)  $\delta$  7.74 (m, 2H), 7.46 (m, 2H), 7.39 – 7.27 (m, 4H), 7.28 – 7.19 (m, 10H), 5.07 (m, 1H), 4.52 (m, 2H), 4.39 (dd,  $J$  = 15.5 Hz, 2H), 4.28 (m, 3H), 4.08 (m, 1H), 3.85 (bs, 1H), 3.66 (m, 2H), 3.47 (m, 1H), 3.18 (m, 1H), 3.04 (m, 1H), 1.74 (m, 1H), 1.47 (m, 1H), 1.33 (m, 1H), 0.94 (m, 3H), 0.91 (s, 3H), 0.83 (s, 6H), 0.03 (s, 3H), 0.00 (s, 3H). <sup>13</sup>C NMR (125 MHz, CDCl<sub>3</sub>)  $\delta$  174.74, 160.12, 155.21, 146.02, 139.30, 138.05, 128.67, 128.57, 127.81, 127.38, 127.13, 126.48, 123.96, 120.07, 74.94, 68.81, 55.92, 52.54, 51.84, 45.96, 41.47, 25.94, 24.95, 22.84, 17.88, -4.25, -4.87. LC-MS ( $m/z$ ): negative mode 763 [M-H]<sup>-</sup>, positive mode 765 [M+H]<sup>+</sup>. Purity by HPLC-UV (214 nm)-ESI-MS: 97.20%. mp 186-188 °C.

**(((2R,3S)-3-((((9H-fluoren-9-yl)methoxy)carbonyl)amino)-2-((tert-butyldimethylsilyl)oxy)-4-phenylbutyl)(benzyl)carbamoyl)-L-alanine (VIIIb).** Hydroxyethylurea **VIIb** (500 mg, 1 mmol) according to the general procedure gave 250 mg of **VIIIb** (55%). <sup>1</sup>H NMR (400 MHz, CDCl<sub>3</sub>) δ 7.74 (d, *J* = 7.6 Hz, 2H), 7.47 (m, 2H), 7.38 (m, 2H), 7.33 (d, *J* = 7.5 Hz, 2H), 7.30 – 7.16 (m, 10H), 5.45 (d, *J* = 6.6 Hz, 1H), 5.22 (d, *J* = 8.3 Hz, 1H), 4.55 (s, 2H), 4.38 (m, 1H), 4.32 – 4.05 (m, 1H), 4.12 (m, 1H), 3.89 (m, 1H), 3.46 (m, 1H), 3.22 (m, 1H), 3.04 (m, 1H), 2.74 (m, 1H), 1.36 (d, *J* = 7.1 Hz, 3H), 0.92 (s, 9H), 0.04 (s, 3H), 0.00 (s, 3H). <sup>13</sup>C NMR (125 MHz, CDCl<sub>3</sub>) δ 174.05, 160.87, 151.57, 143.07, 141.20, 137.84, 129.86, 128.14, 127.36, 127.51, 127.26, 126.72, 124.53, 120.29, 71.14, 65.34, 56.14, 54.02, 50.13, 49.67, 48.47, 39.53, 25.84, 17.98, 17.90, -4.29, -4.40. LC-MS (*m/z*): negative mode 720 [M-H]<sup>-</sup>, positive mode 722 [M+H]<sup>+</sup>. Purity by HPLC-UV (214 nm)-ESI-MS: 98.50%. mp 187-189 °C.

### Solid-phase syntheses

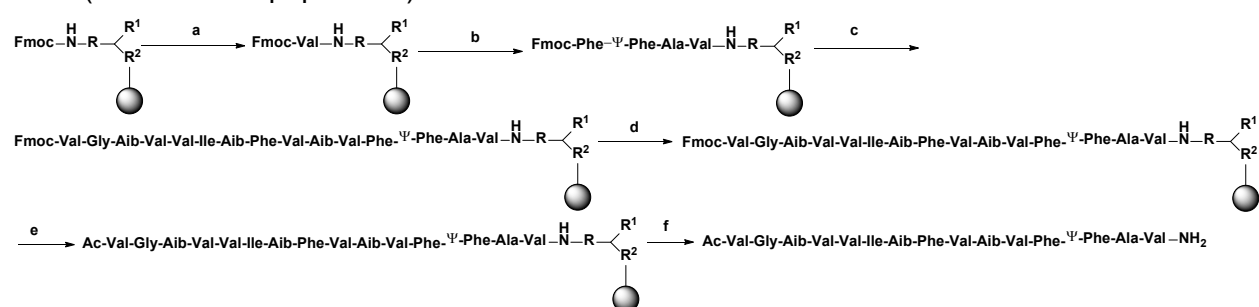
TSAs **1** and **10** were synthesized using building blocks **VIIIa** and **VIIIb**, respectively, by solid-phase coupling on Rink amide resin according to **Scheme S2**. After removal of Fmoc from the resin, *N*-Fmoc-*L*-valine and **VIIIa/b** were consecutively coupled. The peptide analog was then cleaved from the resin, purified by HPLC, and further coupled by solution phase with *N*-Boc-*L*-valine. HPLC purification provided TSAs **1** or **10**. HPI **2** was synthesized as previously described.<sup>3</sup> Leucine-containing HPI-TSAs **3-6** and **9** as well as linker-TSA **7** were synthesized according to **Scheme S3**, using building block **VIIIa**. Note that the *O*-TBDMS protecting group in building blocks **VIIIa** and **VIIIb** was removed during cleavage of peptides from the Rink amide resin, as the cleavage cocktail contains TFA. When 4-Fmoc-hydrazine benzoyl AM resin was used, the peptide was first cleaved from the resin, followed by *O*-TBDMS removal with 2 eq. of TBAF in THF under dry N<sub>2</sub> for 3 h. For control peptide **9**, Fmoc-Leu, Fmoc-Phe and Fmoc-Phe were successively coupled instead of building block **VIIIa**. HPI-TSAs **11** and **13** were accessed from **VIIIb** and *N*-Fmoc-*L*-amino acids by automated solid-phase synthesizer (Focus XC, Aapptec LLC) using Rink amide resin according to **Scheme S3**. Control peptide **12** was synthesized as HPI-TSA **11** and **13**, except Fmoc-Ala, Fmoc-Phe and Fmoc-Phe were successively coupled instead of using building block **VIIIb**. HPI-TSAs **14** and **16** were also accessed using **VIIIb** and Rink amide resin according to **Scheme S2**. HPI-TSA **15** with *N*-terminal Boc and C-terminal methyl ester was synthesized from 4-Fmoc-hydrazine benzoyl AM resins according to **Scheme S4**. TSA **17** was synthesized as previously described.<sup>4</sup> Biotinylated peptides TSA-Bpa-Bt and HPI-Bpa-Bt used for the photoaffinity assay were synthesized as previously described.<sup>5</sup> The purity of all tested peptides were >95%.

**Scheme S2.** Solid-phase synthesis of *N*-Boc, C-amide peptidomimetics using Rink amide resin<sup>a</sup> (for peptide **3**).



<sup>a</sup>Reagents and conditions: (a) two steps: (i) 20% piperidine in DMF; (ii) 0.2 M Fmoc-valine in DMF, 0.2 M DIC in DMF, 0.2 M OXYMA in DMF, 70 °C, 8 min, double coupling; (b) Iteratively: (i) 20% piperidine in DMF; (ii) 0.2 M BB5 in DMF, 0.2 M DIC in DMF, 0.2 M OXYMA in DMF, 70 °C, 8 min, double coupling; (c) Iteratively: i. 20% piperidine in DMF; ii. 0.2 M Fmoc-amino acids in DMF (Val, alkyl linker, Aib, Val, Phe, Aib, Ile, Val, Val, Aib, Gly), 0.2 M DIC in DMF, 0.2 M OXYMA in DMF, 70 °C, 8 min, double coupling; only for peptides **3-9**, **14**, **16** (d) 20% piperidine in DMF; for peptide **9** amino acids are: Aib, Val, Phe, Aib, Ile, <sup>D</sup>Val, <sup>D</sup>Val, Aib, Gly (e) Resin cleavage cocktail TFA:TIPS:H<sub>2</sub>O:DoDt :: 92.5:2.5:2.5:2.5, rt, 2h; (f) 0.1 eq. Boc-valine, 0.09 eq. HCTU, 0.2 eq. DIPEA, 3 mL DMF, rt, 24 h, yield 45-50%. (Note: for the synthesis of peptide **3-9** building block **VIIIa** was used; for the synthesis of peptide **14** and **16** building block **VIIIb** was used; for the synthesis of peptide **1** and **10**, after coupling of building blocks (**VIIIa** for **1** and **VIIIb** for **10**), the peptide was cleaved from resin and Boc-Val-OH was attached in liquid phase; for the synthesis of **7** solid phase coupling ended with addition of building block and Val, then peptide was cleaved from resin and BocNH(CH<sub>2</sub>)<sub>8</sub>CO<sub>2</sub>H was attached by liquid phase; For control peptide **8**, Leu, Phe and Phe were successively coupled instead of building block **VIIIa**).

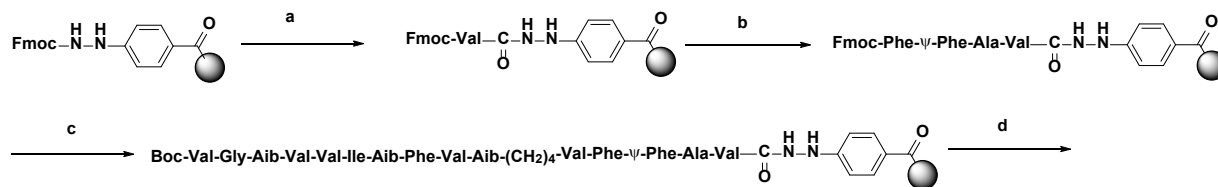
**Scheme S3.** Solid-phase synthesis of *N*-acetylated, C-amide peptidomimetics using Rink amide resin (illustrated for peptide **11**)<sup>a</sup>



<sup>a</sup>Reagents and conditions: (a) i. 20% piperidine in DMF; ii. 0.2 M Fmoc-L-valine in DMF, 0.2 M DIC (N,N'-Diisopropylcarbodiimide) in DMF, 0.2 M OXYMA (Ethyl cyano(hydroxyimino)acetate) in DMF, 70 °C, 8 min, double coupling; (b) i. 20% piperidine in DMF; (ii) 0.2 M **VIIIb** in DMF, 0.2 M DIC (N,N'-Diisopropylcarbodiimide) in DMF, 0.2 M OXYMA in DMF, 70 °C, 8 min, double coupling; (c) Iteratively: i. 20% piperidine in DMF; ii. 0.2 M Fmoc-protected amino acids in DMF (Val, FmocNH(CH<sub>2</sub>)<sub>4</sub>CO<sub>2</sub>H only for peptide **13**, Aib, Val, Phe, Aib, Ile, Val, Val, Aib, Gly, Val), 0.2 M DIC in DMF, 0.2 M OXYMA in DMF, 70 °C, 8 min, double coupling; (d) 20% piperidine in DMF; (e) Ac<sub>2</sub>O, 7% DIPEA in DMF, 60 min (f) TFA:TIPS (Triisopropylsilane): H<sub>2</sub>O: DoDt (2,2'-(Ethylenedioxy)diethanethiol):: 92.5:2.5:2.5:2.5, r.t., 2 h. (<sup>a</sup> Note: for the synthesis of peptide **12**, instead of **VIIIb**, the coupling was carried out with 0.2 M of Ala, Phe and Phe in sequential order).



**Scheme S4.** Solid-phase synthesis of *N*-Boc, C-methyl ester peptidomimetics using 4-Fmoc-hydrazine benzoyl AM resin<sup>a</sup> (illustrated for peptide **15**)



**Boc-Val-Gly-Aib-Val-Val-Ile-Aib-Phe-Val-Aib-(CH<sub>2</sub>)<sub>4</sub>-Val-Phe-ψ-Phe-Ala-Val-OMe**

<sup>a</sup>Reagents and conditions: (a) i. 20% piperidine in DMF; ii. 0.2 M Fmoc-L-valine in DMF, 0.2 M DIC in DMF, 0.2 M OXYMA in DMF, 70 °C, 8 min, double coupling; (b) i. 20% piperidine in DMF; ii. 0.2 M **VIIIb** in DMF, 0.2 M DIC in DMF, 0.2 M OXYMA in DMF, 70 °C, 8 min, double coupling; (c) Iteratively: i. 20% piperidine in DMF; ii. 0.2 M *N*-Fmoc-protected amino acids in DMF (Val, Aib, Val, Phe, Aib, Ile, Val, Val, Aib, Gly) and Boc-Val (last cycle), 0.2 M DIC in DMF, 0.2 M OXYMA in DMF, 70 °C, 8 min, double coupling;; (d): i. 3 eq. NBS, 2 eq. pyridine, 5 mL DCM, r.t., 5 min; ii. 5 eq. methanol, 5 mL DCM, r.t., 4 h; iii. 2.0 eq. TBAF in THF, 3h.

**Table S1:** Measured mass, HPLC peak retention time and LC-MS purity of tested peptides

<b>Compound name</b>	<b>Mass calc.</b>	<b>Mass measured (ESI) M+Na<sup>+</sup></b>	<b>Mass measured (TOF) M+H<sup>+</sup></b>	<b>Retention time (Method A)<sup>a</sup> min</b>	<b>Retention time (Method B)<sup>b</sup> min</b>	<b>LC-MS % Purity</b>
<b>1</b>	724.4523	747.4491	725.9508	6.94	8.86	100
<b>2</b>	1100.6845	1123.6813	1101.6910	10.33	10.35	99
<b>3</b>	1693.0582	1716.0093	1694.0693	7.86	8.55	95
<b>4</b>	1764.0954	1787.0621	1765.1017	6.51	6.50	100
<b>5</b>	1792.1267	1815.0834	1793.1305	4.84	4.82	96
<b>6</b>	1848.1893	1871.1791	1849.2210	10.98	10.99	96
<b>7</b>	879.5834	902.5788	880.5914	8.40	9.87	97
<b>8</b>	1846.1534	1869.1432	1847.1930	6.28	6.46	96
<b>9</b>	1848.1915	1871.1813	1849.2134	10.99	6.48	96
<b>10</b>	682.4054	705.3768	683.4105	6.99	7.19	98
<b>11</b>	1592.9694	1615.9903	1594.0015	5.19	4.78	96
<b>12</b>	1590.9538	1613.9194	1591.9633	8.03	8.10	96
<b>13</b>	1692.0378	1715.9730	1693.0389	8.55	8.54	98
<b>14</b>	1750.0797	1773.0626	1751.0575	7.31	7.14	95
<b>15</b>	1765.0794	1788.0547	1766.0887	11.06	11.04	97
<b>16</b>	1806.1423	1829.1754	1807.1272	10.49	11.58	99
<b>17</b>	739.4521	762.4420	740.4608	8.84	8.81	97

<sup>a</sup>gradient of water/methanol: 2-propanol (1: 1) (containing 0.02% formic acid) from 60:40 to 0:100

<sup>b</sup>gradient of water/acetonitrile (containing 0.05% trifluoroacetic acid) from 50:40 to 0:100

**Table S2. Inhibition of  $\gamma$ -secretase by helical peptide/transition-state analogue conjugates: P2' = Ala.**

Compound	Helical Peptide	Linker	Transition-State Analogue <sup>a</sup>	IC <sub>50</sub> <sup>b</sup>
	<i>APP transmembrane residues 707-717:</i> ---Val-Gly-Gly-Val-Val-Ile-Ala-Thr-Val-Ile---		-----Optimized TSA----- ----P2 - P1 - P1' - P2' - P3'-----	
<b>10</b>			Boc-Val-Phe- $\psi$ -Phe-Ala-Val-NH <sub>2</sub>	123 $\pm$ 4
<b>2</b>	Boc-Val-Gly-Aib-Val-Val-Ile-Aib-Phe-Val-Aib-OCH <sub>3</sub>			58 $\pm$ 6
<b>11</b>	Ac-Val-Gly-Aib-Val-Val-Ile-Aib-Phe-Val-Aib-	-	-Val-Phe- $\psi$ -Phe-Ala-Val-NH <sub>2</sub>	17 $\pm$ 3
<b>12</b>	Ac-Val-Gly-Aib-Val-Val-Ile-Aib-Phe-Val-Aib-	-	-Val-Phe - Phe-Ala-Val-NH <sub>2</sub>	>1000
<b>13</b>	Ac-Val-Gly-Aib-Val-Val-Ile-Aib-Phe-Val-Aib-	-NH(CH <sub>2</sub> ) <sub>4</sub> CO-	-Val-Phe- $\psi$ -Phe-Ala-Val-NH <sub>2</sub>	15 $\pm$ 2
<b>14</b>	Boc-Val-Gly-Aib-Val-Val-Ile-Aib-Phe-Val-Aib-	-NH(CH <sub>2</sub> ) <sub>4</sub> CO-	-Val-Phe- $\psi$ -Phe-Ala-Val-NH <sub>2</sub>	5.8 $\pm$ 0.2
<b>15</b>	Boc-Val-Gly-Aib-Val-Val-Ile-Aib-Phe-Val-Aib-	-NH(CH <sub>2</sub> ) <sub>4</sub> CO-	-Val-Phe- $\psi$ -Phe-Ala-Val-OCH <sub>3</sub>	28 $\pm$ 2
<b>16</b>	Boc-Val-Gly-Aib-Val-Val-Ile-Aib-Phe-Val-Aib-	-NH(CH <sub>2</sub> ) <sub>8</sub> CO-	-Val-Phe- $\psi$ -Phe-Ala-Val-NH <sub>2</sub>	0.5 $\pm$ 0.1

<sup>a</sup>  $\psi$  represents hydroxyethylurea replacement of the peptide backbone; <sup>b</sup> Concentration that inhibits 50% activity of 1 nM purified  $\gamma$ -secretase.

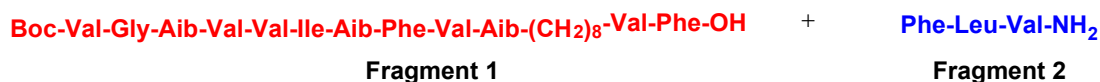
## General protocol for LC-MS/MS analysis of proteolysis of control peptides

To 25  $\mu\text{L}$  aliquots of 30 nM enzyme in  $\gamma$ -secretase assay buffer was added either 0.5  $\mu\text{L}$  of either DMSO alone or 0.5  $\mu\text{M}$  of control peptide **8** in DMSO, and the reaction mixtures were incubated at 37  $^{\circ}\text{C}$  for 4 h. Reactions were stopped on ice and stored at -20  $^{\circ}\text{C}$ . Samples were analyzed on Q-Tof-2<sup>TM</sup> (Micromass Ltd., Manchester UK), a quadrupole and time-of-flight tandem mass analyzer with an electrospray ion source coupled with LC (Aquity-Waters).

## LC-MS/MS study of control peptide **8**

Boc-Val-Gly-Aib-Val-Val-Ile-Aib-Phe-Val-Aib-(CH<sub>2</sub>)<sub>8</sub>-Val-Phe-Phe-Leu-Val-NH<sub>2</sub>  $\xrightarrow{\gamma\text{-secretase, } 37^{\circ}\text{C, } 4\text{ h}}$

**Peptide 8**



Both fragments were detected by LC-MS. Fragment 1 calculated M+H: 1489.9; Found: 1489.9. Fragment 2 calculated M+H: 377.2; Found: 377.3. LC-MS/MS of fragment 1 shown in **Fig. S1**.

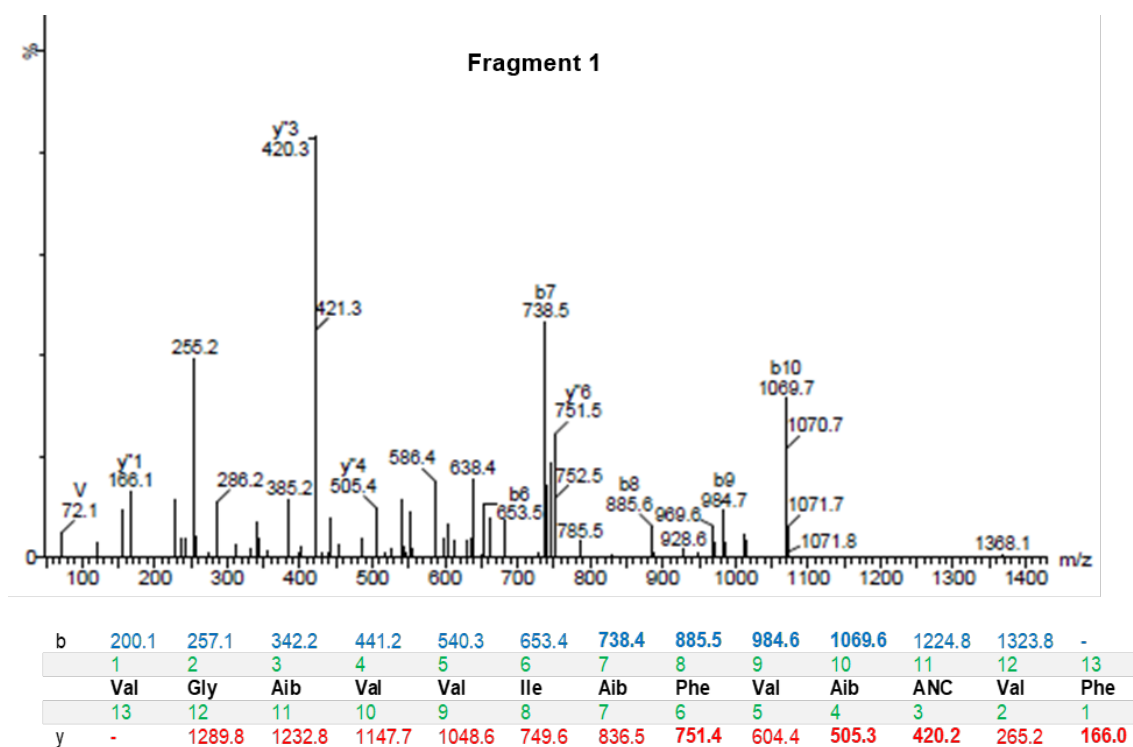


**Figure S1:** Confirmation of the LC/ESI-MS peak corresponding to **fragment 1** ( $m/z = 1488.9367$ ) from peptide **8** by the analysis of product ions (detected product ions in bold).

## LC-MS/MS study of control peptide 12

Ac-Val-Gly-Aib-Val-Val-Ile-Aib-Phe-Val-Aib-Val-Phe-Phe-Ala-Val-NH<sub>2</sub>  $\xrightarrow{\gamma\text{-secretase, } 37\text{ }^\circ\text{C, } 4\text{ h}}$

**Peptide 12**

**Ac-Val-Gly-Aib-Val-Val-Ile-Aib-Phe-Val-Aib-Val-Phe-OH** + **Phe-Ala-Val-NH<sub>2</sub>**

**Fragment 1**

**Fragment 2**

Both fragments were detected by LC-MS. Fragment 1 calculated M+H: 1275.76; Found: 1275.76. Fragment 2 calculated M+H: 335.20; Found: 335.17. LC-MS/MS of fragment 1 shown in **Fig. S2**.

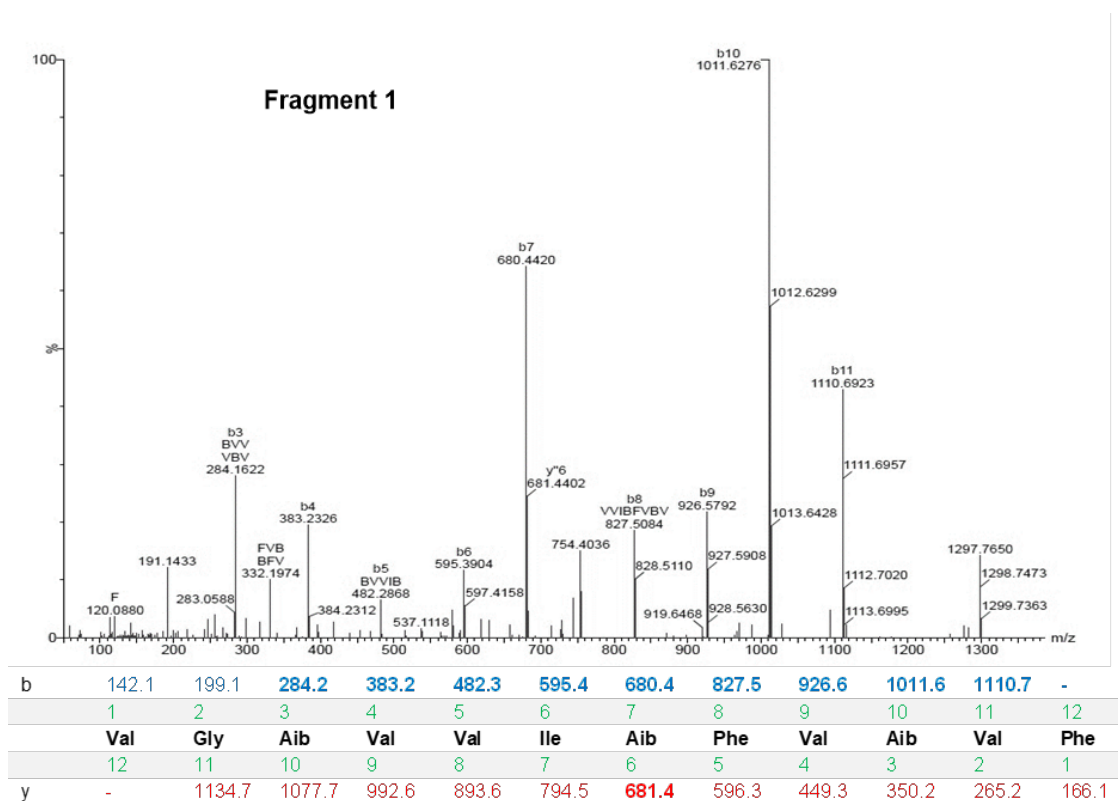


**Figure S2:** Confirmation of the LC/ESI-MS peak corresponding to **fragment 1** ( $m/z = 1274.7638$ ) of peptide **12** by the analysis of product ions (detected product ions in bold).

## Conformational Analysis of Compounds 6 and 9 by 2D NMR.

### NMR experiments:

All NMR spectra were recorded on a Bruker 800 MHz NMR spectrometer with a 5 mm TCI probe, with probe temperature 278 °K. A series of 2D COSY, TOCSY, ROESY and <sup>1</sup>H-<sup>13</sup>C HSQC experiments were performed using standard pulse sequences from the Bruker library. Data were collected with 4K data points in t2 and 400 data points in t1. The relaxation delay was 2 s. Mixing times of 70 ms and 300 ms were used for the TOCSY and ROESY experiments, respectively. Data were processed and analyzed using MestReNova.

### Compound 6

#### Boc-Val-Gly-Val-Val-Ile-Aib-Phe-Val-Aib-(CH<sub>2</sub>)<sub>8</sub>-Val-Phe-ψ-Phe-Leu-Val-NH<sub>2</sub>

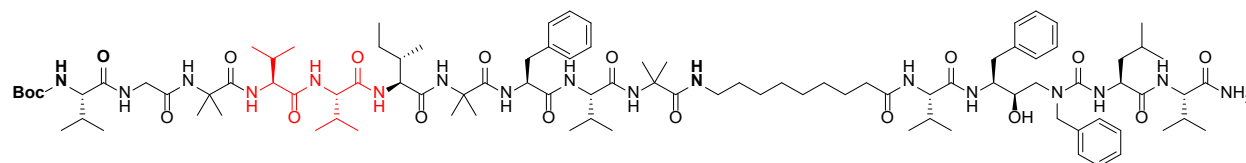


**Table S3:** <sup>1</sup>H NMR chemical shifts (ppm) of 6

Residue	NH	C <sup>α</sup> H	C <sup>β</sup> H	Others
Val (1)	7.13	3.77	2.05	H <sup>r</sup> 0.99, 0.99
Gly (2)	8.90	3.79, 3.73		
Aib (3)	8.16		1.51, 1.51	
Val (4)	7.51	3.68	2.24	H <sup>r</sup> 1.06, 0.98
Val (5)	7.73	3.68	2.25	H <sup>r</sup> 1.06, 0.98
Ile (6)	7.65	3.67	2.02	H <sup>r</sup> 1.62, 1.32 CH <sub>3</sub> - H <sup>r</sup> 0.91 H <sup>δ</sup> 0.82
Aib (7)	7.81		1.44, 1.44	
Phe (8)	7.81	4.27	3.19, 3.19	H <sup>δ</sup> 7.21, 7.21 H <sup>ε</sup> 7.28 7.28 H <sup>ξ</sup> 7.16
Val (9)	8.06	3.86	2.27	H <sup>r</sup> 1.10, 1.00
Aib (10)	7.89		1.45, 1.45	
(CH <sub>2</sub> ) <sub>8</sub> (11)	7.29	3.15	1.51	1.29, 1.29, 1.29, 1.29, 1.50, 2.13
Val (12)	7.77	3.97	1.76	H <sup>r</sup> 0.67, 0.69
Pseudo Phe (13)	7.98	3.99	3.07, 2.61	H <sup>δ</sup> 7.15, 7.15 H <sup>ε</sup> 7.17, 7.17 H <sup>ξ</sup> 7.11
ψ (14)		3.77	3.32, 3.32	
Pseudo Phe (15)		4.47		H <sup>r</sup> 7.19, 7.19 H <sup>δ</sup> 7.28, 7.28 H <sup>ε</sup> 7.33
Leu (16)	Missing*	4.30	1.55, 1.55	H <sup>r</sup> 1.55 H <sup>ε</sup> 0.90, 0.90
Val (17)	7.91	4.21	2.06	H <sup>r</sup> 0.96, 0.96

Solvent: CD<sub>3</sub>OH. Temperature: 278 °K. Boc-CH<sub>3</sub> chemical shifts: 1.47 ppm

\*Leu(16) backbone NH peak is broadened beyond detection, most likely due to NH exchange.

## Compound 9

Boc-Val-Gly-Aib-<sup>D</sup>Val-<sup>D</sup>Val-Ile-Aib-Phe-Val-Aib-(CH<sub>2</sub>)<sub>8</sub>-Val-Phe-ψ-Phe-Leu-Val-NH<sub>2</sub>

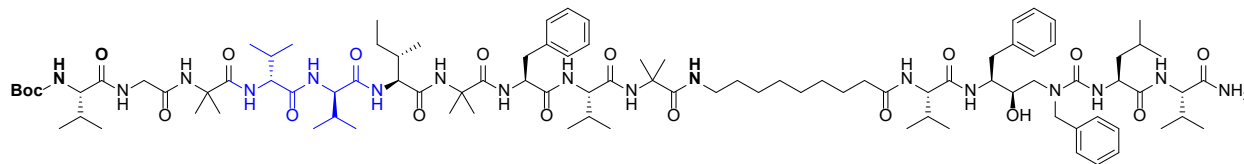


**Table S4:** <sup>1</sup>H NMR chemical shifts (ppm) of **9**

Residue	NH	C <sup>α</sup> H	C <sup>β</sup> H	Others
Val (1)	6.99	3.78	2.04	H <sup>r</sup> 0.94, 0.94
Gly (2)	8.68	3.72, 3.72		
Aib (3)	8.17		1.45, 1.45	
<sup>D</sup> Val (4)	7.46	4.05	2.21	H <sup>r</sup> 0.97, 0.97
<sup>D</sup> Val (5)	7.80	4.12	2.22	H <sup>r</sup> 0.92, 0.92
Ile (6)	8.05	4.06	2.05	H <sup>r</sup> 1.48, 1.24 CH <sub>3</sub> - H <sup>r</sup> 0.91 H <sup>δ</sup> 0.91
Aib (7)	8.07		1.25, 1.36	
Phe (8)	7.57	4.47	3.29, 3.06	H <sup>δ</sup> 7.22, 7.22 H <sup>ε</sup> 7.26, 7.26 H <sup>ξ</sup> 7.18
Val (9)	7.83	3.90	2.20	H <sup>r</sup> 0.97, 0.99
Aib (10)	7.72		1.45, 1.45	
(CH <sub>2</sub> ) <sub>8</sub> (11)	7.39	3.13	1.49	1.29, 1.29, 1.29, 1.29, 1.53, 2.13
Val (12)	7.73	3.97	1.76	H <sup>r</sup> 0.67, 0.69
Pseudo Phe (13)	7.97	4.02	3.04, 2.62	H <sup>δ</sup> 7.15, 7.15 H <sup>ε</sup> 7.17, 7.17 H <sup>ξ</sup> 7.11
ψ (14)		3.76	3.51, 3.24	
Pseudo Phe (15)		4.42		H <sup>r</sup> 7.13, 7.13 H <sup>δ</sup> 7.22, 7.22 H <sup>ε</sup> 7.29
Leu (16)	6.22	4.32	1.50, 1.50	H <sup>δ</sup> 1.40 H <sup>ε</sup> 0.85, 0.85
Val (17)	7.77	4.20	2.04	H <sup>r</sup> 0.92, 0.92

Solvent: CD<sub>3</sub>OH. Temperature: 278 °K. Boc-CH<sub>3</sub> chemical shifts: 1.44 ppm

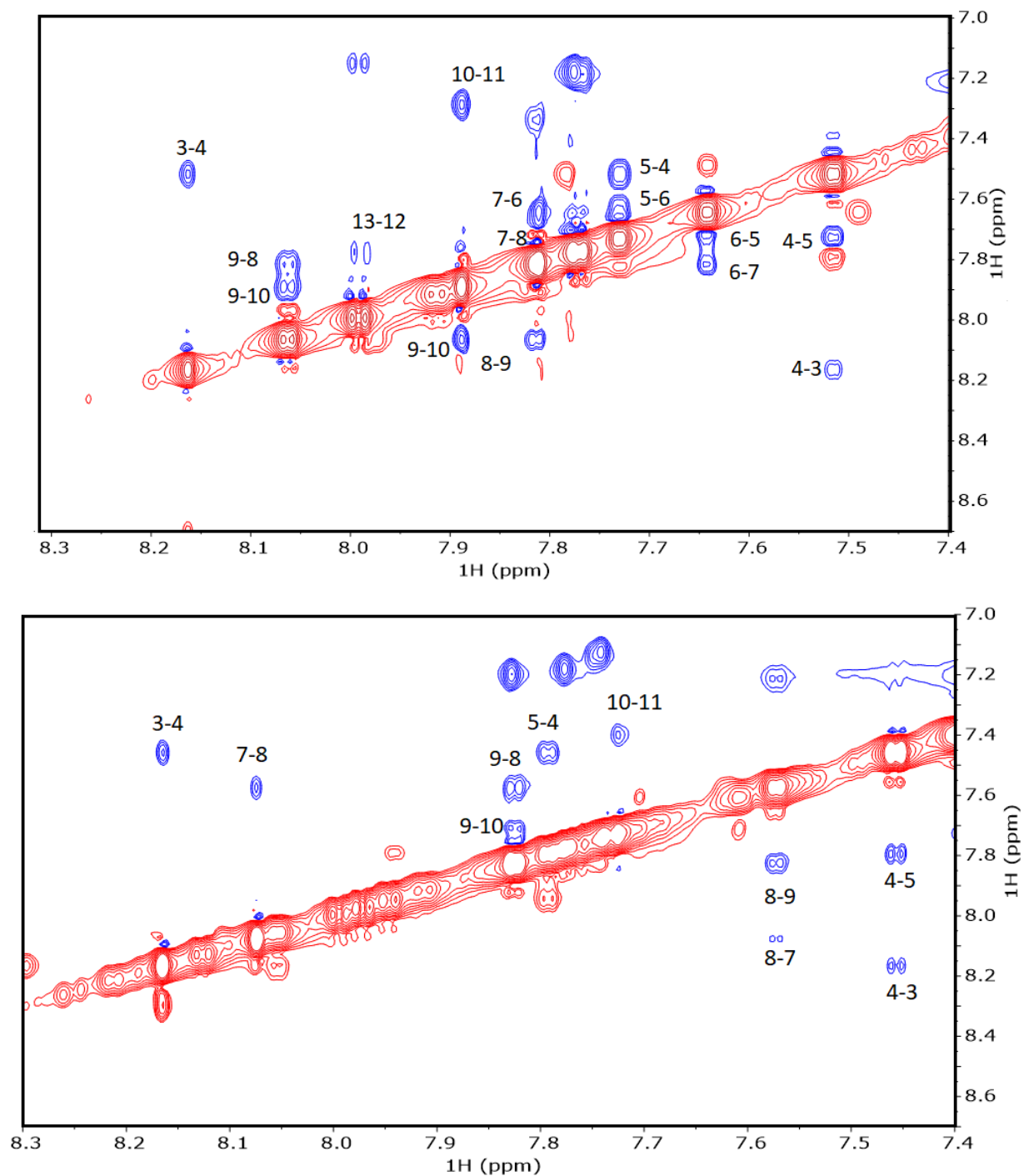


**Figure S3:** Portion of 800 MHz ROESY spectra of **6** (top) and **9** (bottom) in CD<sub>3</sub>OH at 278 K highlighting NH↔NH NOEs. Cross peaks are annotated using their corresponding residue numbers. Cross-peak intensities of **6** (5↔6, 6↔7, 7↔8) are increased compared to **9**, consistent with the HPI region of **6** being more helical.



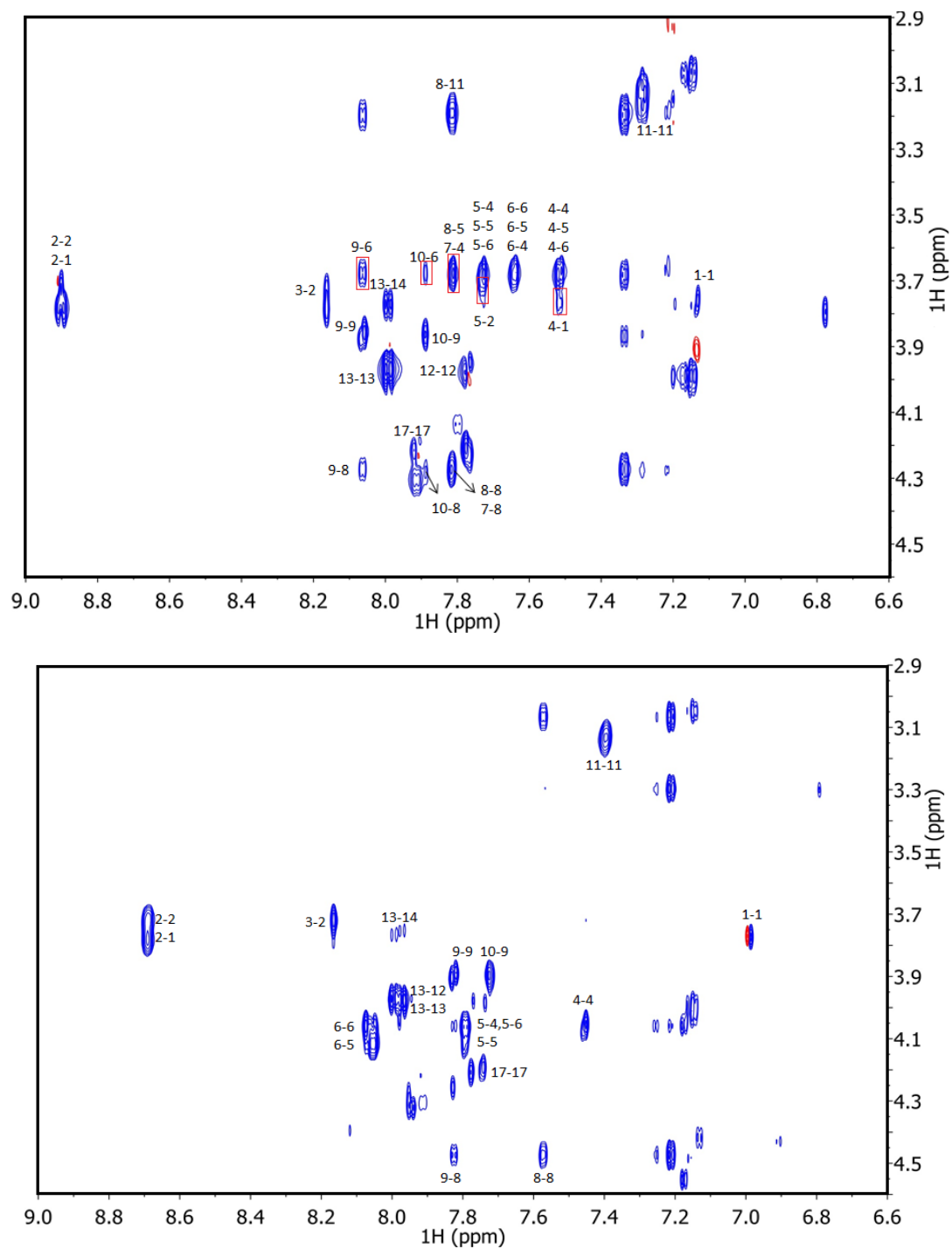


**Figure S4:** Portion of 800 MHz ROESY spectra of **6** (top) and **9** (bottom) in CD<sub>3</sub>OH at 278 K highlighting NH↔CaH NOEs. Cross peaks are annotated using their corresponding residue numbers. Medium range NOEs (1↔4, 2↔5, 4↔7, 5↔8, 6↔9, 6↔10) of the HPI region of **6** are diagnostic for a helical conformation.

## Protein overexpression and purification

The  $\gamma$ -secretase complex was expressed in suspension human embryonic kidney (HEK) 293 cells from a tetracistronic vector as previously described.<sup>6</sup> The protease complex was isolated and purified by affinity chromatography as we have previously reported.<sup>7</sup> APP-based recombinant substrate C100Flag was expressed in *E. coli* and isolated and purified as previously reported.<sup>8</sup>

## $\gamma$ -Secretase activity assays

Standard assay buffer contained 50 mM HEPES, pH 7.0, 150 mM NaCl, 0.025% DOPC (18:1 ( $\Delta$ 9-Cis) PC, Avanti Polar Lipids), 0.1% DOPE (18:1 ( $\Delta$ 9-Cis) PE, Avanti Polar Lipids), and 0.25% CHAPSO (Sigma). For  $IC_{50}$  determination, 1 nM purified  $\gamma$ -secretase in standard assay buffer was incubated at 37 °C for 30 min before addition of varying concentrations of inhibitor in DMSO and 0.5  $\mu$ M C100Flag (final 2% DMSO concentration in all cases). The reaction was incubated for 2 h at 37 °C, and A $\beta$ 40 produced was determined by specific sandwich ELISA (Invitrogen). The 2 h timepoint for A $\beta$ 40 production under these conditions is within the linear range with respect to time,<sup>9</sup> which we validated for the present study (data not shown), and therefore provides an appropriate indication of initial rate. Peptide  $IC_{50}$  inhibition was fit to the equation 1 using KaleidaGraph (Synergy Software). For  $K_i$  determination, enzyme reactions were run as above, but varying concentrations of C100Flag (0-5.4  $\mu$ M) and inhibitor. Kinetic data of peptide inhibition was fit to the noncompetitive equation (equation 2) using KaleidaGraph. (see **Fig. S5 and S6** for kinetic analysis of inhibition by HPI-TSA **6** and **16** respectively).

Peptide  $IC_{50}$  inhibition was determined by using the following equation:

$$\frac{v_i}{v_o} = \frac{1}{\left(1 + \frac{[I]}{IC_{50}}\right)}$$

Where  $v_i$  and  $v_o$  are the initial velocity in the presence and absence of inhibitor at concentration  $[I]$ .

$K_i$  values for noncompetitive inhibition were determined using the following equation:

$$v = \frac{V_{max}[S]}{[S] \left(1 + \frac{[I]}{K_{ii}}\right) + K_m \left(1 + \frac{[I]}{K_i}\right)}$$

where,  $v$  is the initial rate,  $S$  is the substrate concentration,  $K_i$  and  $K_{ii}$  are dissociation constant for inhibitor binding to free enzyme and enzyme-substrate complex respectively.

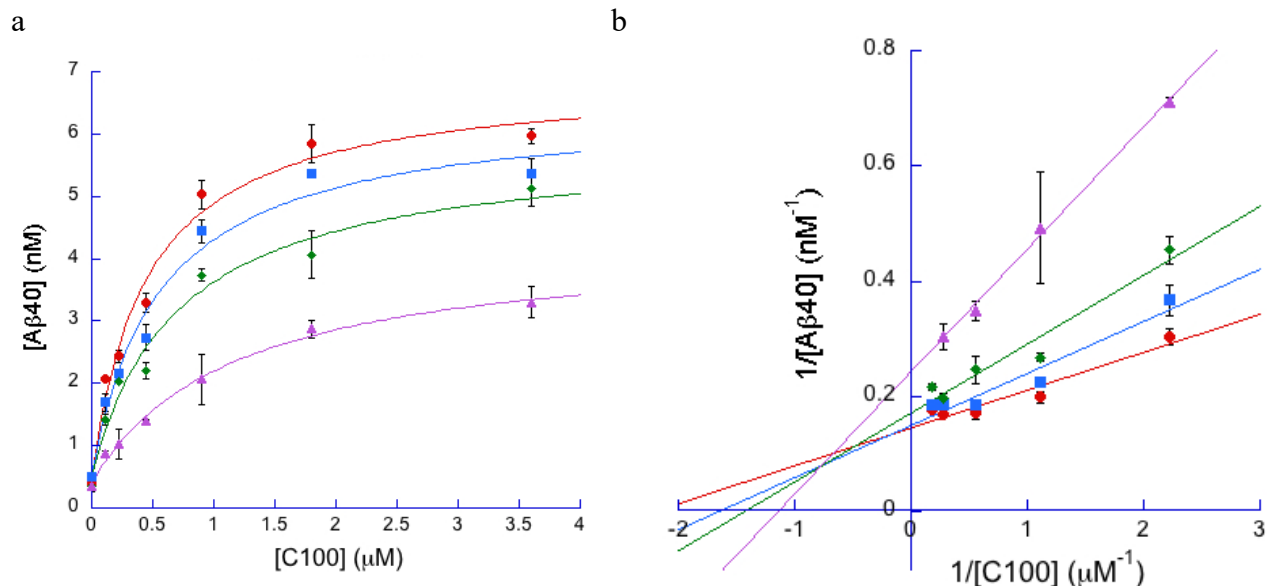


**Figure S5: Noncompetitive inhibition by HPI-TSA 6.** Michaelis-Menten (a) and double-reciprocal (b) Reciprocal plot of  $\gamma$ -secretase activity with **6** at concentrations of 0 nM (●), 0.5 nM (■), 1 nM (●), and 2.5 nM (●) showing noncompetitive inhibition with  $K_i$  of  $0.42 \pm 0.12$  nM.

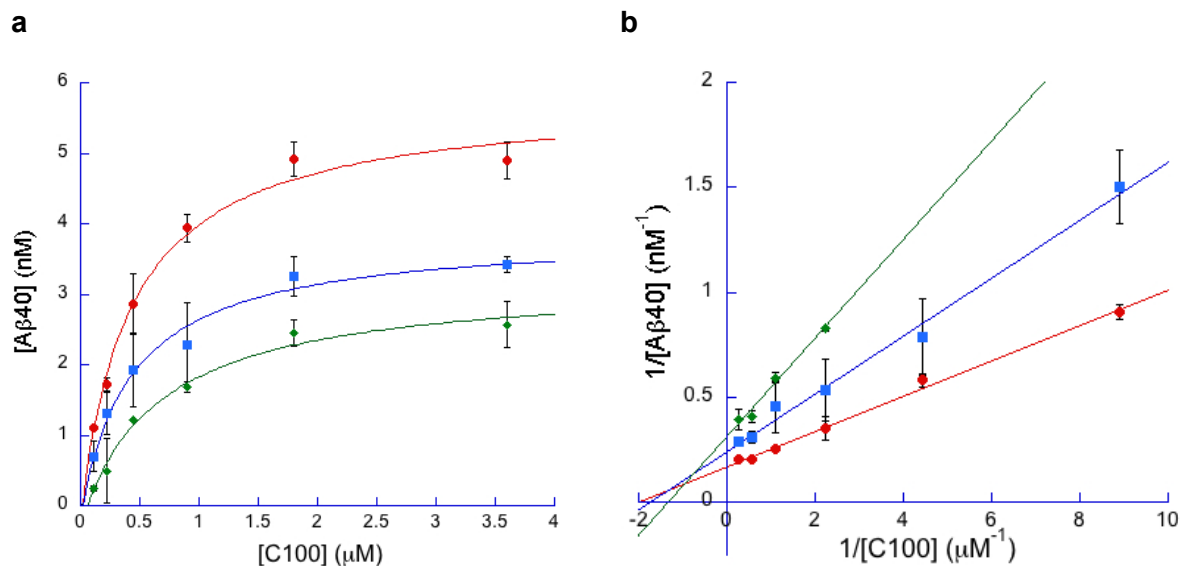


**Figure S6: Noncompetitive inhibition by HPI-TSA 16.** Michaelis-Menten (a) and double-reciprocal (b) plots of  $\gamma$ -secretase with **16** at concentrations of 0 nM (●), 0.5 nM (■), and 1 nM (◆) showing noncompetitive inhibition with  $K_i$  of  $0.84 \pm 0.07$  nM.

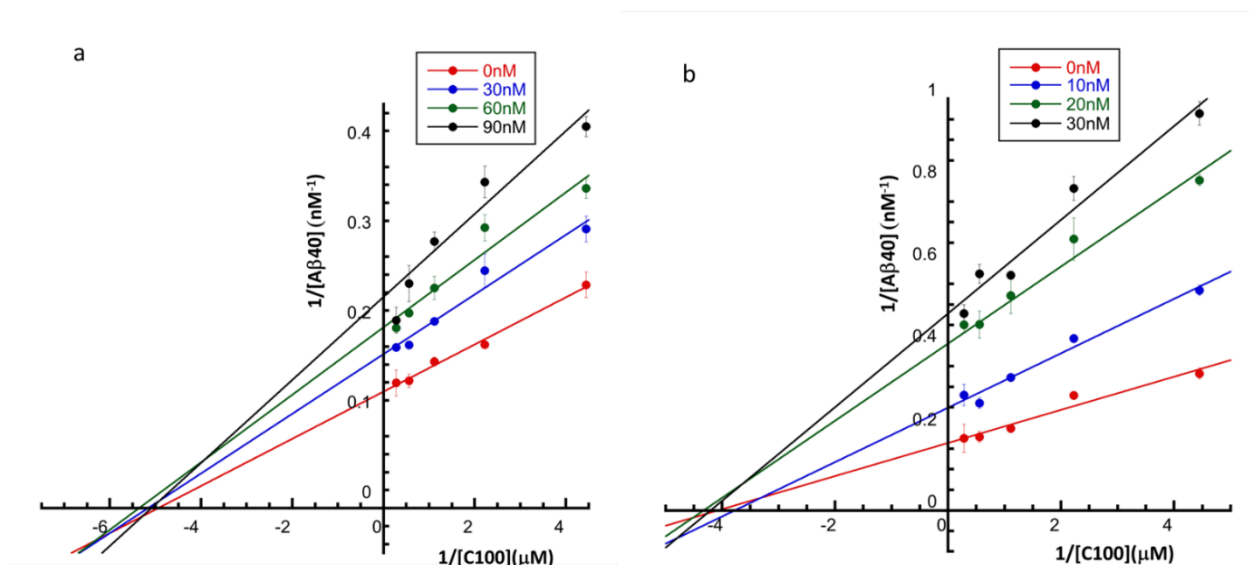


**Figure S7:** Noncompetitive inhibition with HPI **2** and TSA **17**. (a) Reciprocal plot of  $\gamma$ -secretase inhibition with HPI **2** at  $[2] = 0$  nM (●), 30 nM (●), 60 nM (●), and 90 nM (●). (b) Reciprocal plot of  $\gamma$ -secretase with TSA **17** at  $[17] = 0$  nM (●), 10 nM (●), 20 nM (●), and 30 nM (●).

### Cross-competition kinetic experiments

For cross-competition studies between two inhibitors, enzyme reactions were run as activity assays, where varying concentration of two inhibitors were titrated against each-other, keeping the concentrations of C100 ( $0.50 \mu\text{M}$ ) constant.<sup>10, 11</sup> Reciprocal plots were generated, and data were fit using KaleidaGraph (Synergy Software). Inhibitor cross-competition data was fit into the following equation:

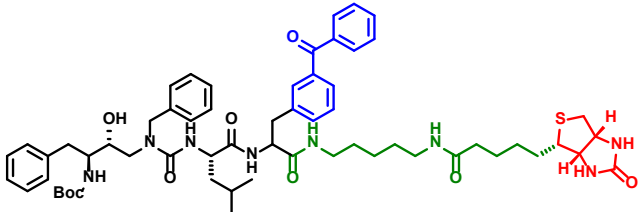
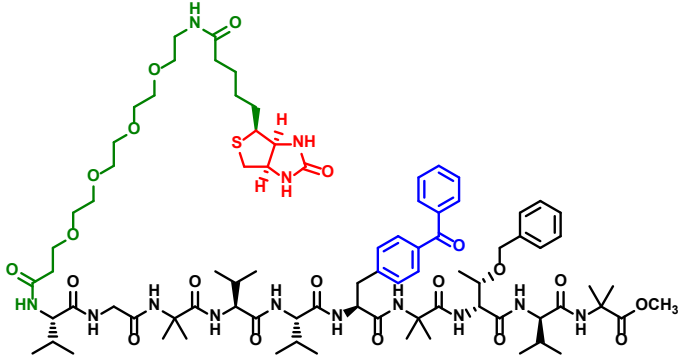
$$\frac{1}{v_{ij}} = 1/v_0 \left( 1 + \frac{[I]}{K_i} + \frac{[J]}{K_j} + \frac{[I][J]}{\alpha K_i K_j} \right)$$

where,  $v_{ij}$  and  $v_0$  are the initial rate in the presence and absence of inhibitors,  $K_i$  and  $K_j$  are the dissociation constants for inhibitors  $I$  and  $J$ , respectively and  $\alpha$  is the constant defining the interaction between the two inhibitors  $I$  and  $J$ .

## Photoaffinity labeling experiments

Enzyme (2 nM) in standard assay buffer was incubated at 37 °C for 30 min before addition of 1 μM **TSA-BPa-Bt** or **HPI-BPa-Bt** biotinylated photoaffinity probe (structures and IC<sub>50</sub>s below) with or without 10 μM inhibitor. The reaction was incubated for 1.5 h at 37 °C, and irradiated at 320 nm for 30 min on ice (Rayonet Photochemical Reactor). Biotin-bound γ-secretase was pulled down using streptavidin beads (Sigma), washed 6 times with standard assay buffer, eluted from the beads with SDS loading buffer, and heated to 70 °C for 10 min. Presenilin N-terminal fragment (NTF) was detected by western blot using rat anti-presenilin-1 monoclonal antibody (Millipore).

**Table S5:** Inhibition of gamma-secretase by photoprobes

Photoprobe	Structure	IC <sub>50</sub> (nM)
<b>TSA-Bpa-Bt</b>		313 ± 68
<b>HPI-Bpa-Bt</b>		107 ± 17

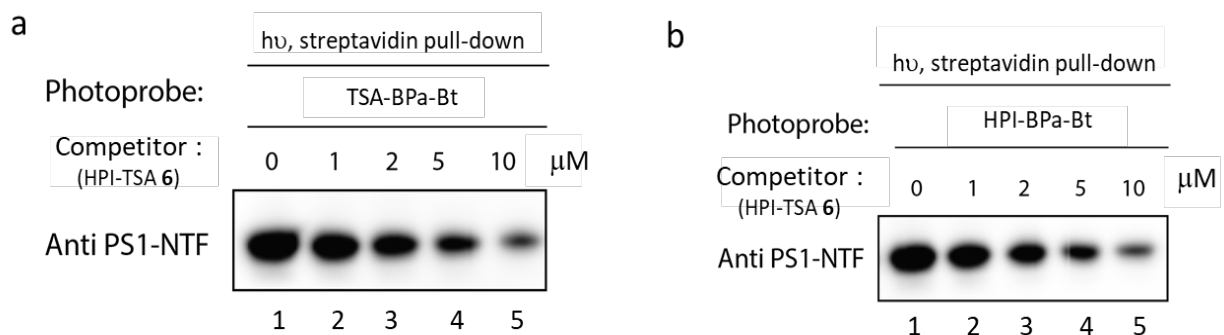


**Figure S8:** Dose response for HPI-TSA 6 against photoprobe TSA-Bpa-Bt (a) and HPI-Bpa-Bt (b).

## NMR Data Acquisition, Analysis and Structure Calculation of 6

All NMR data was acquired using a Bruker AVANCE 800 MHz NMR spectrometer equipped with a triple-resonance inverse cryoprobe. Sample temperature was set to approximately 5° C. NMR data was processed using NMRPipe<sup>12</sup> and analyzed using CCPN Analysis<sup>13</sup> on NMRBox.<sup>14</sup> Backbone and sidechain resonance assignments were completed using 2D <sup>1</sup>H-<sup>1</sup>H COSY, TOCSY and ROESY collected using the Bruker standard pulse programs and parameter sets. ROE assignments were performed iteratively with structure calculation.

NMR structure calculation was performed using Xplor-NIH.<sup>15</sup> A summary of the experimentally-derived restraints input used for the final structure are included in **Table S6**. The force field for the non-standard moieties (e.g. the alkyl linker and the TSA) were generated using the PRODRG2 server<sup>16</sup> and patched into the standard protein parameter and topology files. 200 total structures were calculated using modified versions of the scripts “fold.py” and “refine.py”.<sup>17</sup> Statistics for the 10 lowest energy structures are included in **Table S6**.

**Table S6. Statistics for the 10 lowest-energy structures**

<b>Experimental Restraints</b>		
	NOEs total	152
	Intraresidue NOEs	88
	Sequential NOEs	38
	Medium range NOEs	26
	Dihedrals	17
<b>Structure Results</b>		
	NOE violations > 0.5 Å	0
	Dihedral violations > 5°	0
	Bond length RMS	0.003 ± 0.000 Å
	Bond angle RMS	0.573 ± 0.007°
	Improper angle RMS	0.452 ± 0.041°
	NOE RMS	0.052 ± 0.005 Å
	Dihedral RMS	0.544 ± 0.352°
	Xplor-NIH total energy	270 ± 15 kcal
	Xplor-NIH NOE energy	12 ± 2 kcal
	Xplor-NIH Dihedral energy	0.45 ± 0.42 kcal

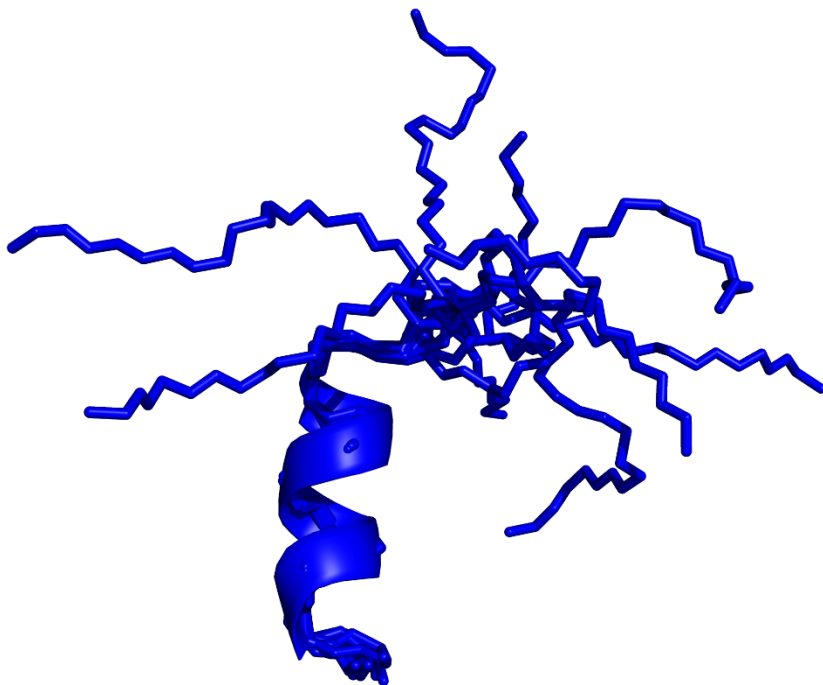


**Figure S9:** Summary of 10 lowest energy structures.

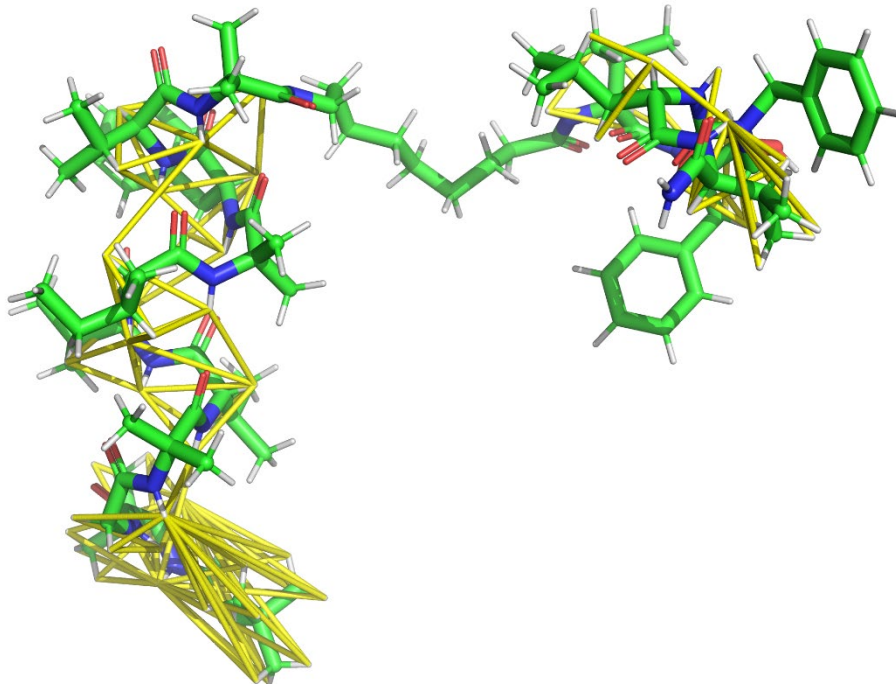


**Figure S10:** Summary of restrains on structure.

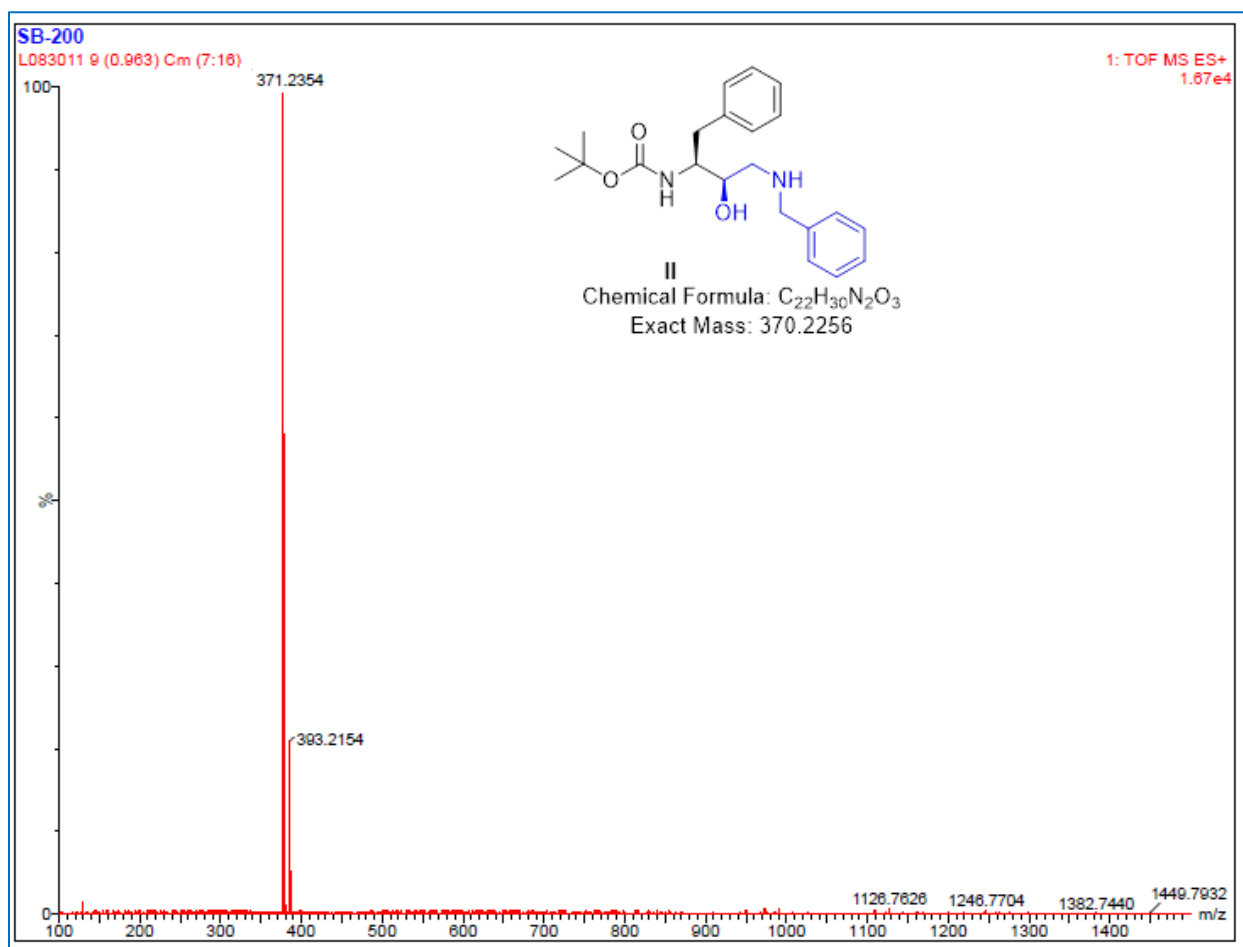


**Figure S11:** Section of HRMS (ESI):  $m/z$   $[M + H]^+$  spectra for the intermediate **II**. calcd for  $C_{22}H_{30}N_2O_3$ : 371.2336; found: 371.2354.



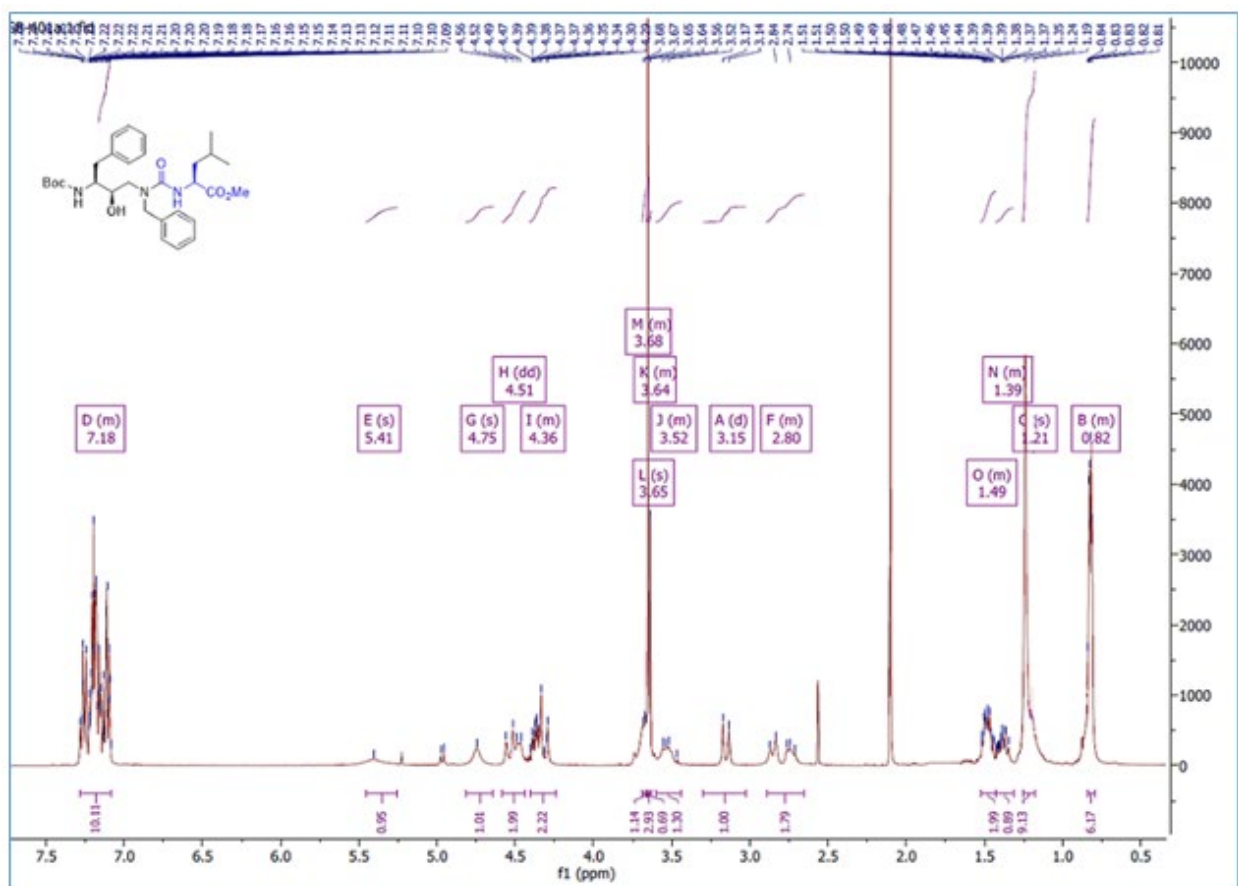


Figure S12: Section of the  $^1\text{H}$  NMR spectra (400 MHz,  $\text{CDCl}_3$ ) for the intermediate IIIa.

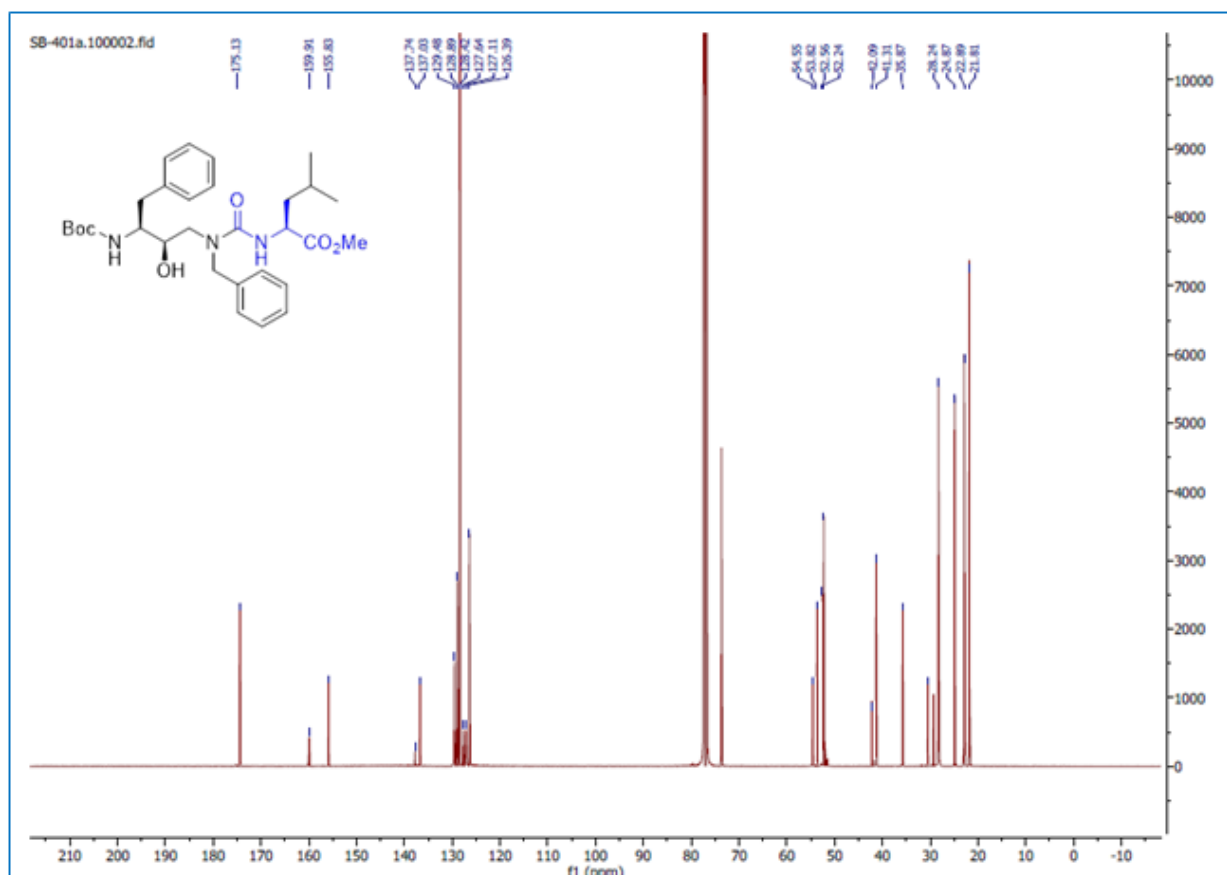
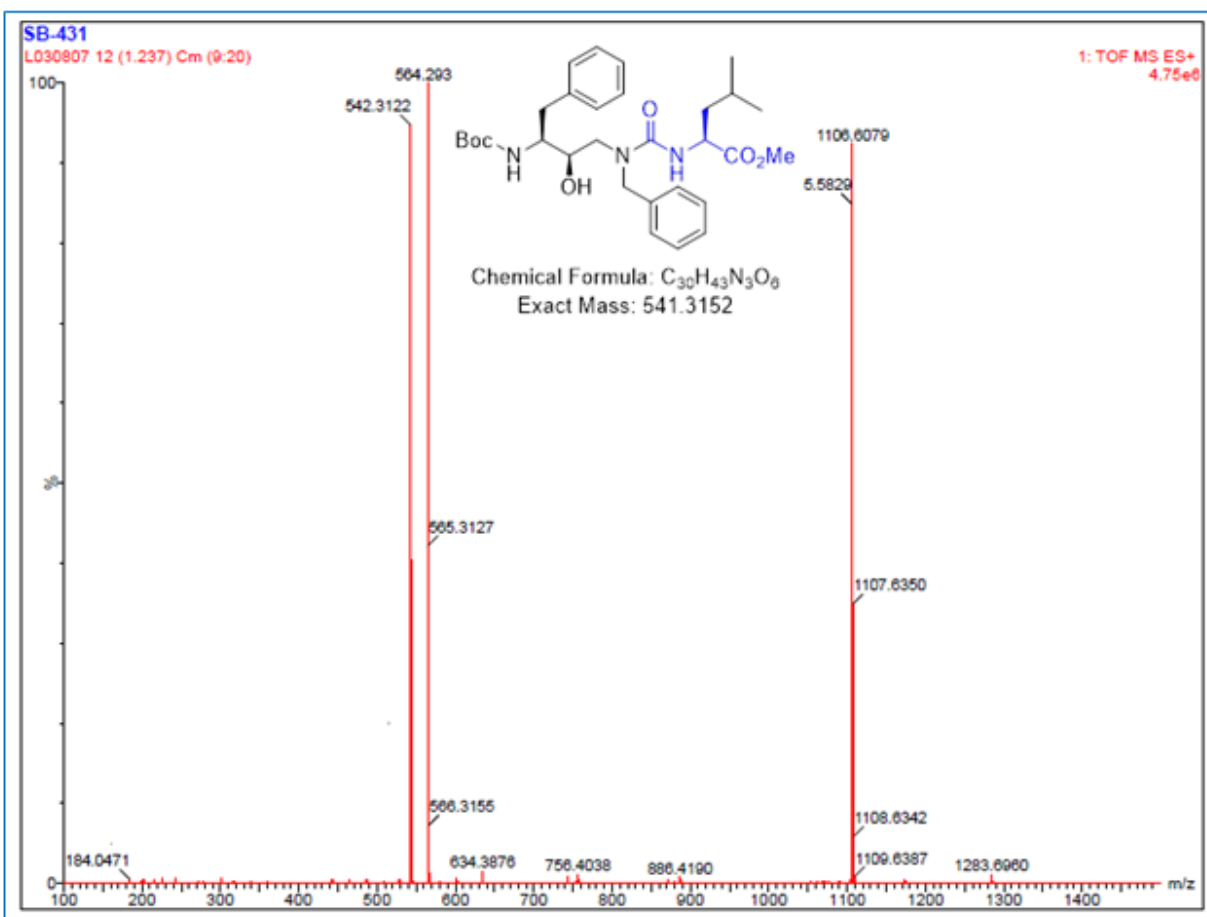
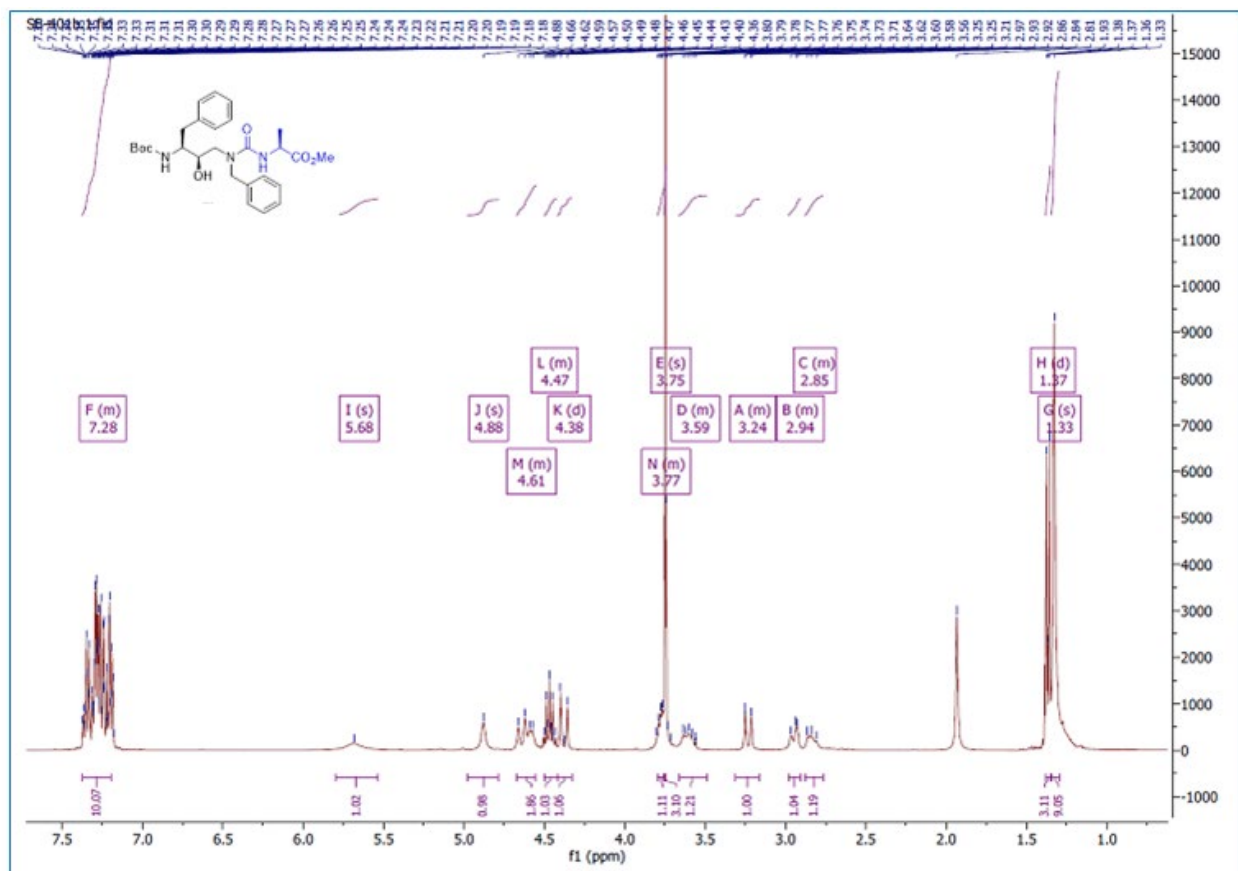


Figure S13: Section of the  $^{13}\text{C}$  NMR spectra (126 MHz,  $\text{CDCl}_3$ ) for the intermediate **IIIa**.



**Figure S14:** Section of HRMS (ESI):  $m/z$   $[M + H]^+$  spectra for the intermediate **IIIa**. calcd for  $C_{30}H_{43}N_3O_6$ : 542.3232; found: 542.3122.



**Figure S15:** Section of the  $^1\text{H}$  NMR spectra (400 MHz,  $\text{CDCl}_3$ ) for the intermediate **IIIb**.

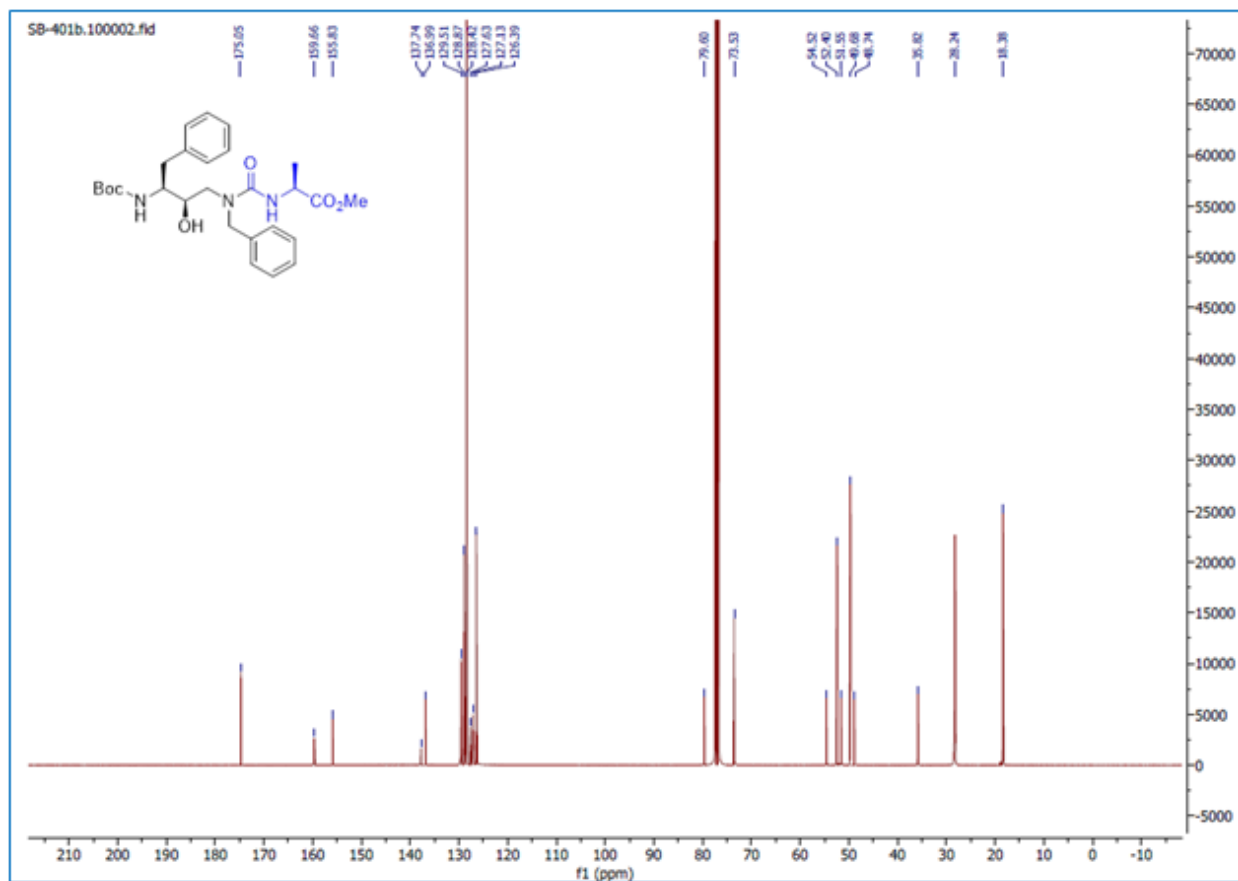


**Figure S16:** Section of the  $^{13}\text{C}$  NMR spectra (126 MHz,  $\text{CDCl}_3$ ) for the intermediate **IIIb**.

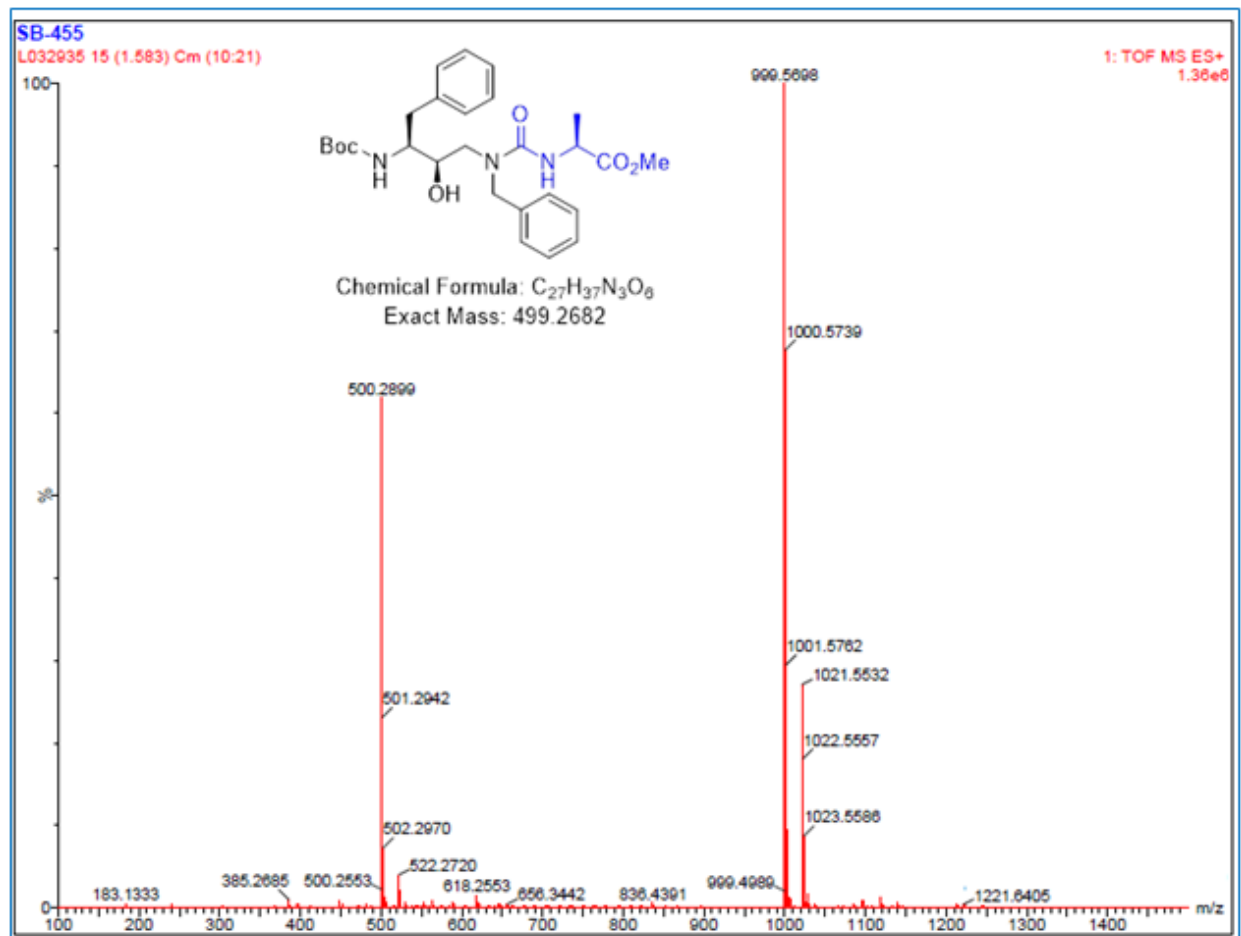


**Figure S17:** Section of HRMS (ESI):  $m/z$   $[M + H]^+$  spectra for the intermediate **IIIb**. calcd for  $C_{27}H_{37}N_3O_6$ : 500.2762; found: 500.2899.

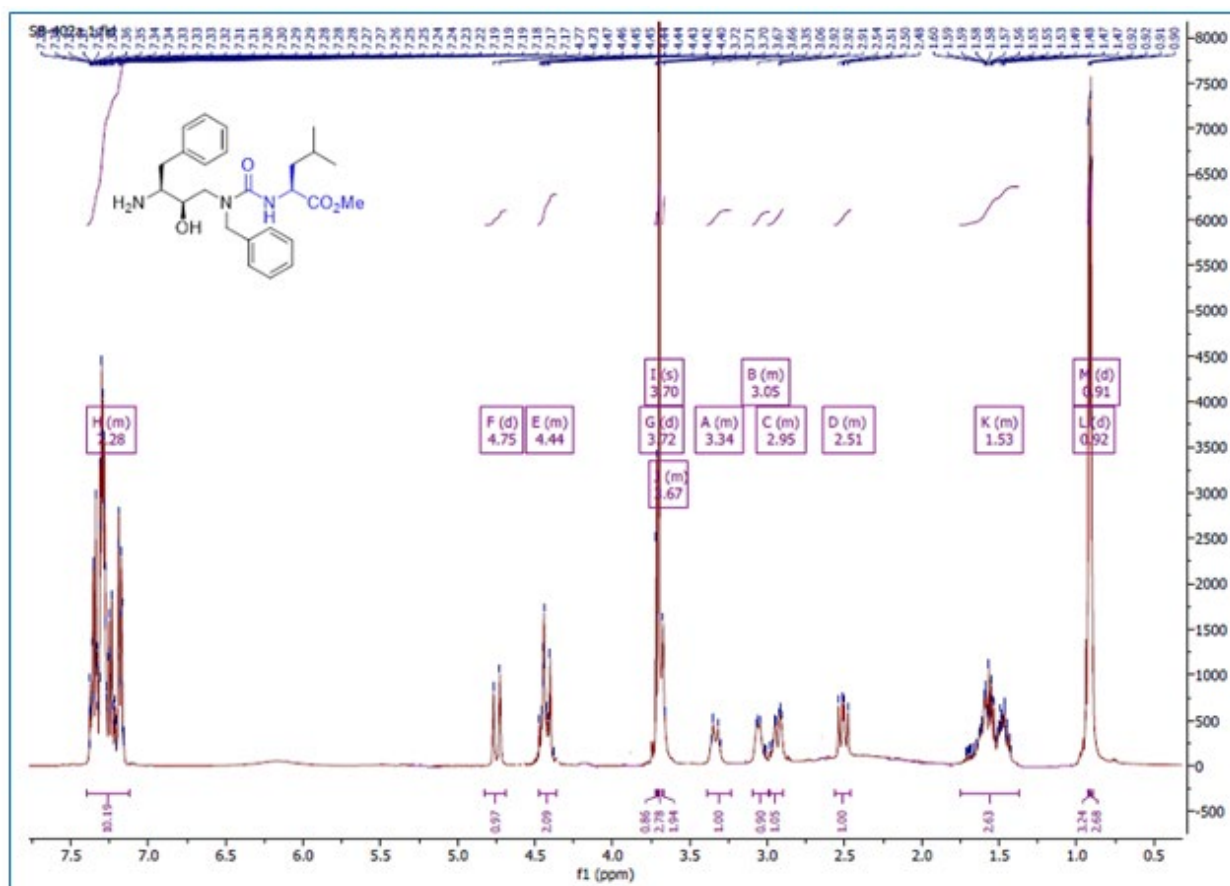
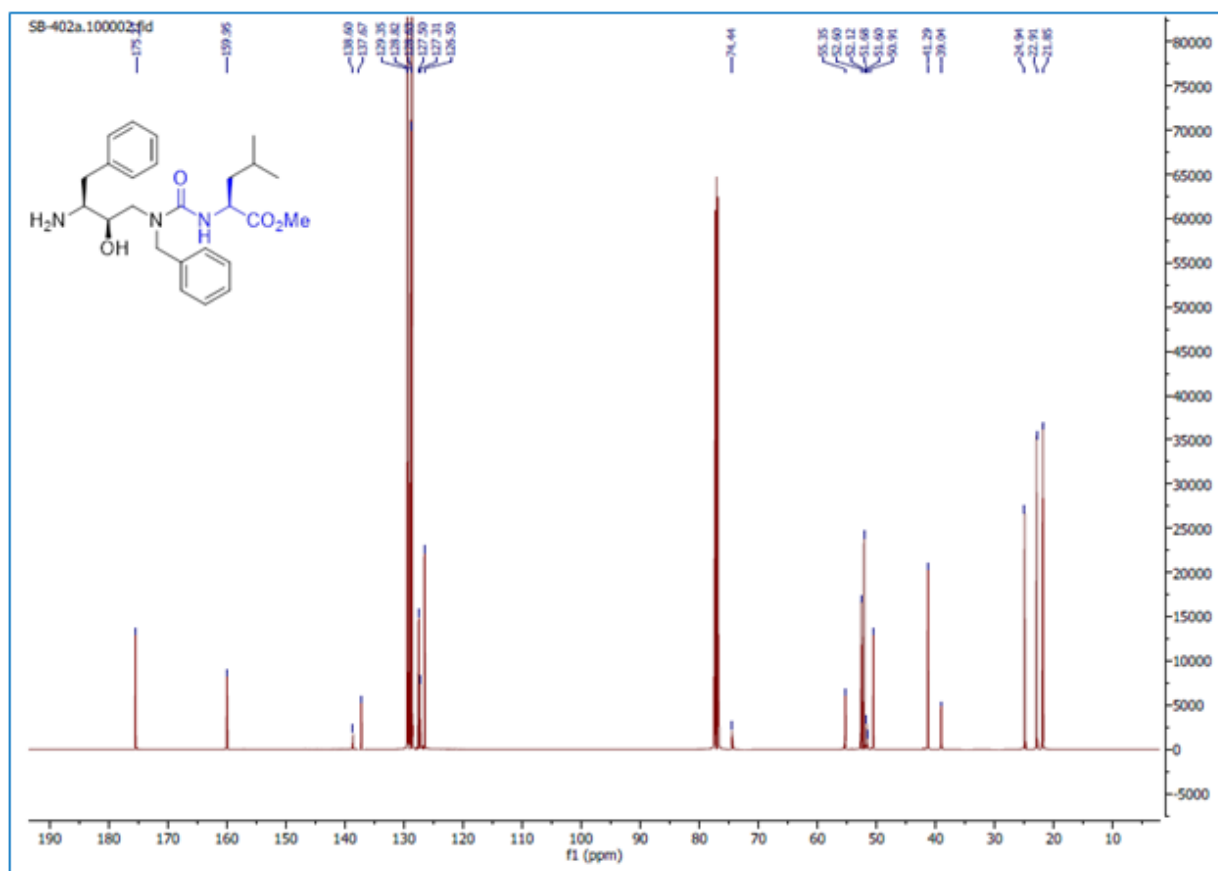
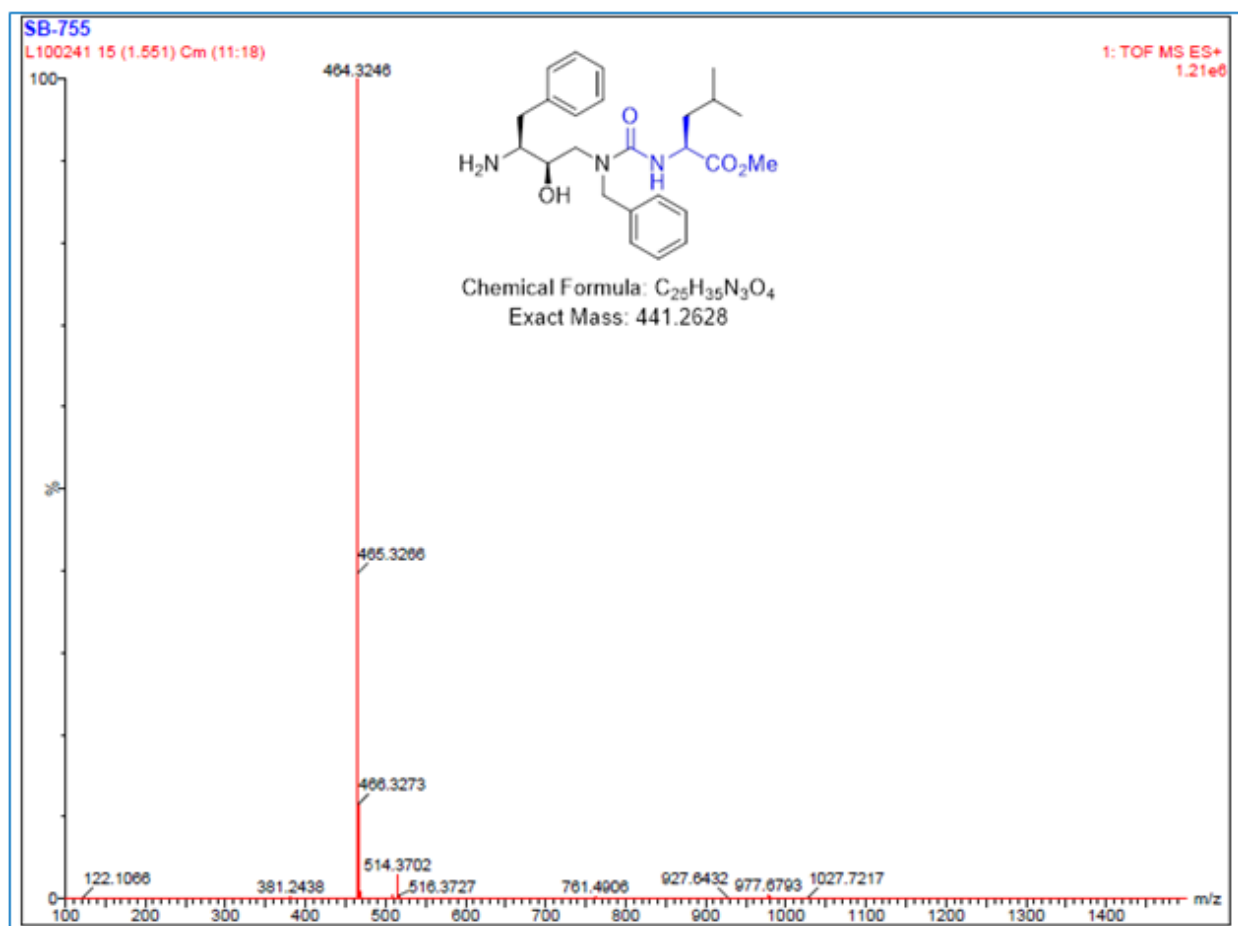


Figure S18: Section of the  $^1\text{H}$  NMR spectra (400 MHz,  $\text{CDCl}_3$ ) for the intermediate IVa.



**Figure S19:** Section of the  $^{13}\text{C}$  NMR spectra (126 MHz,  $\text{CDCl}_3$ ) for the intermediate IVa.





**Figure S20:** Section of HRMS (ESI):  $m/z$   $[M + Na]^+$  spectra for the intermediate **IVa**. calcd for  $C_{25}H_{35}N_3O_4Na$ : 464.2526; found: 464.3246.

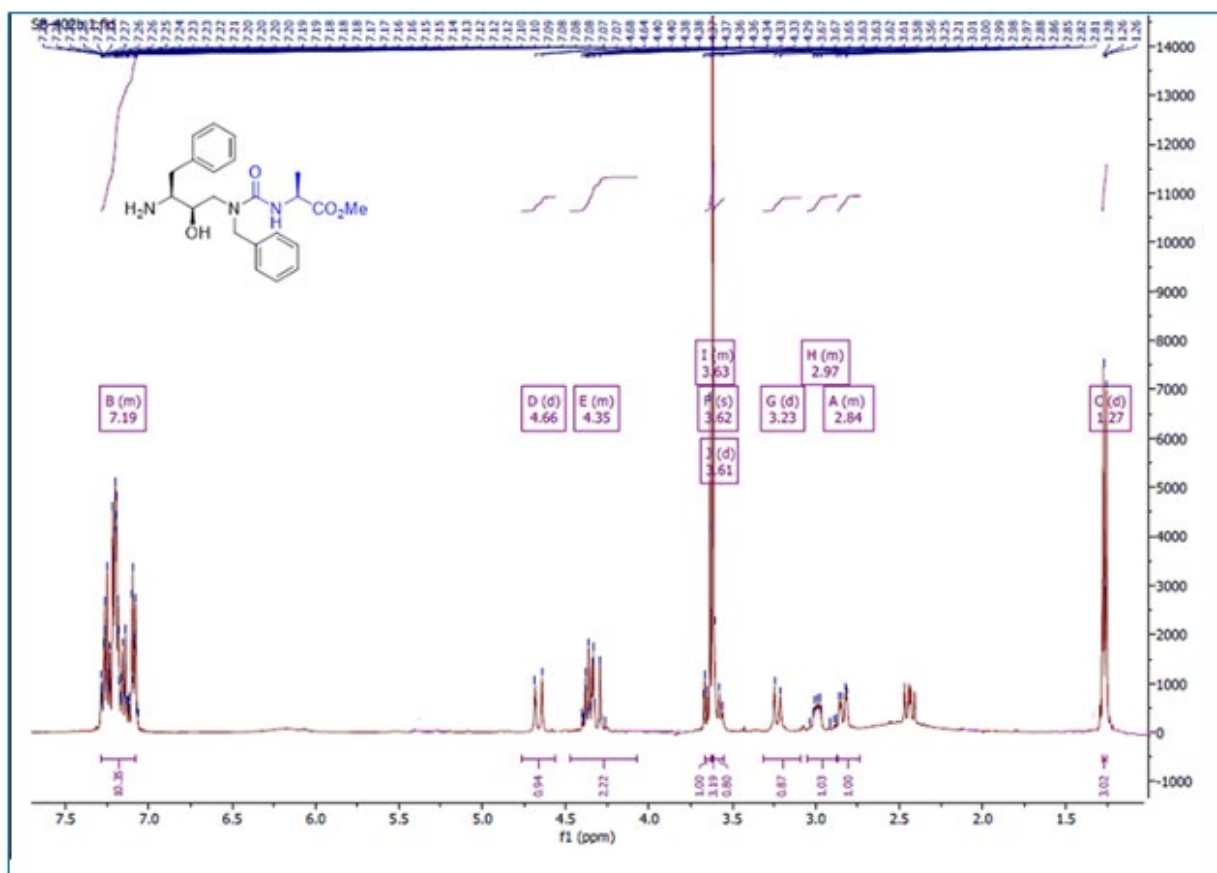
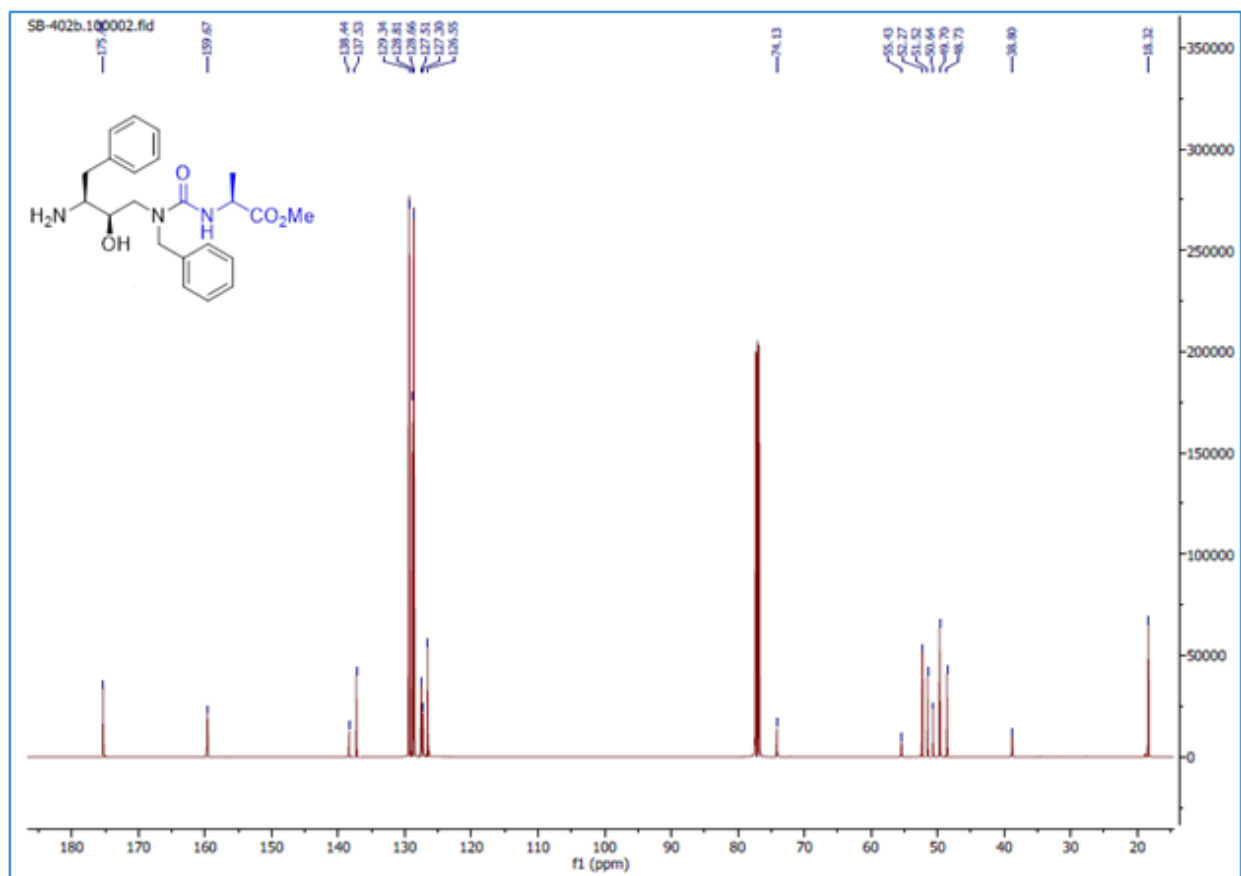
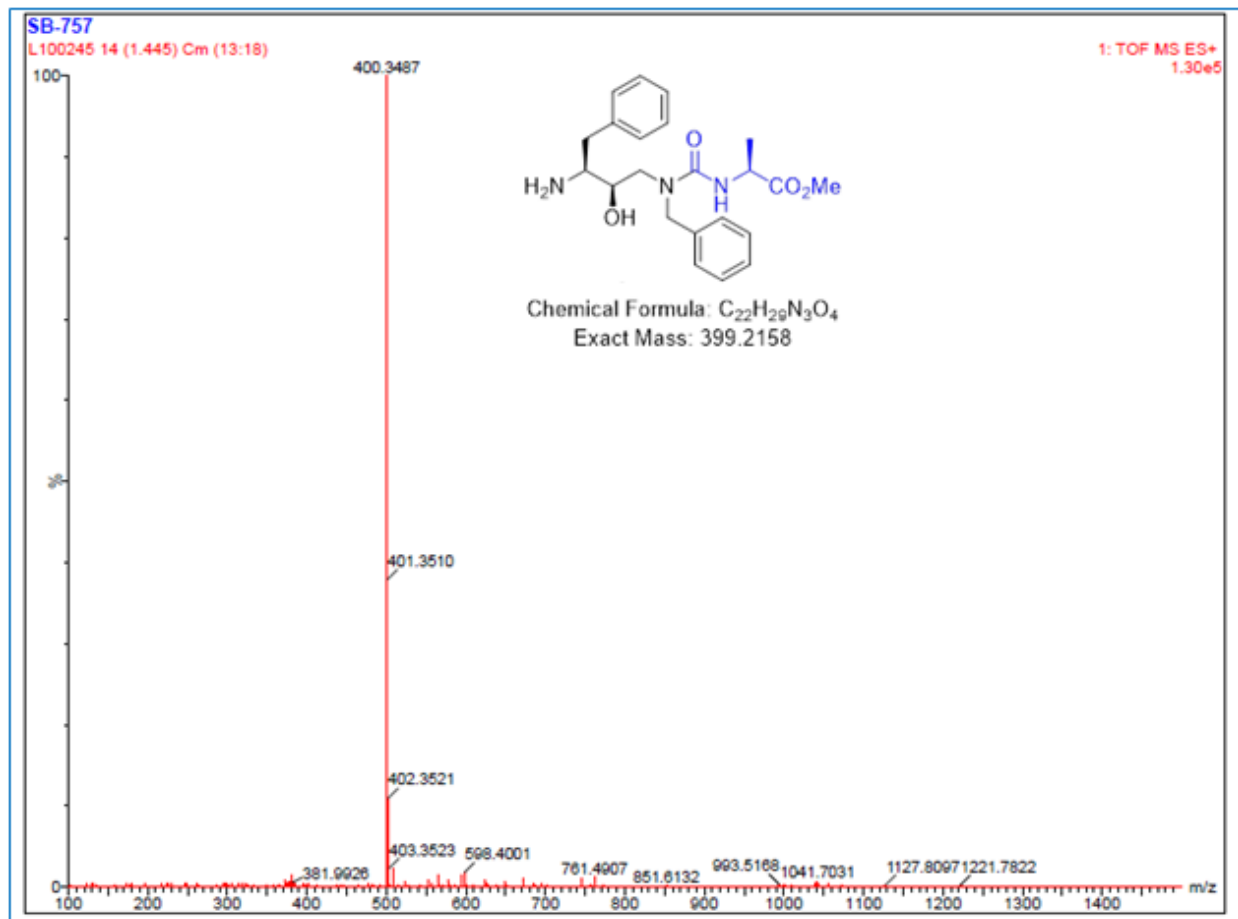


Figure S21: Section of the  $^1\text{H}$  NMR spectra (400 MHz,  $\text{CDCl}_3$ ) for the intermediate IVb.



**Figure S22:** Section of the  $^{13}\text{C}$  NMR spectra (126 MHz,  $\text{CDCl}_3$ ) for the intermediate IVb.



**Figure S23:** Section of HRMS (ESI):  $m/z$   $[M + Na]^+$  spectra for the intermediate **IVb**. calcd for C<sub>22</sub>H<sub>29</sub>N<sub>3</sub>O<sub>4</sub>: 400.2238; found: 400.3487.

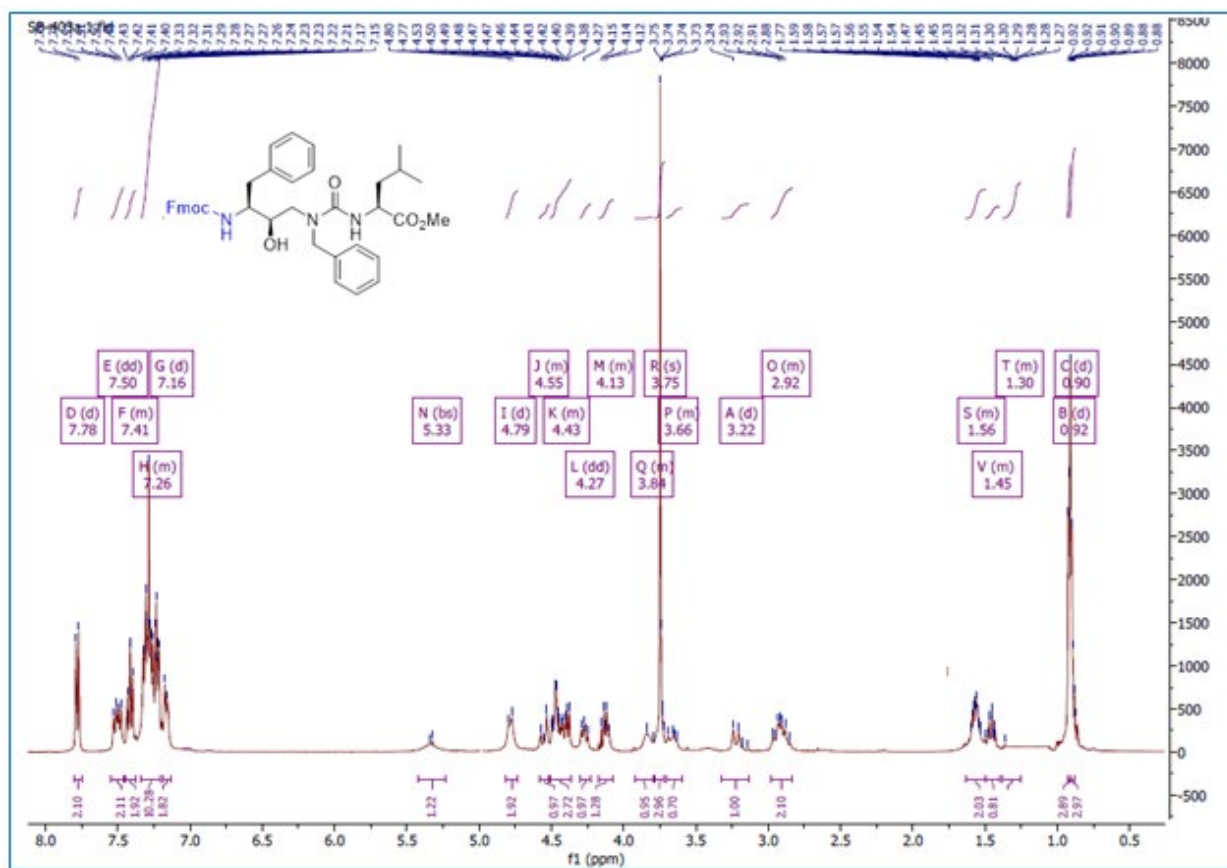


**Figure S24:** Section of the <sup>1</sup>H NMR spectra (400 MHz, CDCl<sub>3</sub>) for the intermediate **Va**.

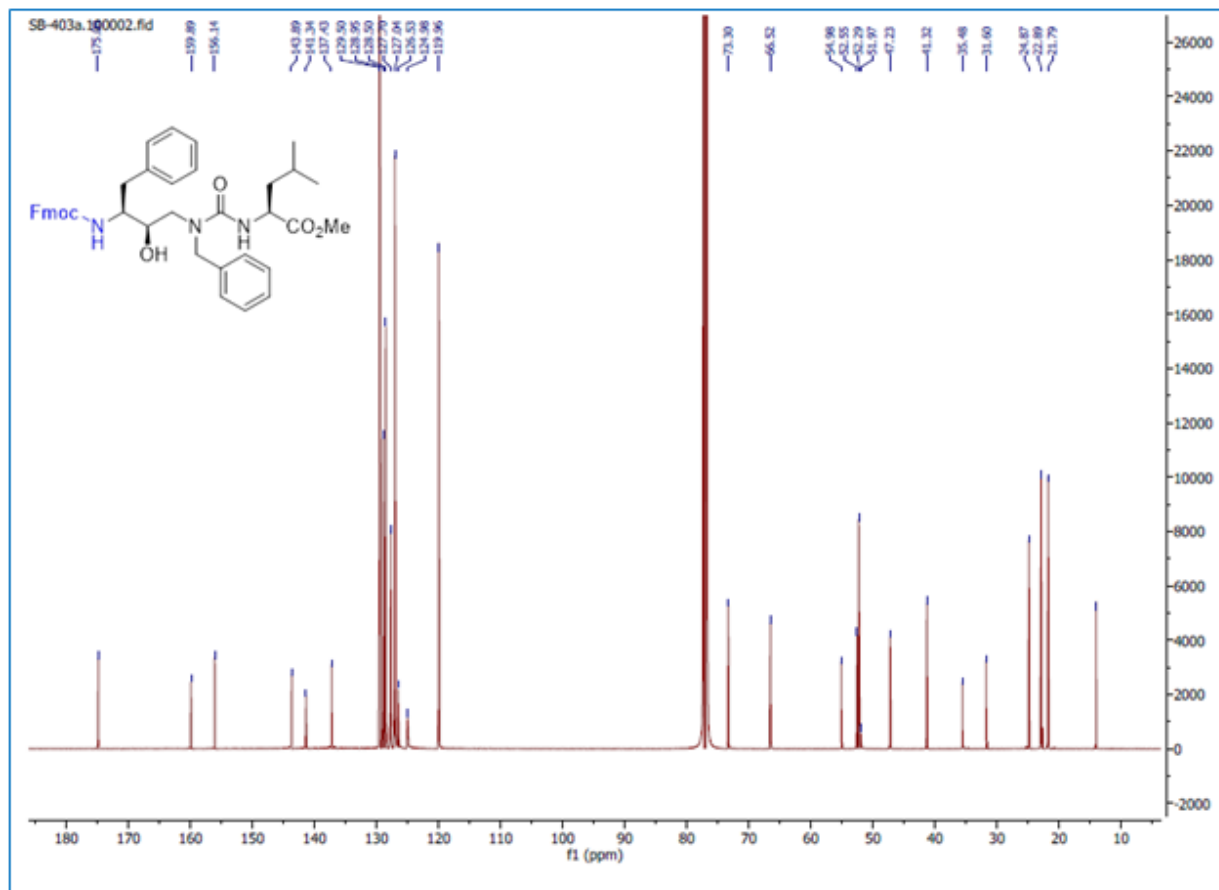


**Figure S25:** Section of the  $^{13}\text{C}$  NMR spectra (126 MHz,  $\text{CDCl}_3$ ) for the intermediate Va.

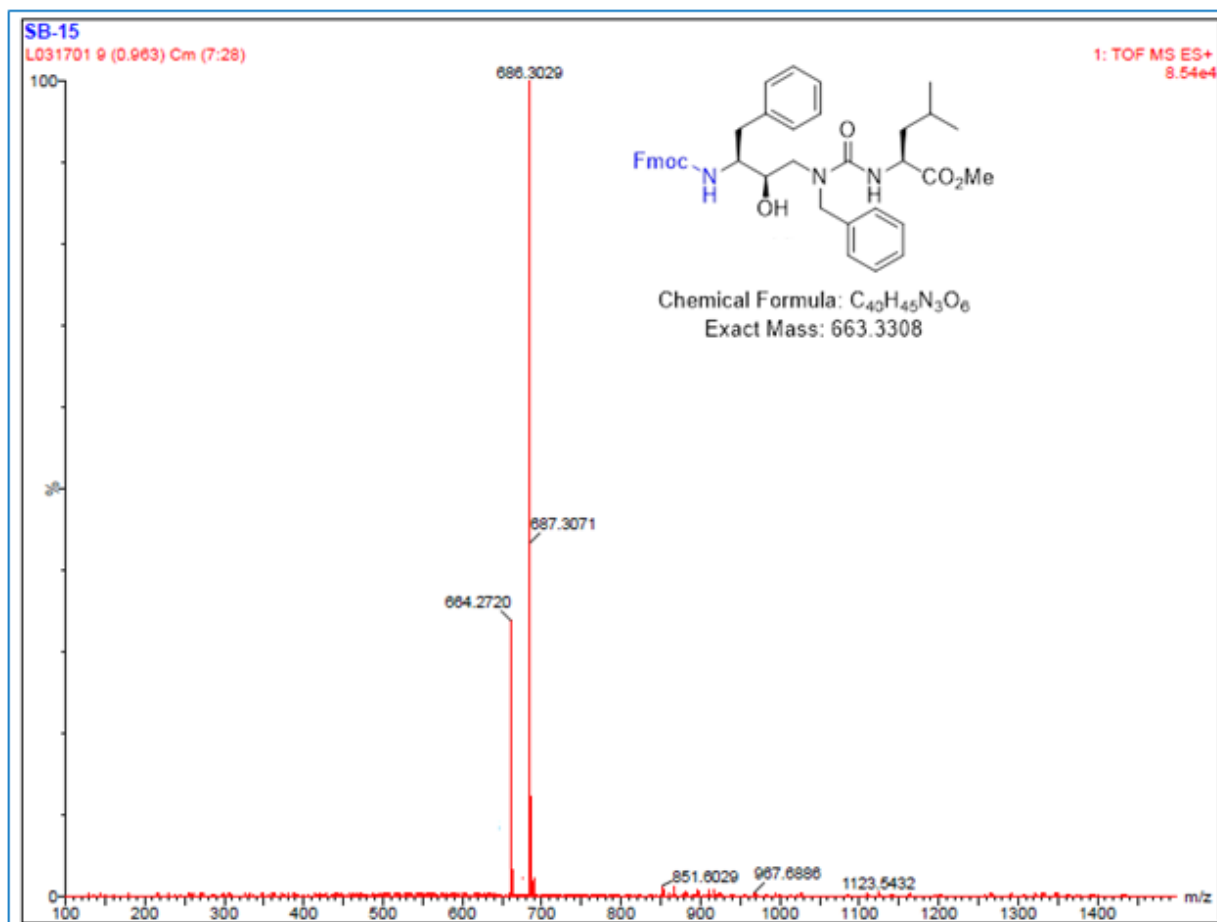


**Figure S26:** Section of HRMS (ESI):  $m/z$   $[M + H]^+$  spectra for the intermediate **Va**. calcd for C<sub>40</sub>H<sub>45</sub>N<sub>3</sub>O<sub>6</sub>: 664.3388; found: 664.2720.

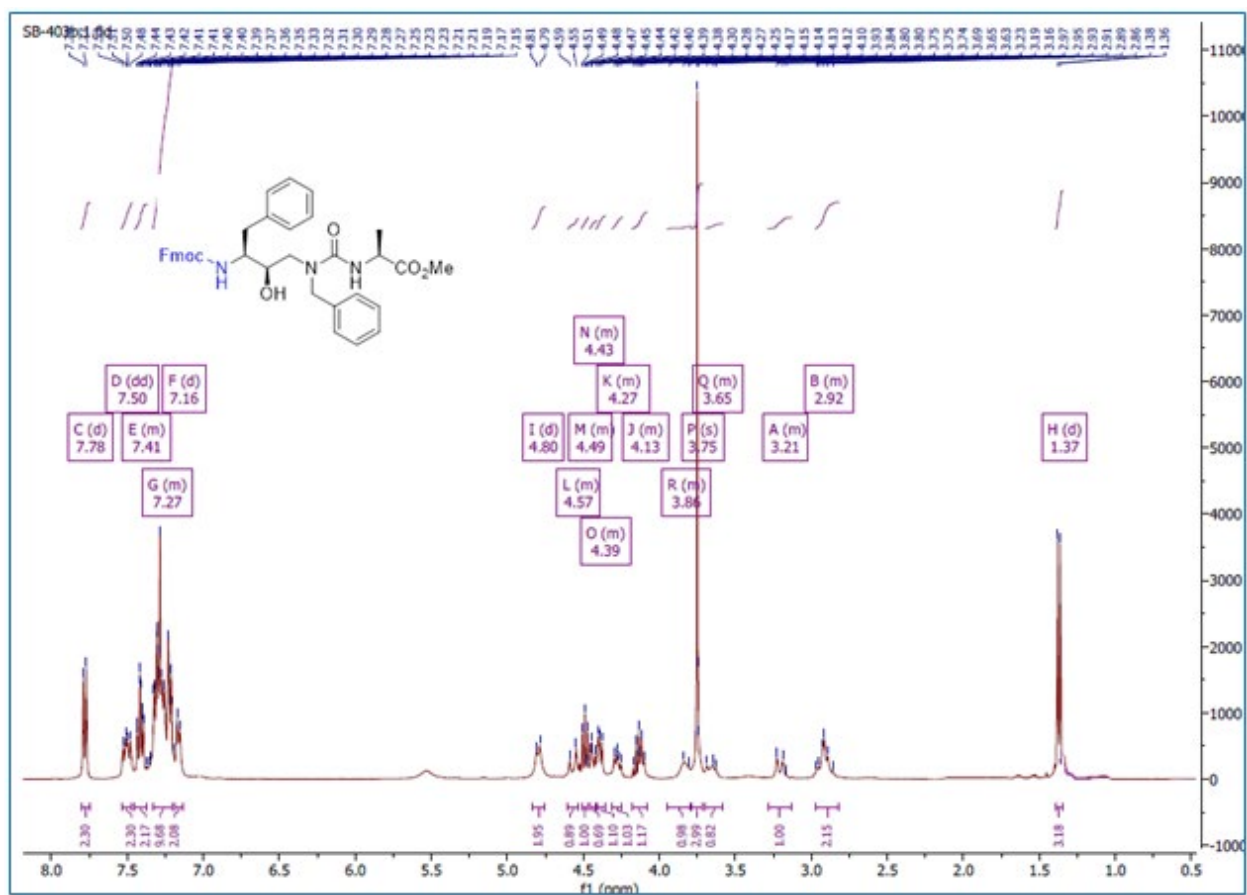


Figure S27: Section of the  $^1\text{H}$  NMR spectra (400 MHz,  $\text{CDCl}_3$ ) for the intermediate Vb.



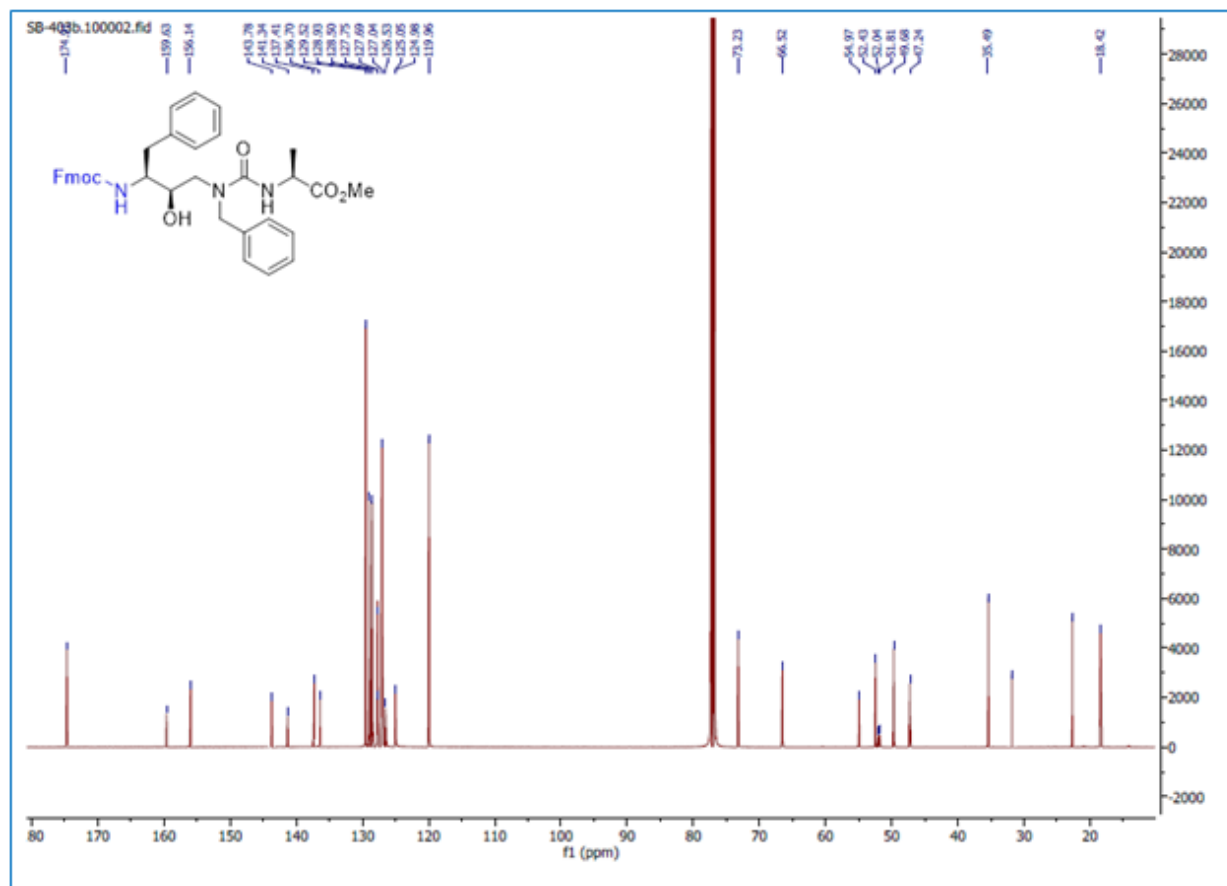
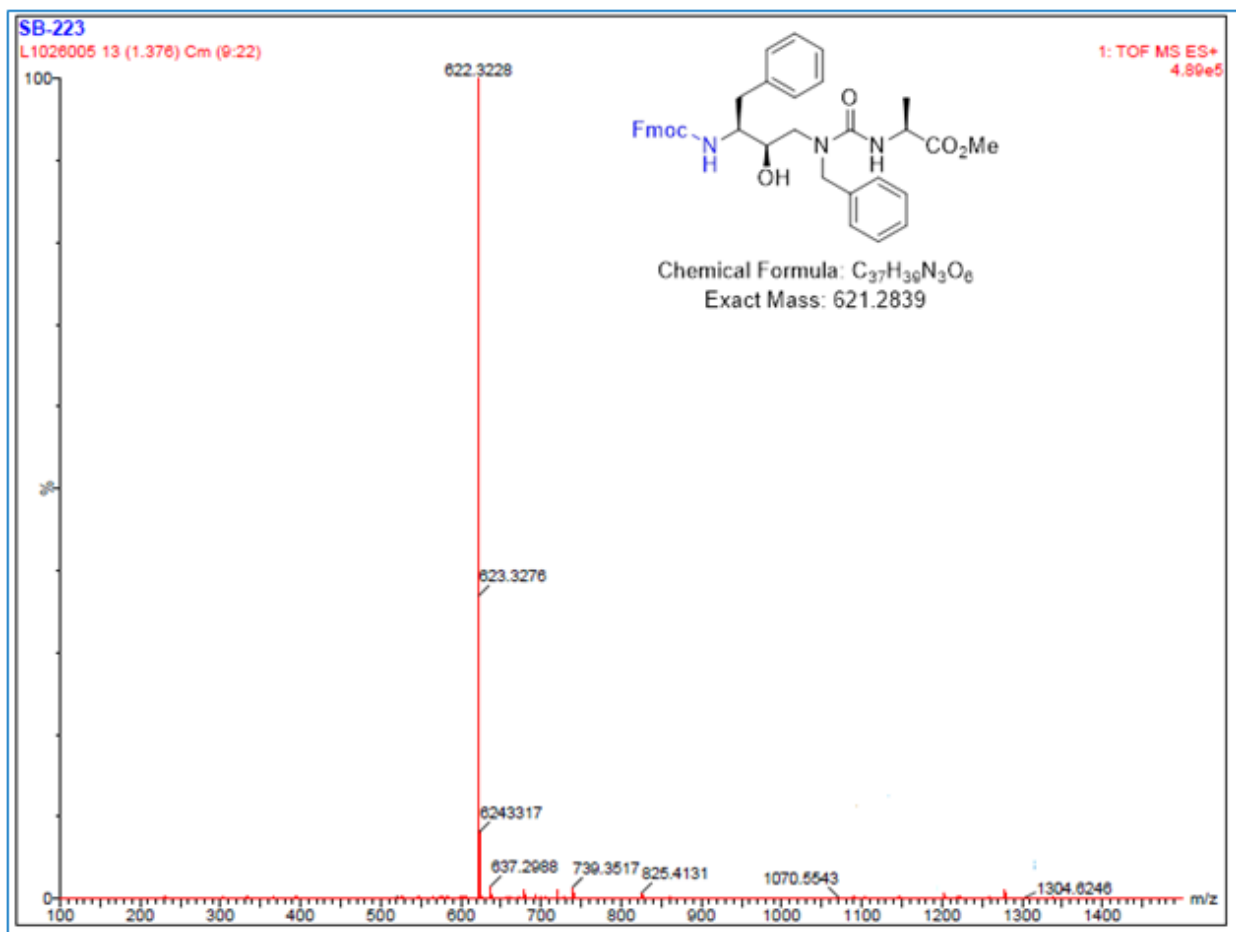


Figure S28: Section of the <sup>13</sup>C NMR spectra (126 MHz, CDCl<sub>3</sub>) for the intermediate Vb.



**Figure S29:** Section of HRMS (ESI):  $m/z$   $[M + H]^+$  spectra for the intermediate **Vb**. calcd for  $C_{37}H_{39}N_3O_6$ : 622.2919; found: 622.3228.



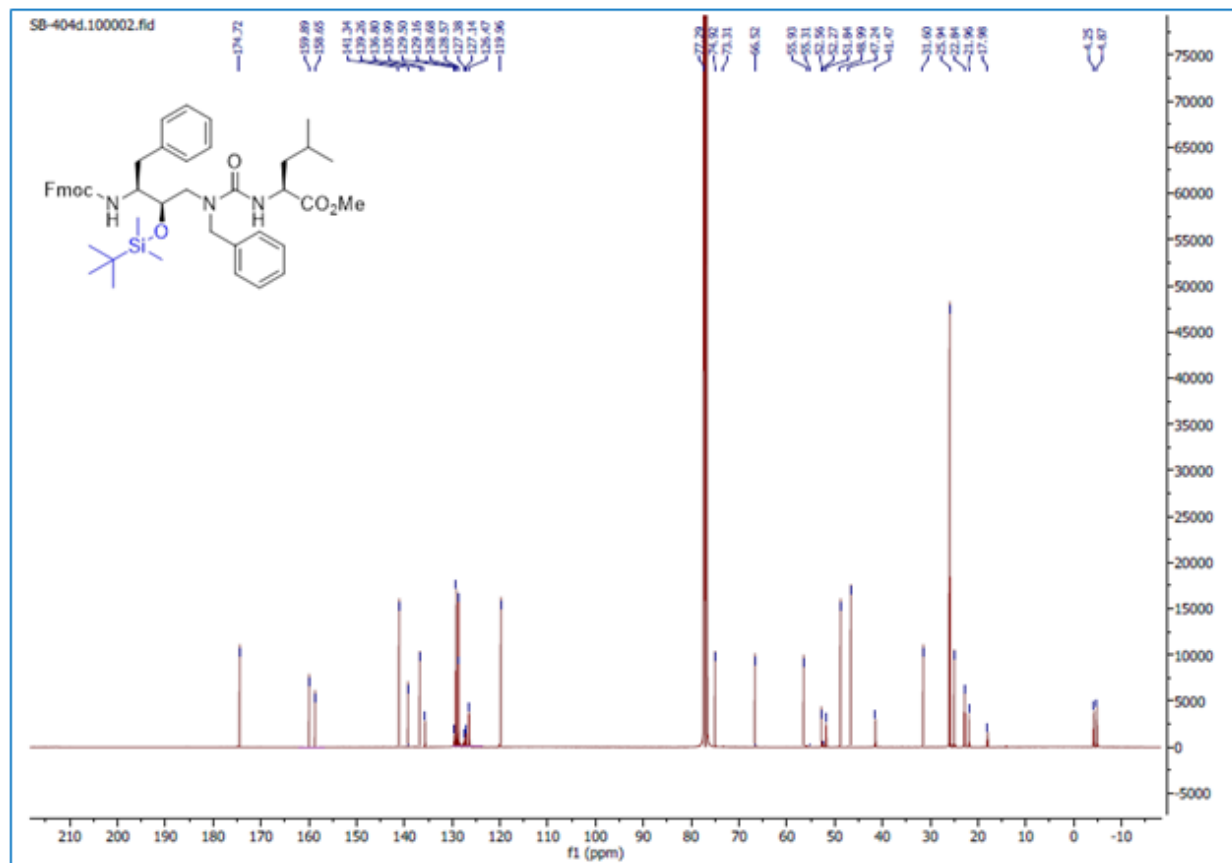
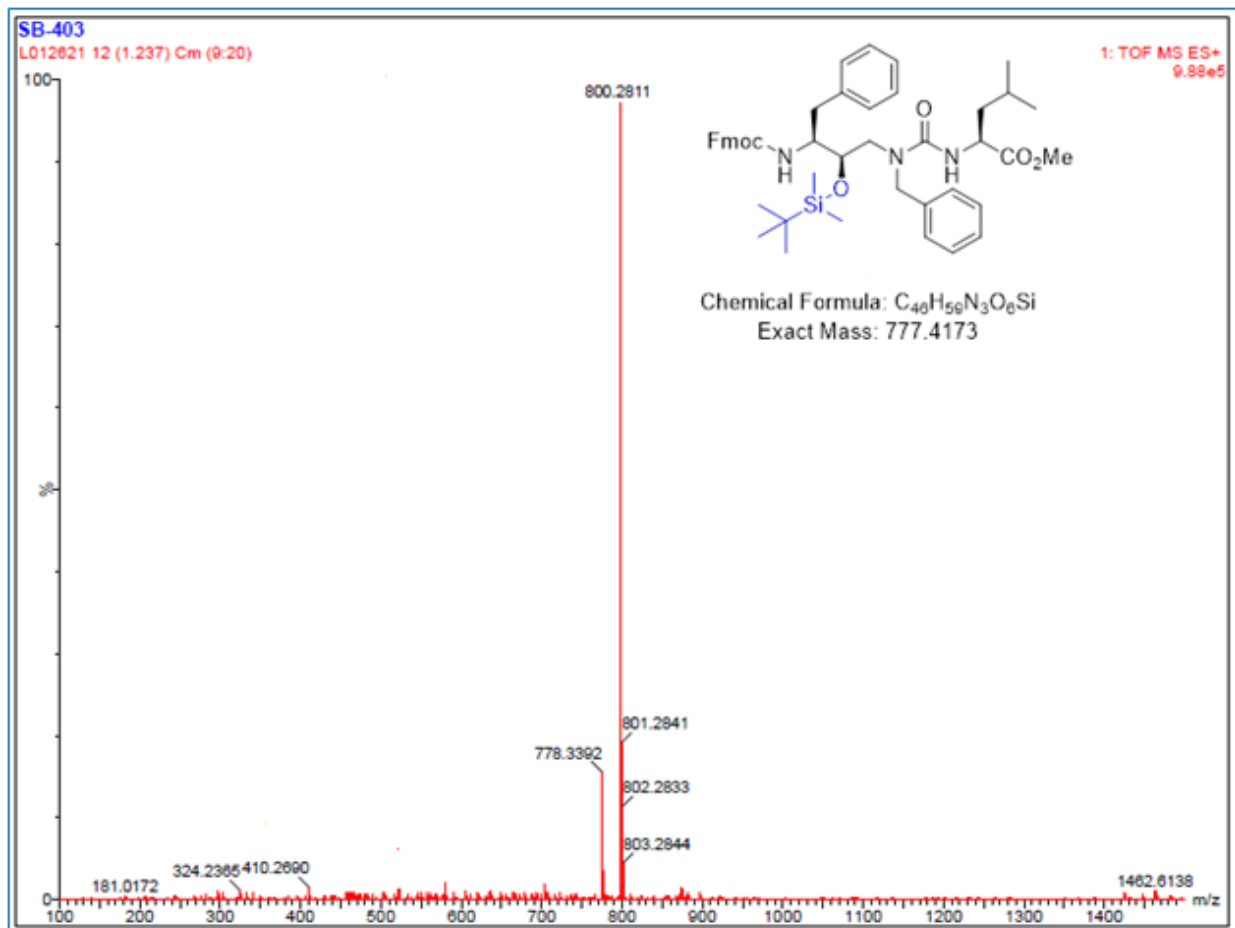


Figure S31: Section of the  $^{13}\text{C}$  NMR spectra (126 MHz,  $\text{CDCl}_3$ ) for the intermediate VIa.



**Figure S32:** Section of HRMS (ESI):  $m/z$   $[M + H]^+$  spectra for the intermediate **VIa**. calcd for  $C_{46}H_{59}N_3O_6Si$ : 778.4253; found: 778.3392.

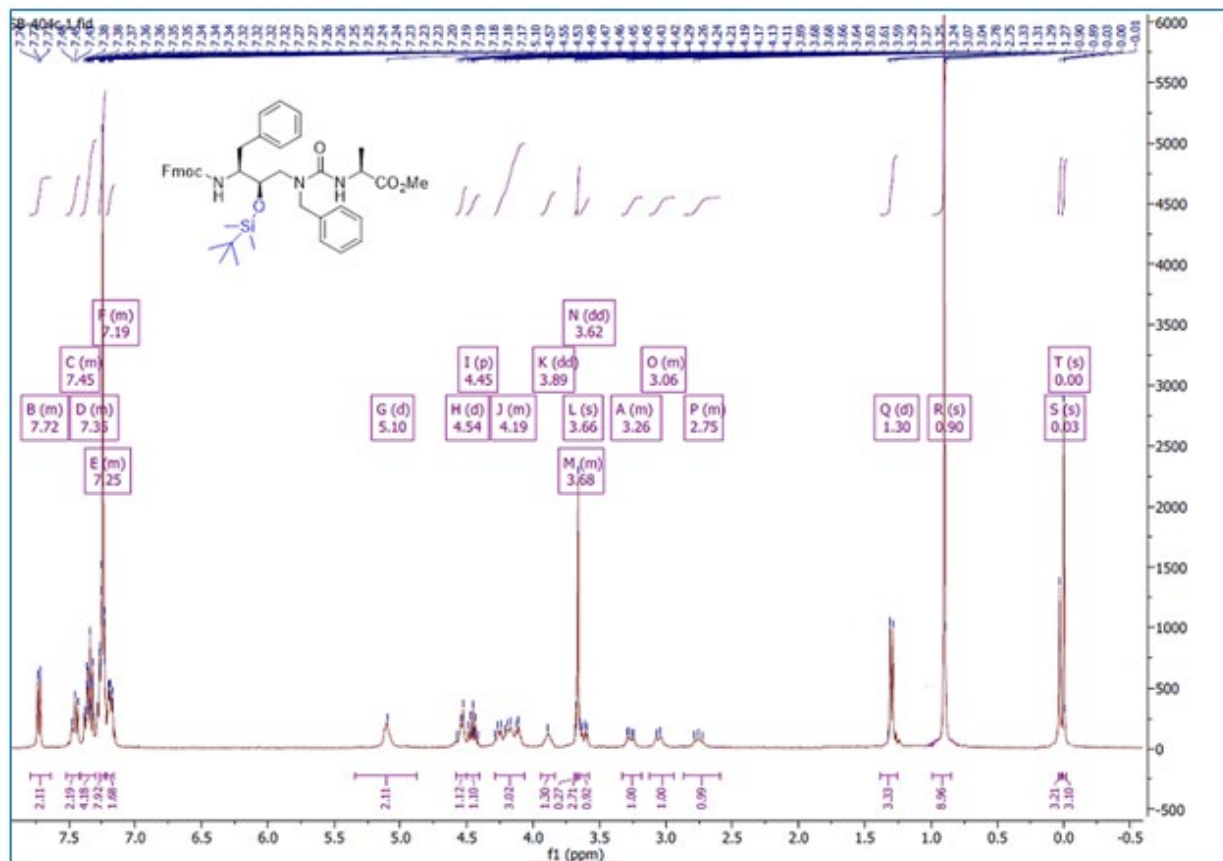
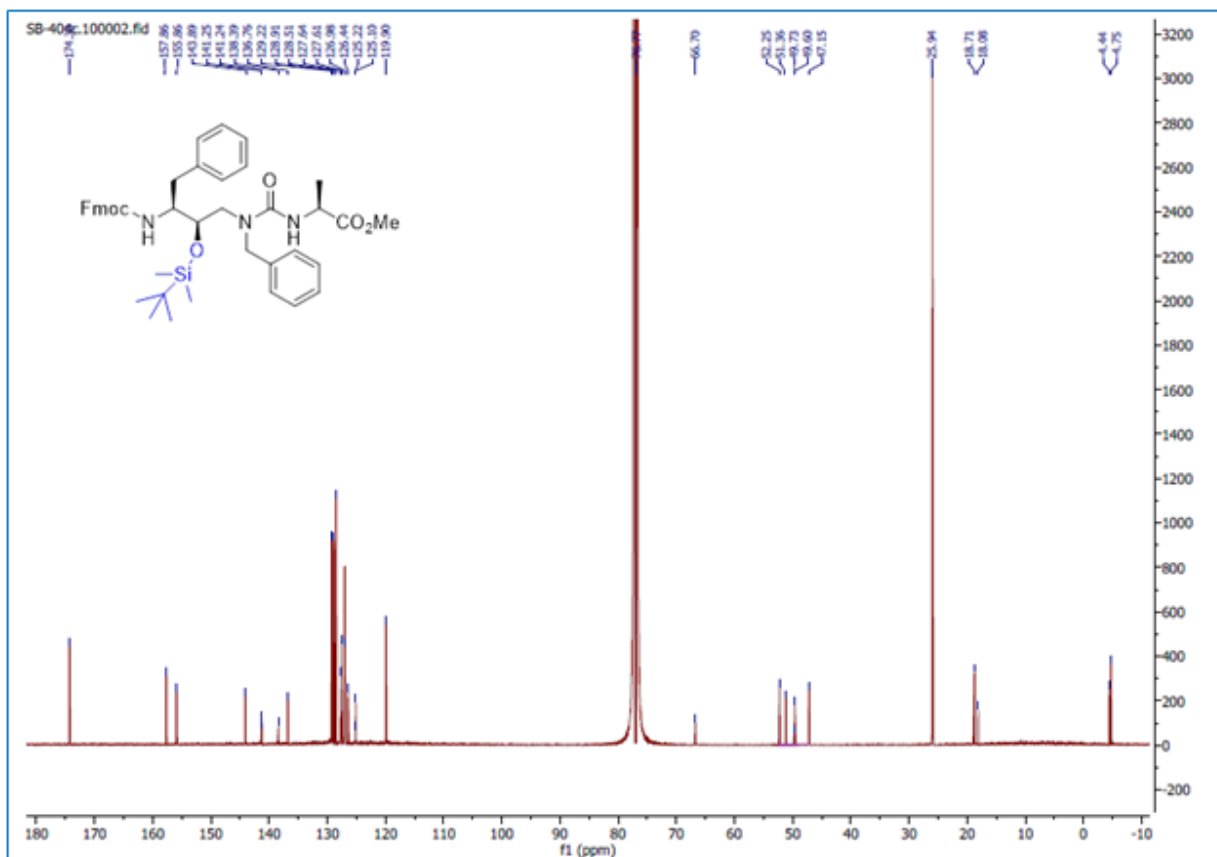
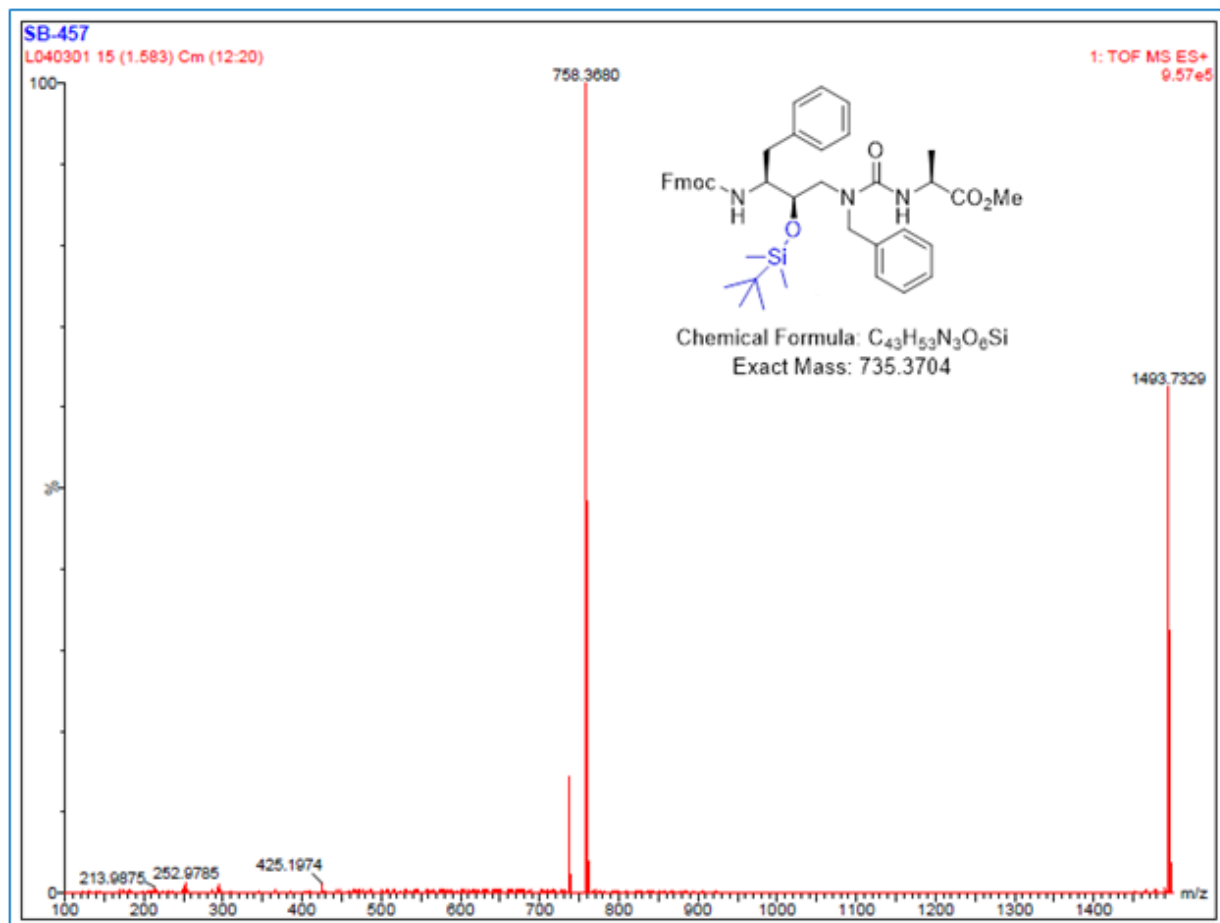


Figure S33: Section of the  $^1\text{H}$  NMR spectra (400 MHz,  $\text{CDCl}_3$ ) for the intermediate VIb.



**Figure S34:** Section of the  $^{13}\text{C}$  NMR spectra (126 MHz,  $\text{CDCl}_3$ ) for the intermediate **VIb**.



**Figure S35:** Section of HRMS (ESI):  $m/z$   $[M + Na]^+$  spectra for the intermediate **Vib**. calcd for  $C_{43}H_{53}N_3O_6SiNa$ : 758.3602; found: 758.3680.



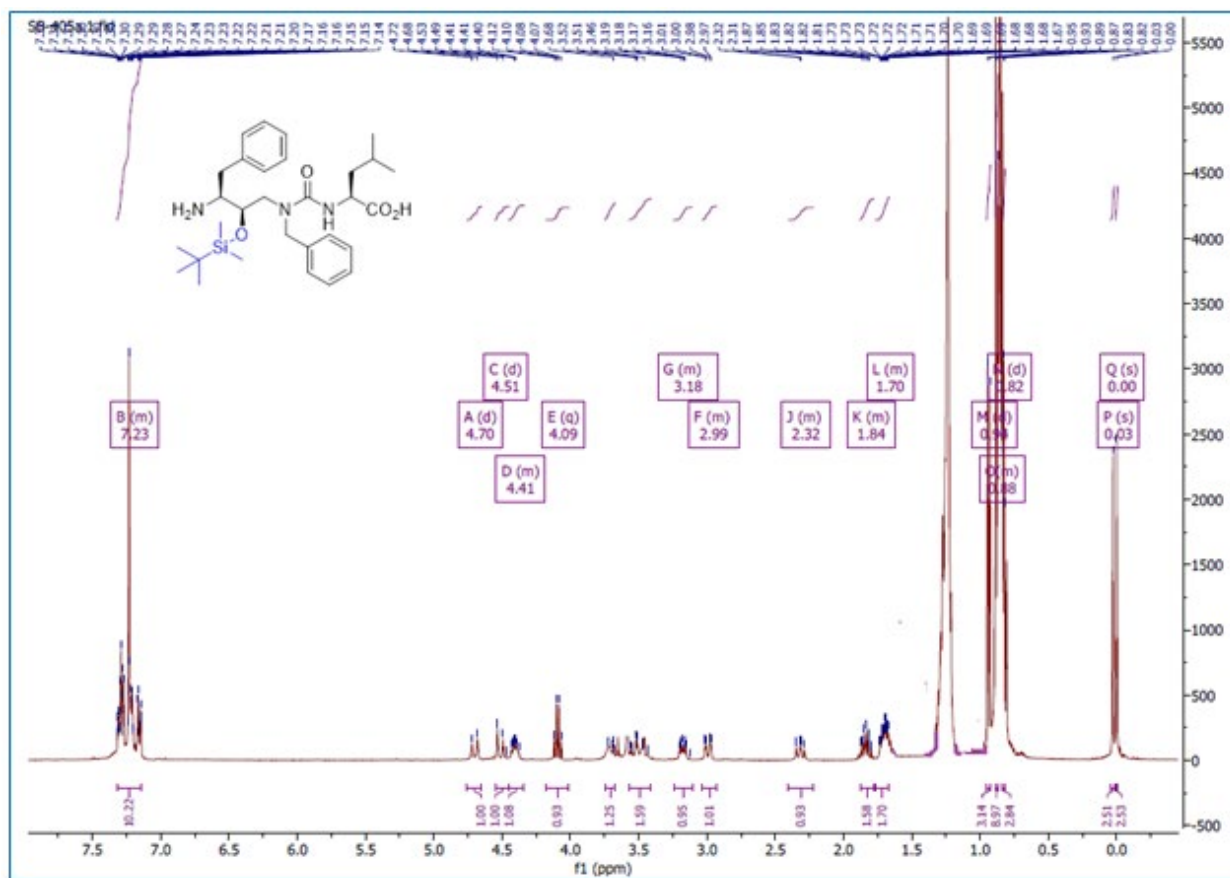
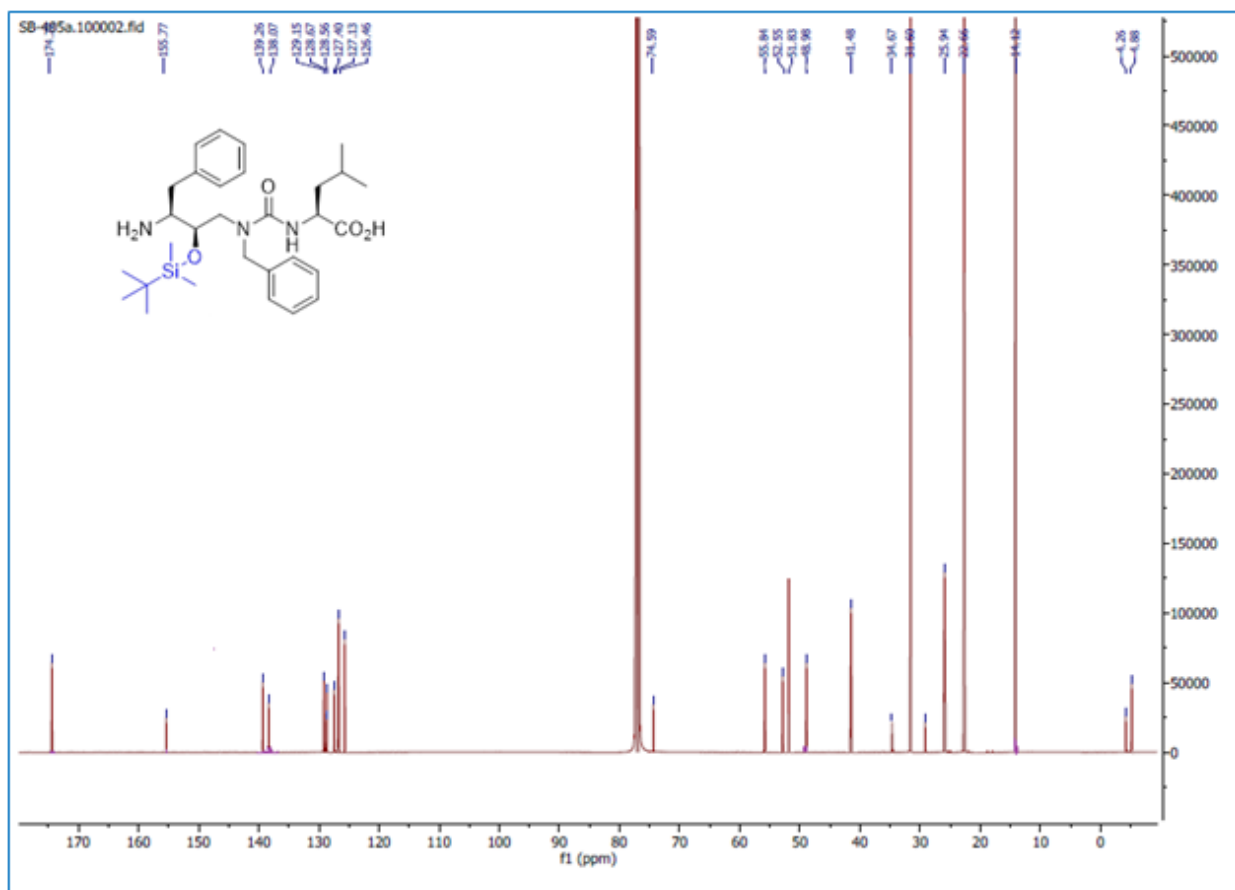
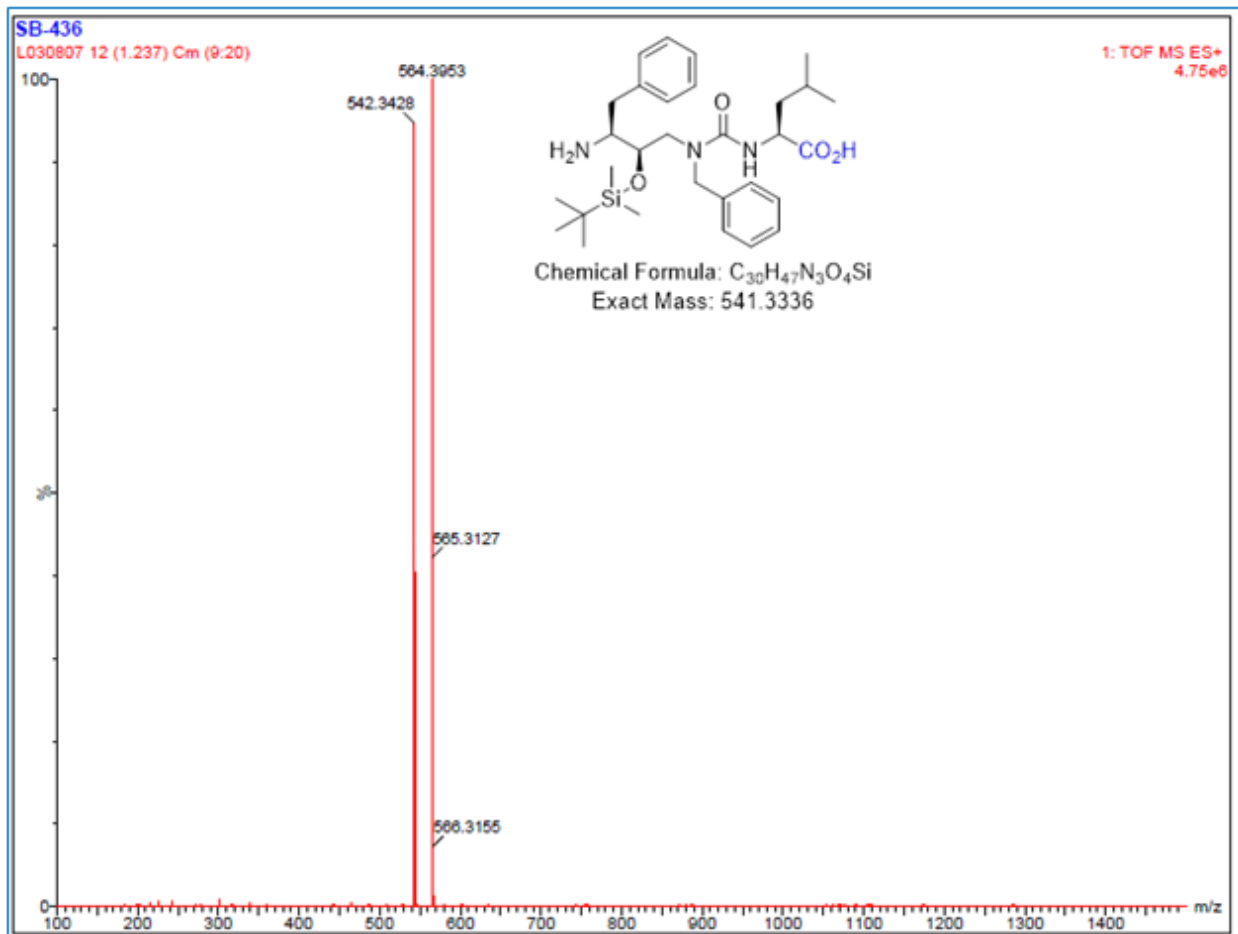


Figure S36: Section of the  $^1\text{H}$  NMR spectra (400 MHz,  $\text{CDCl}_3$ ) for the intermediate VIIa.



**Figure S37:** Section of the  $^{13}\text{C}$  NMR spectra (126 MHz,  $\text{CDCl}_3$ ) for the intermediate **VIIa**.



**Figure S38:** Section of HRMS (ESI):  $m/z$   $[M + H]^+$  spectra for the intermediate **VIIa**. calcd for C<sub>30</sub>H<sub>47</sub>N<sub>3</sub>O<sub>5</sub>Si: 542.4316; found: 542.3428.



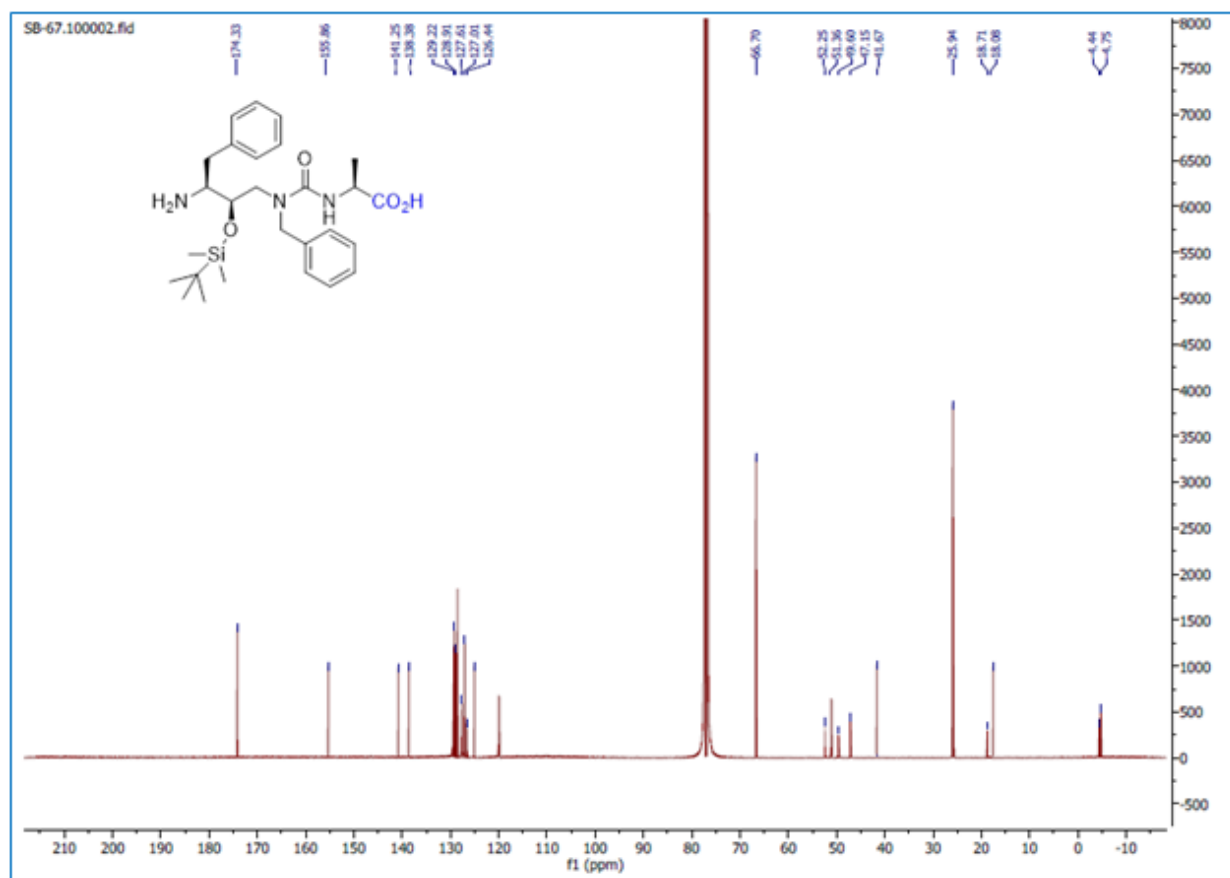


**Figure S40:** Section of the  $^{13}\text{C}$  NMR spectra (126 MHz,  $\text{CDCl}_3$ ) for the intermediate **VIIb**.

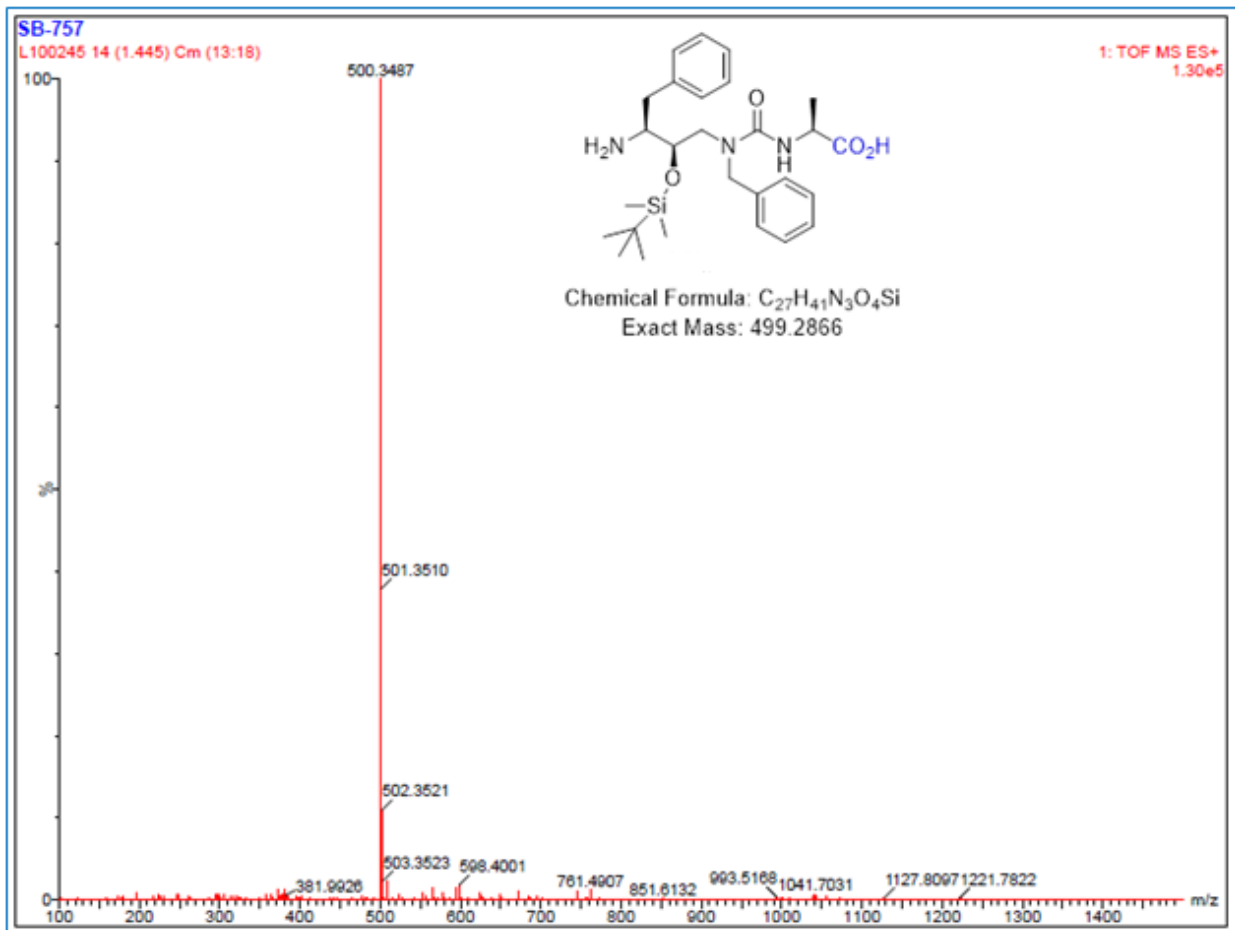


**Figure S41:** Section of HRMS (ESI):  $m/z$   $[M + H]^+$  spectra for the intermediate **VIIb**. calcd for C<sub>27</sub>H<sub>41</sub>N<sub>3</sub>O<sub>4</sub>Si: 500.2946; found: 500.3487.

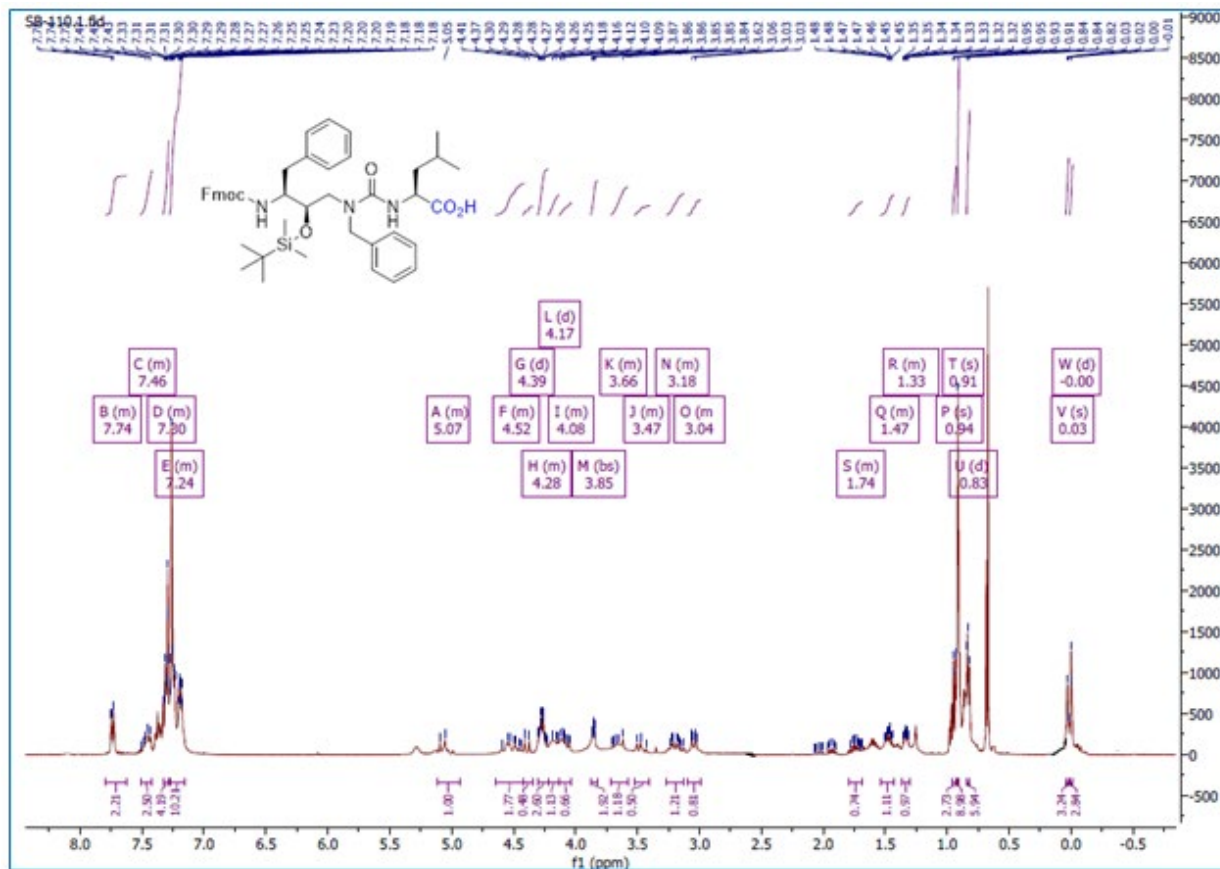
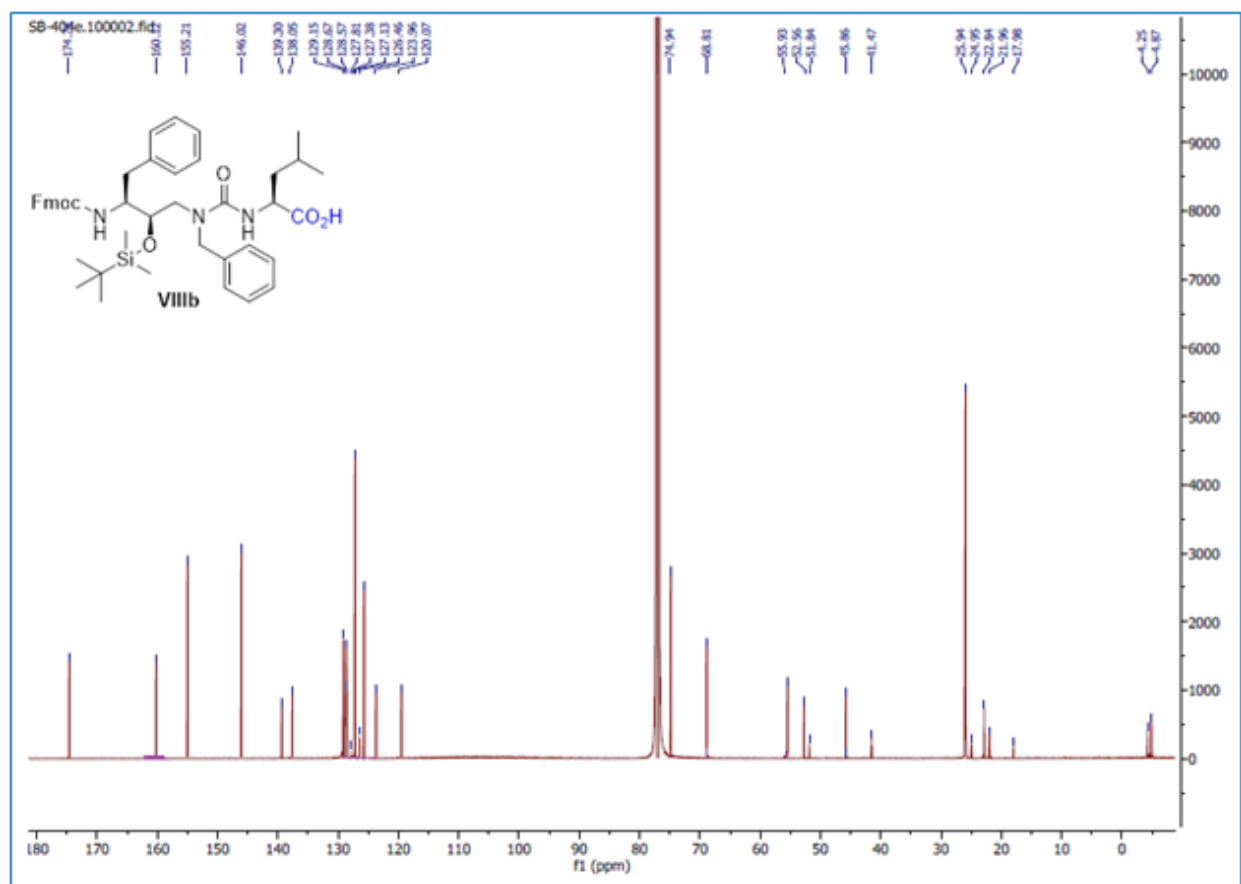
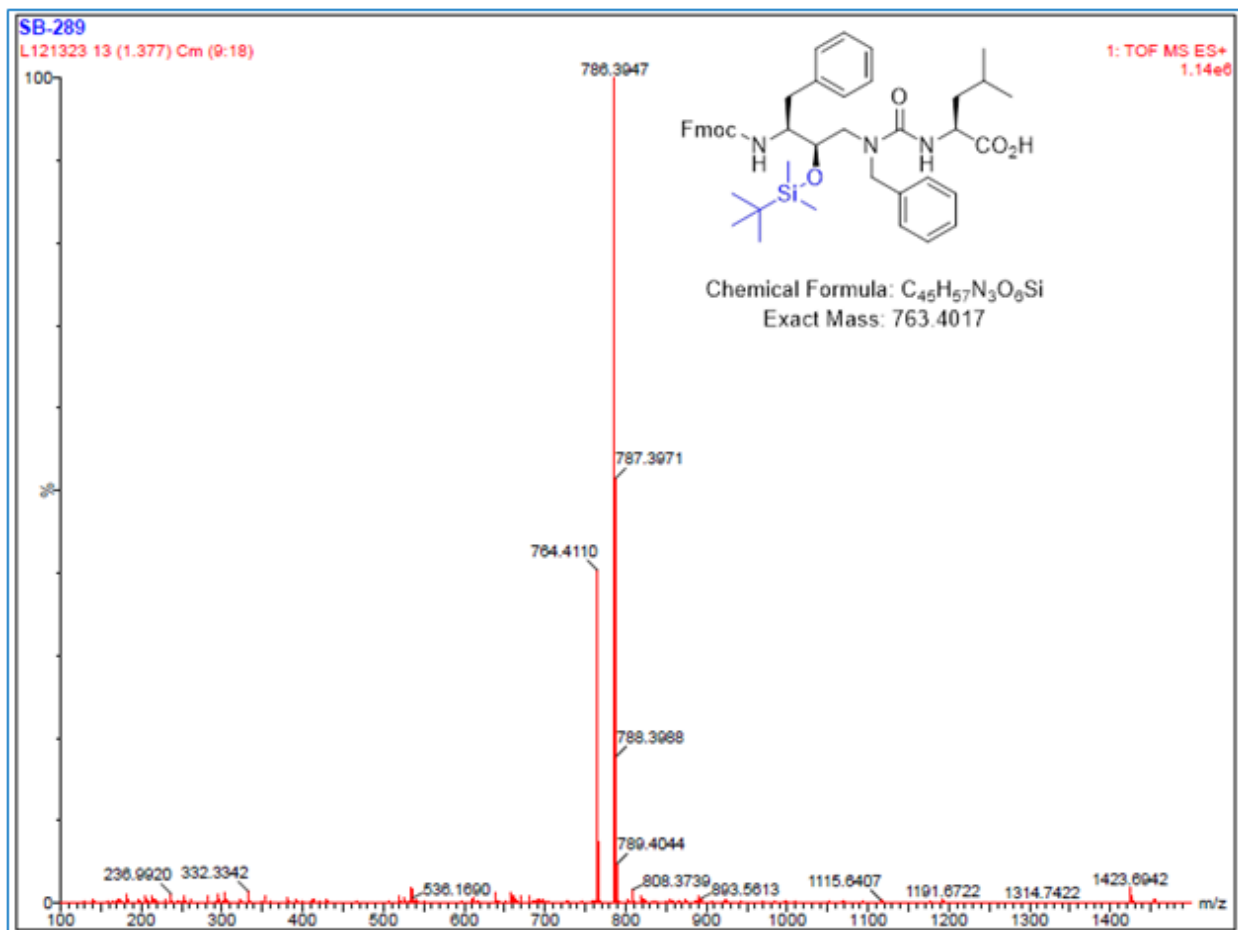


Figure S42: Section of the  $^1\text{H}$  NMR spectra (400 MHz,  $\text{CDCl}_3$ ) for the intermediate VIIIa.



**Figure S43:** Section of the  $^{13}\text{C}$  NMR spectra (126 MHz,  $\text{CDCl}_3$ ) for the intermediate **VIIIa**.





**Figure S44:** Section of HRMS (ESI):  $m/z$   $[M + H]^+$  spectra for the intermediate **VIIa**. calcd for  $C_{45}H_{57}N_3O_6Si$ : 764.4097; found: 764.4110.

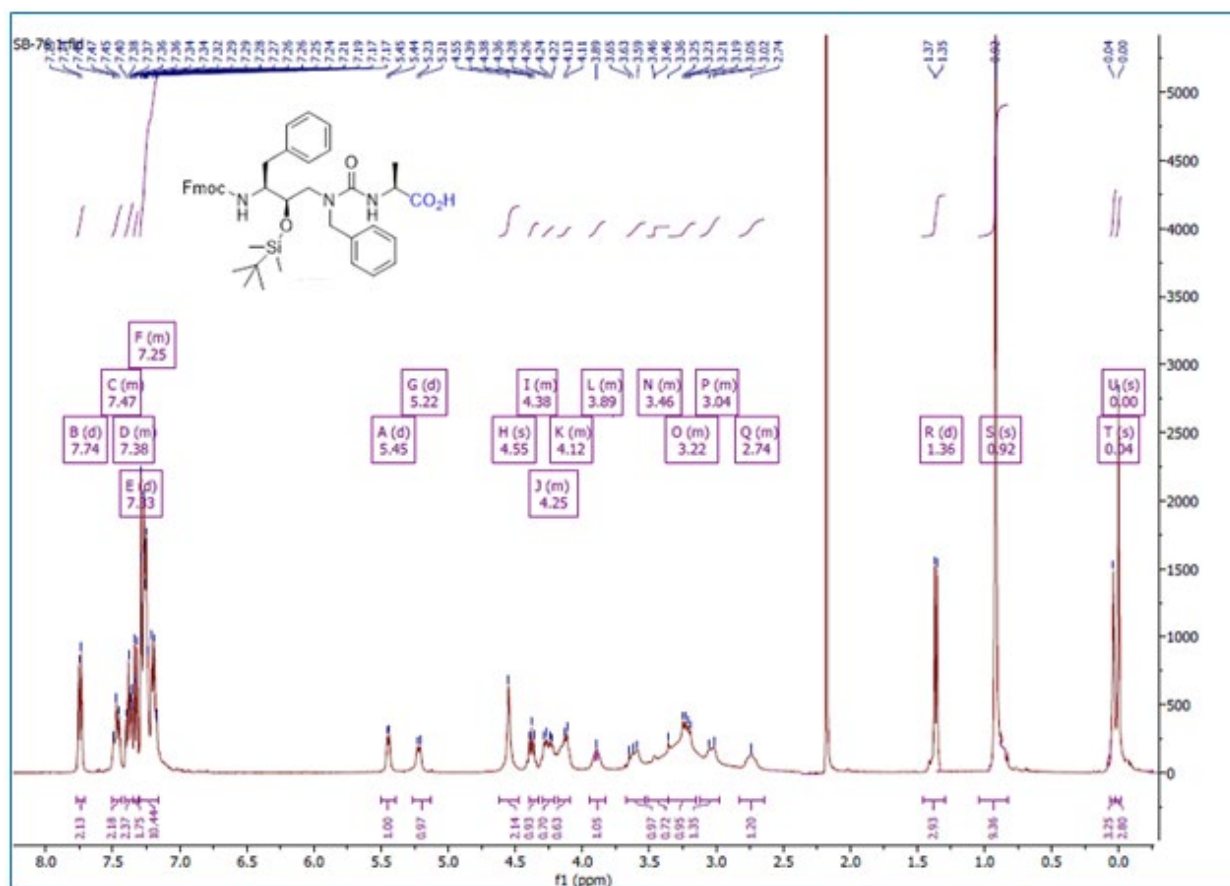
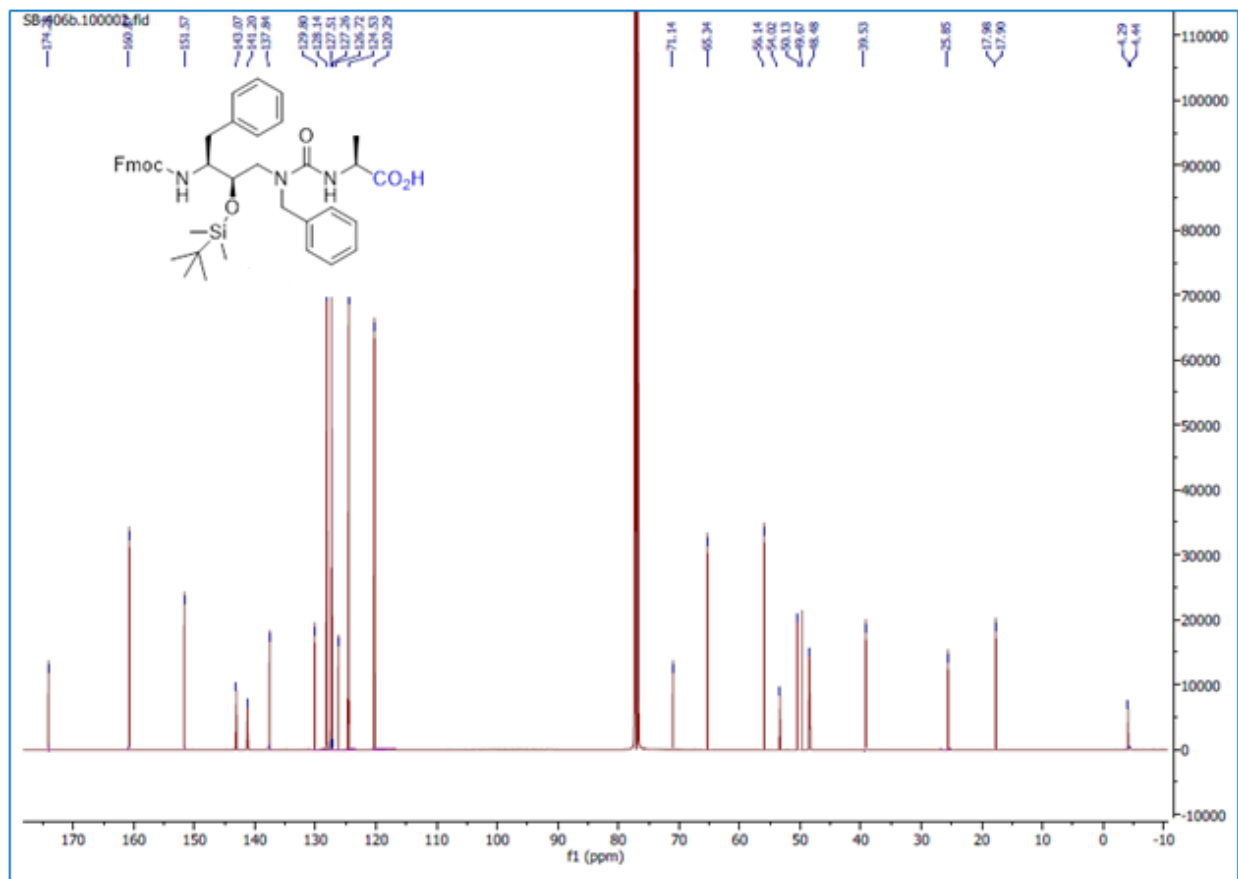
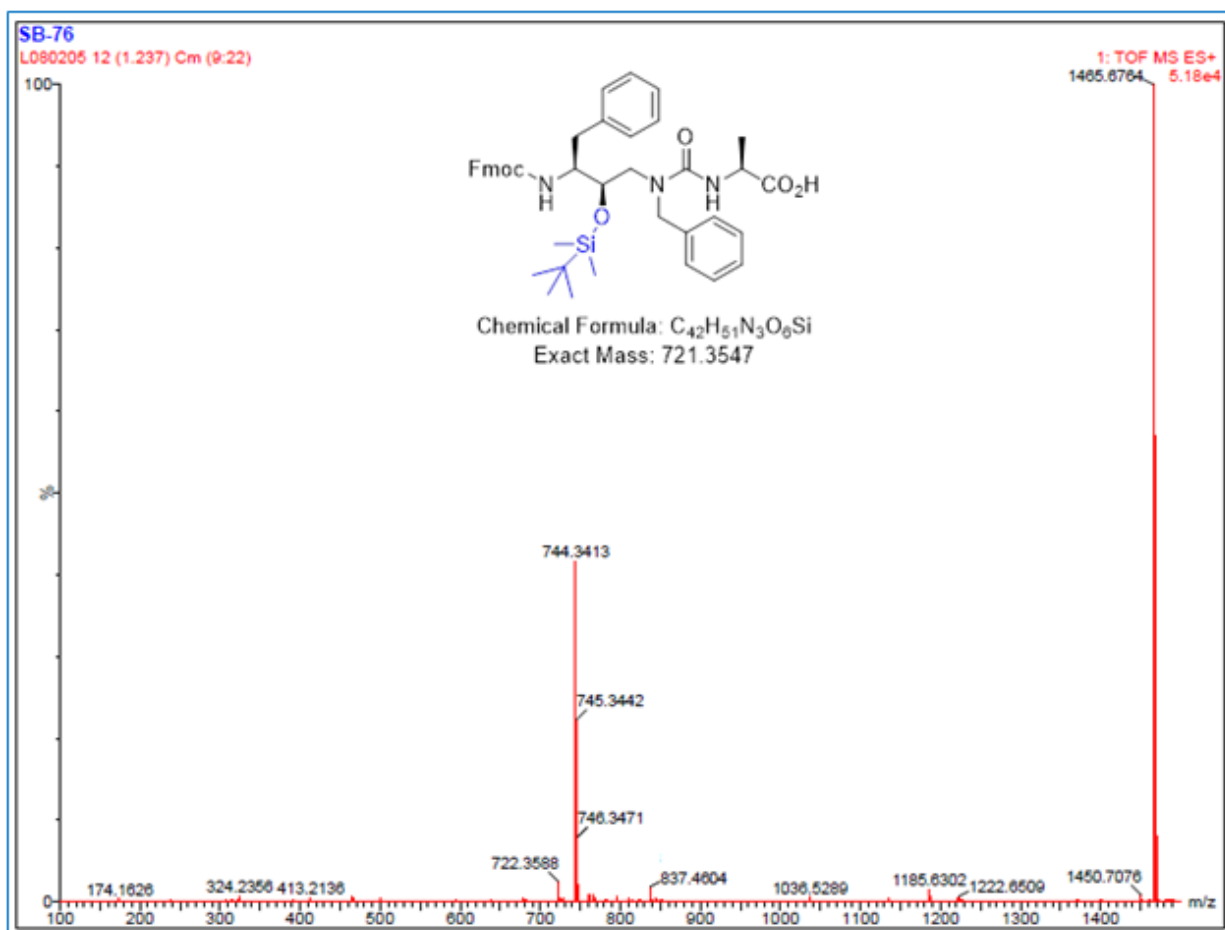


Figure S45: Section of the  $^1\text{H}$  NMR spectra (400 MHz,  $\text{CDCl}_3$ ) for the intermediate VIIIb.



**Figure S46:** Section of the  $^{13}\text{C}$  NMR spectra (126 MHz,  $\text{CDCl}_3$ ) for the intermediate **VIIIb**.



**Figure S47:** Section of HRMS (ESI):  $m/z$   $[M + H]^+$  spectra for the intermediate **VIIIb**. calcd for  $C_{42}H_{51}N_3O_6Si$ : 722.3627; found: 722.3588.

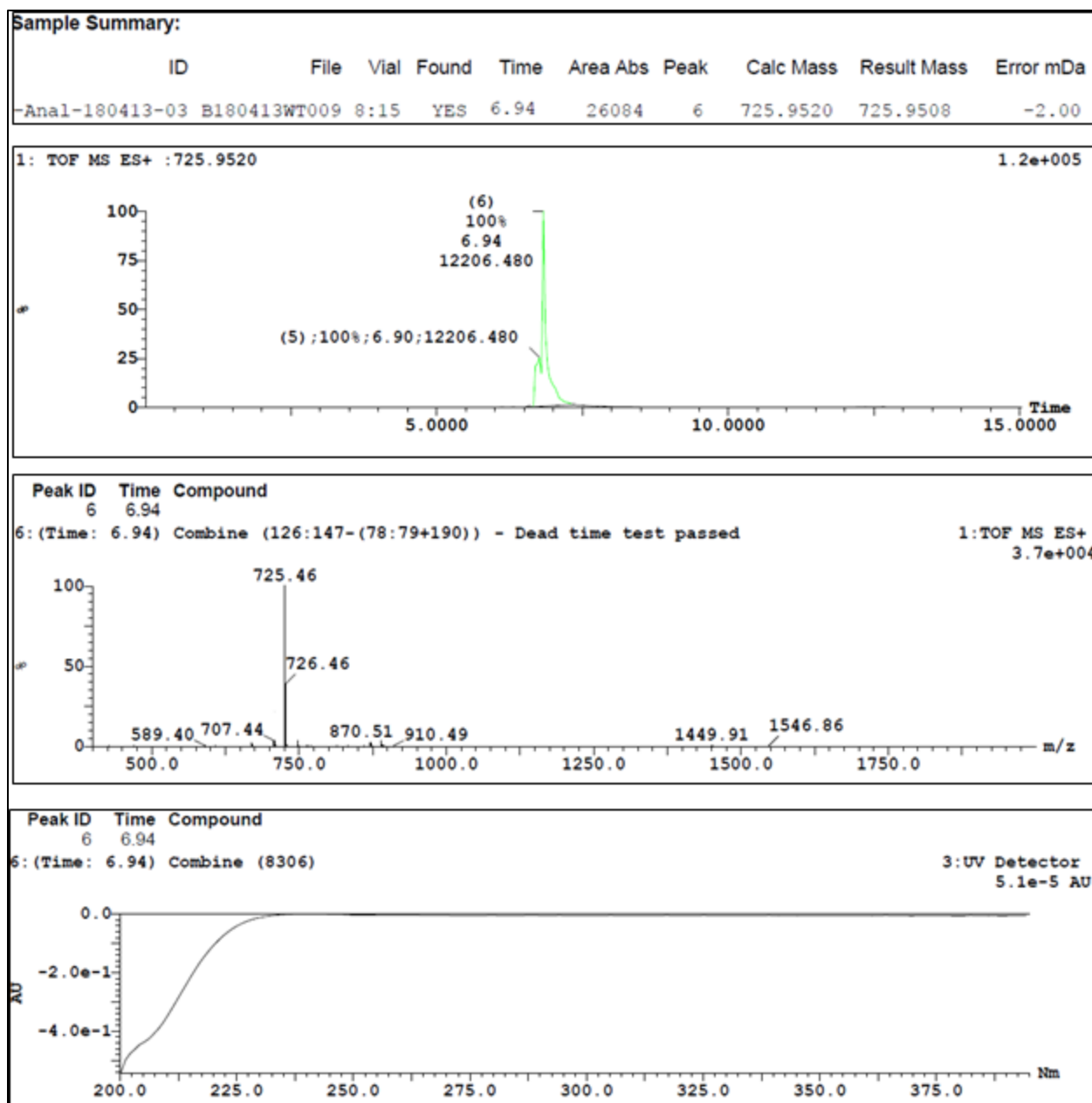


**Figure S48.** LC/TOF-ES-MS spectra of the synthesized peptide **1** (mass spectra in the positive mode), HPLC chromatogram with **1** and its purity determined by HPLC-DAD from 200-375 nm (100%). The peak at 6.94 min belongs to **1** ( $m/z = 725$ ).

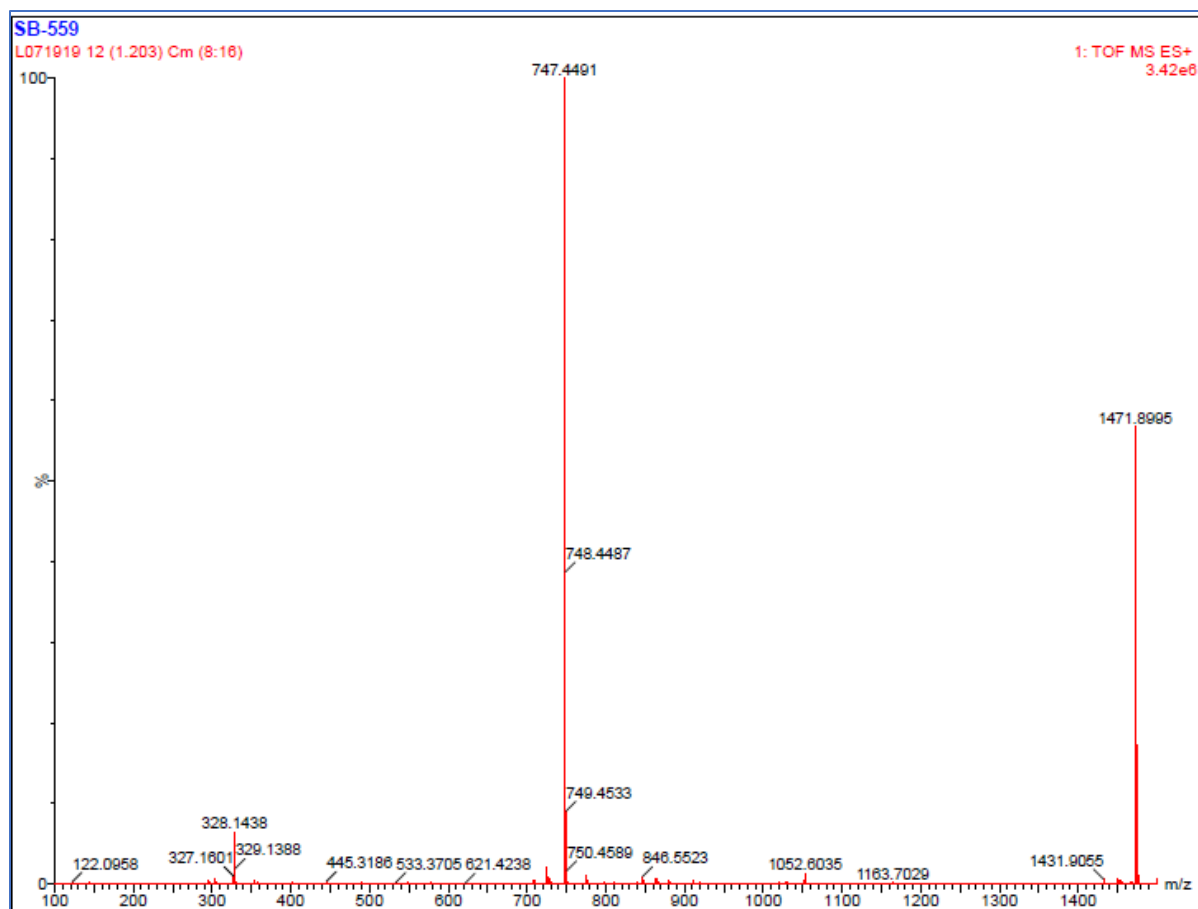


**Figure S49:** Section of HRMS (ESI):  $m/z$   $[M + Na]^+$  spectra for the synthesized peptide **1**. calcd for  $C_{39}H_{60}N_6O_7Na$ : 747.4421; found: 747.4491.

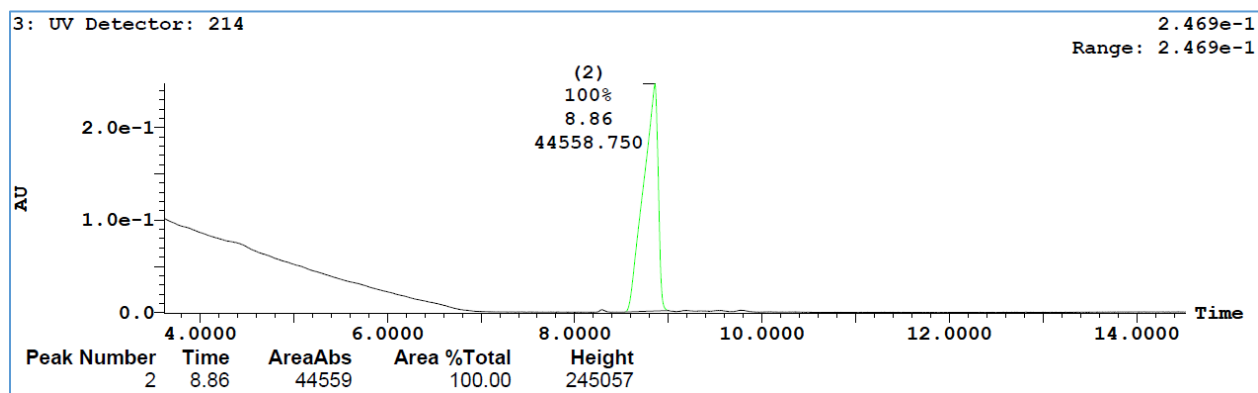


**Figure S50:** Purity of peptide **1** determined by HPLC-UV (214 nm)-ESI-MS and was found to be 100%.

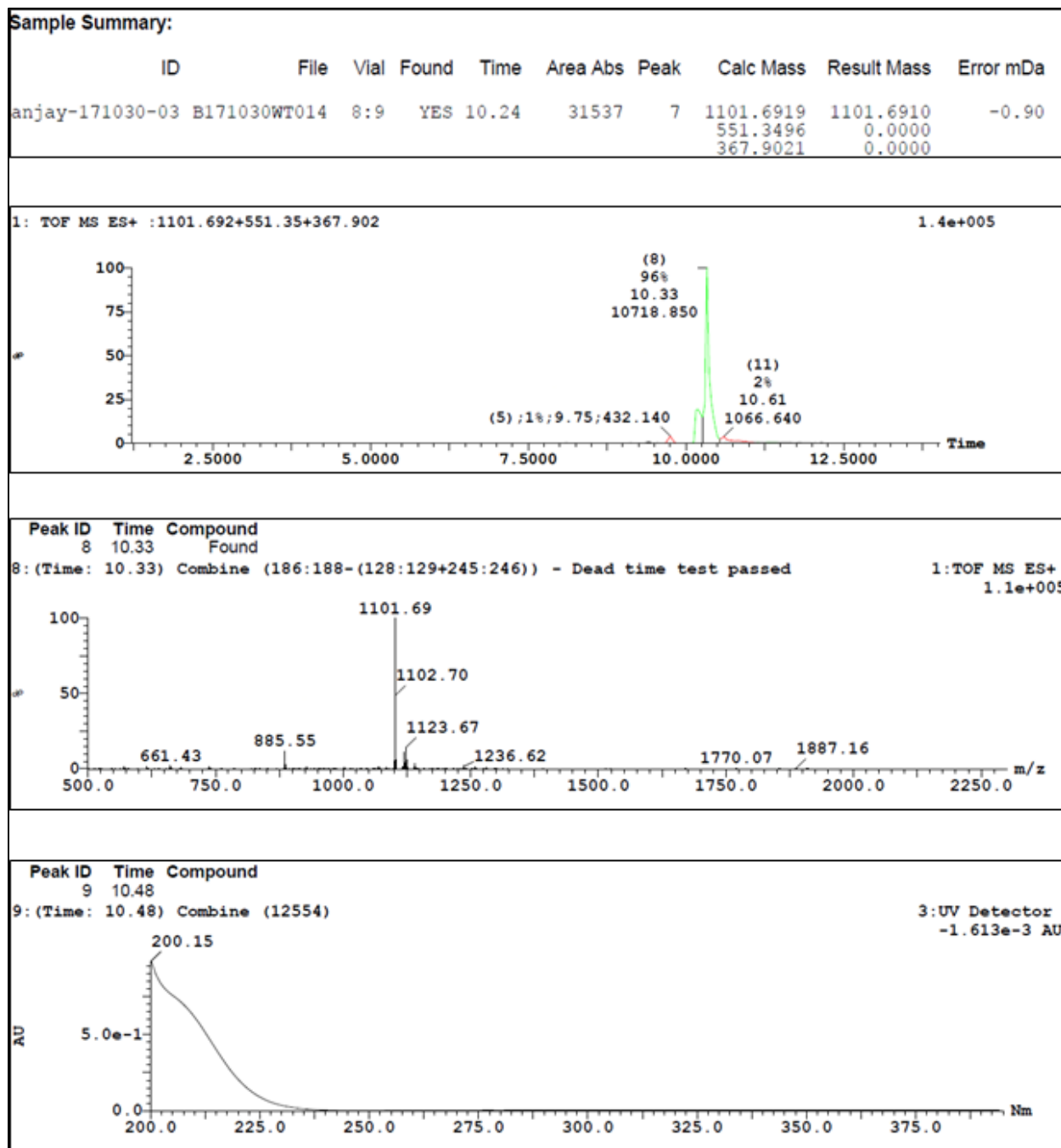


**Figure S51.** LC/TOF-ES-MS spectra of the synthesized peptide **2** (mass spectra in the positive mode), HPLC chromatogram with **2** and its purity determined by HPLC-DAD from 200-370 nm (96%). The peak at 10.33 min belongs to **2** ( $m/z = 1101$ ).

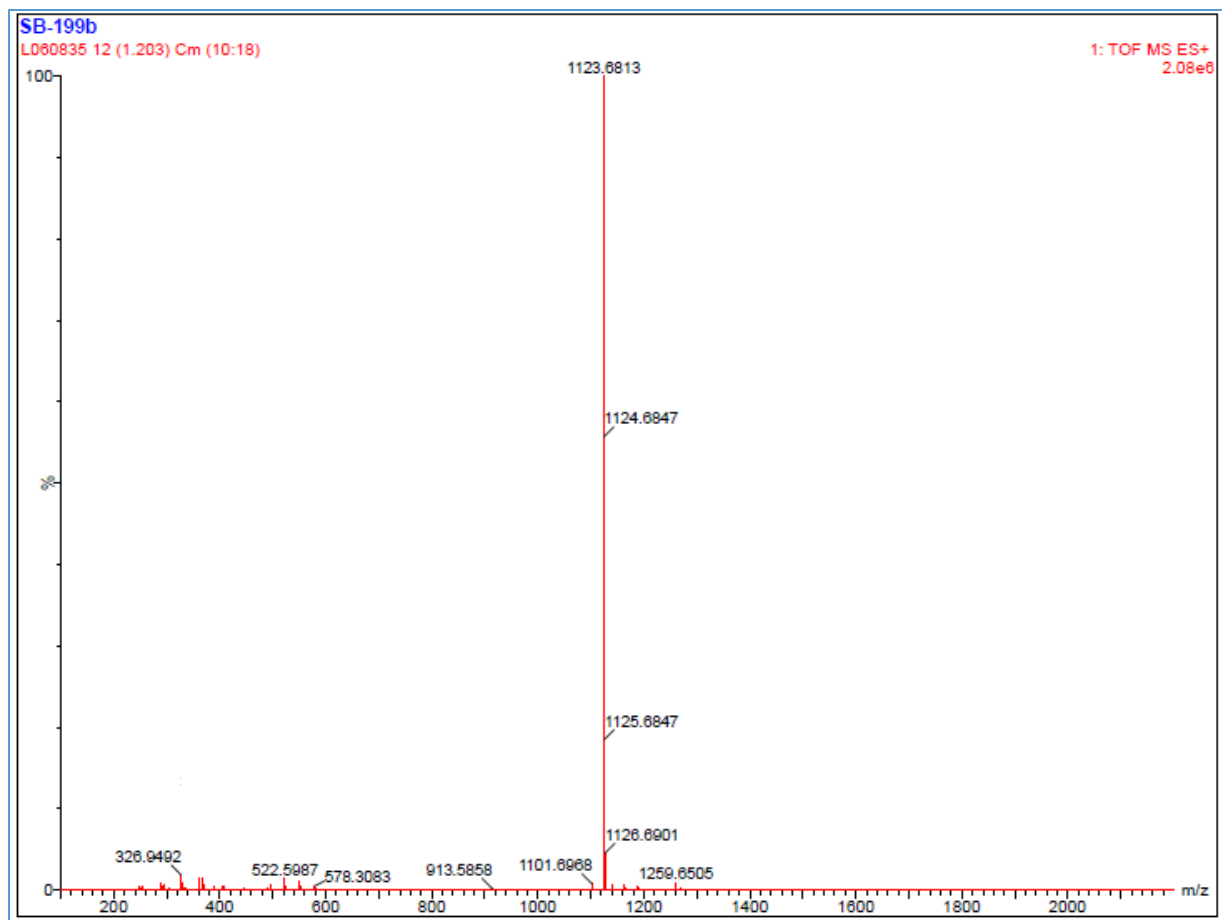


**Figure S52:** Section of HRMS (ESI):  $m/z$   $[M + Na]^+$  spectra for the synthesized peptide **2**. calcd for  $C_{55}H_{92}N_{10}O_{13}Na$ : 1123.6743; found: 1123.6813.

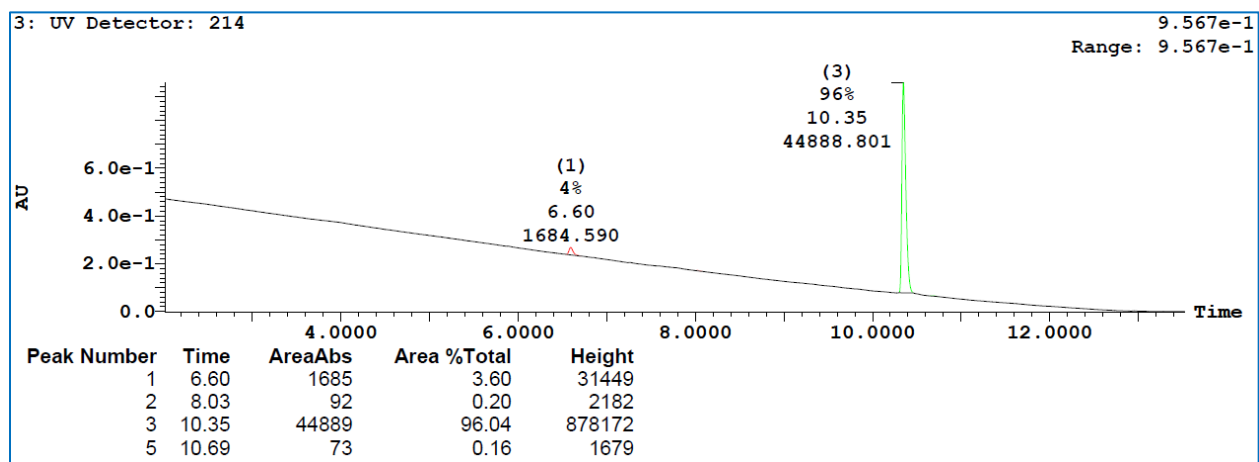


**Figure S53:** Purity of peptide **2** determined by HPLC-UV (214 nm)-ESI-MS and was found to be 96%.



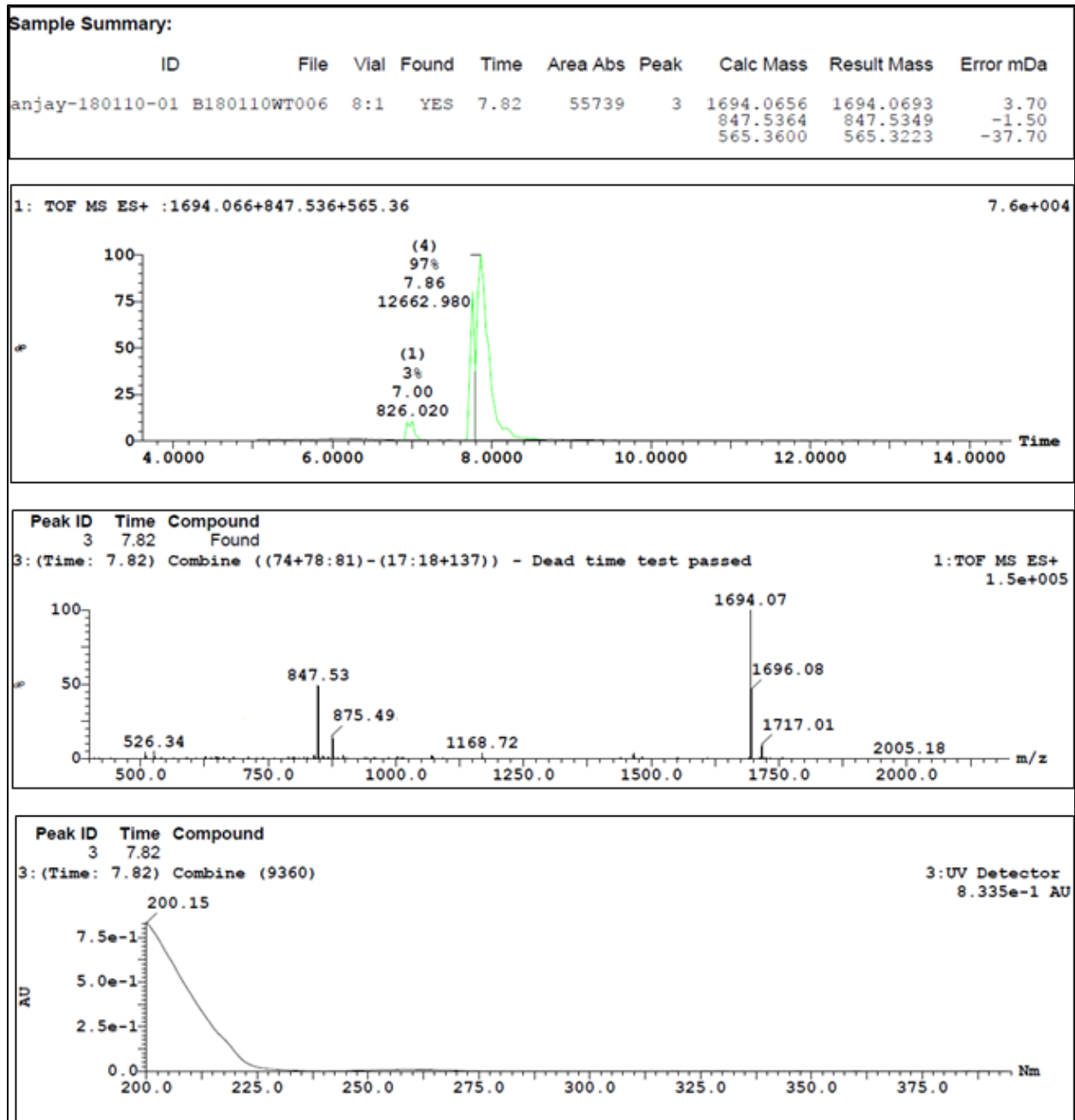


**Figure S54.** LC/TOF-ES-MS spectra of the synthesized peptide **3** (mass spectra in the positive mode), HPLC chromatogram with **3** and its purity determined by HPLC-DAD from 200-375 nm (97%). The peak at 7.82 min belongs to **3** ( $m/z = 1694$ ).

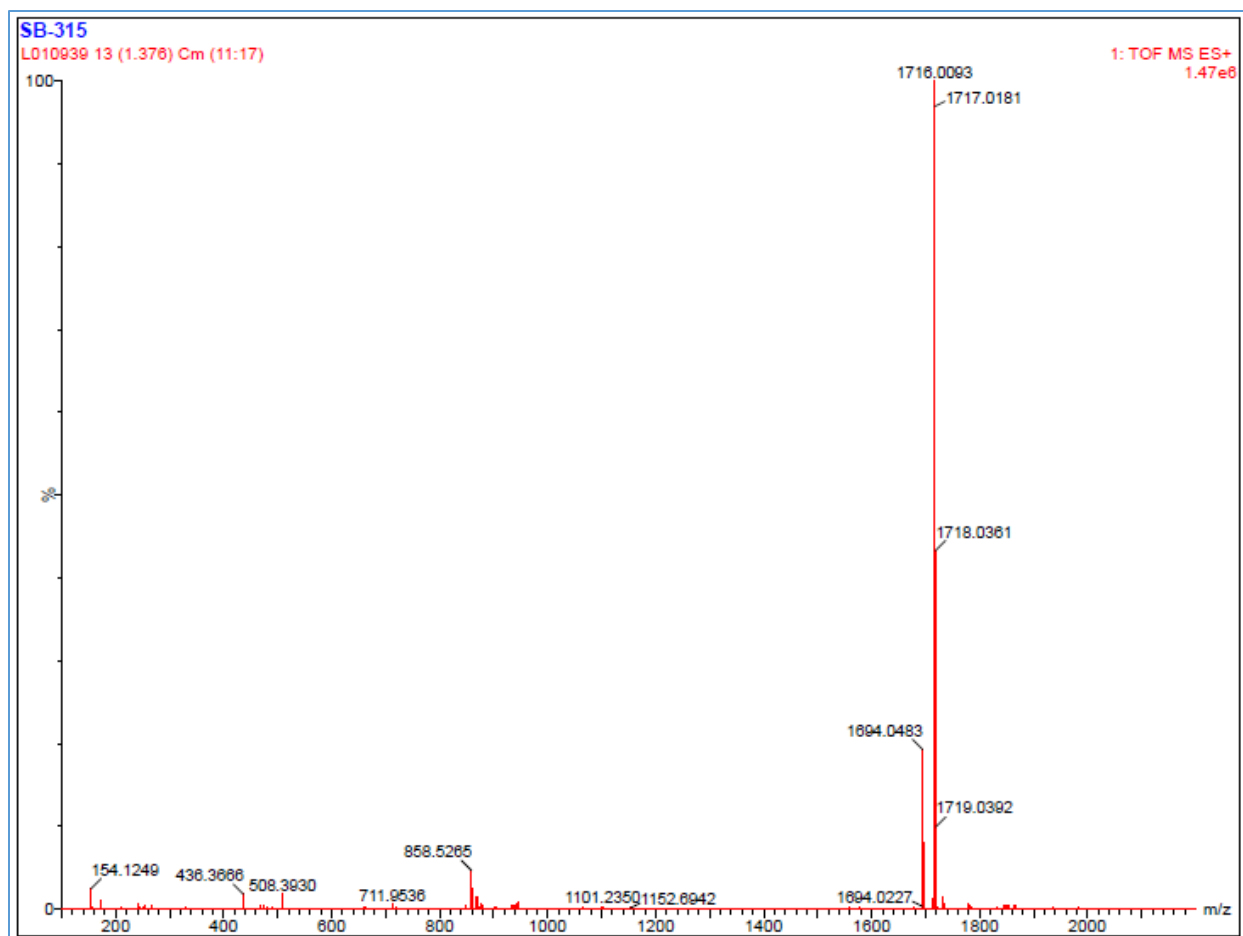


**Figure 55:** Section of HRMS (ESI):  $m/z$   $[M + H]^+$  spectra for the synthesized peptide **3**. calcd for  $C_{88}H_{140}N_{16}O_{17}$ : 1694.0662; found: 1694.0483.

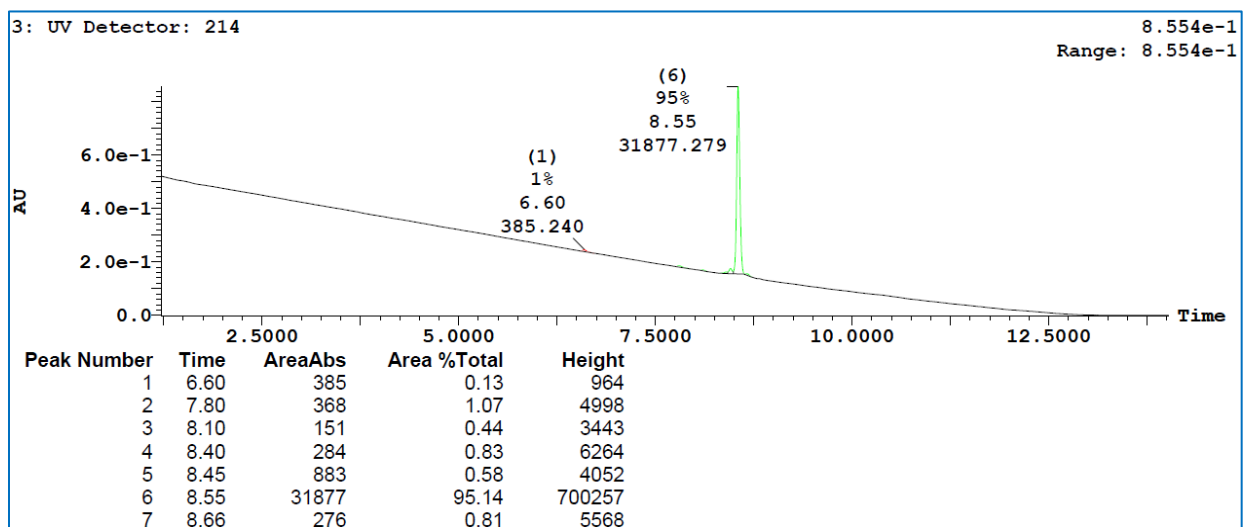


**Figure S56:** Purity of peptide **3** determined by HPLC-UV (214 nm)-ESI-MS and was found to be 95%.

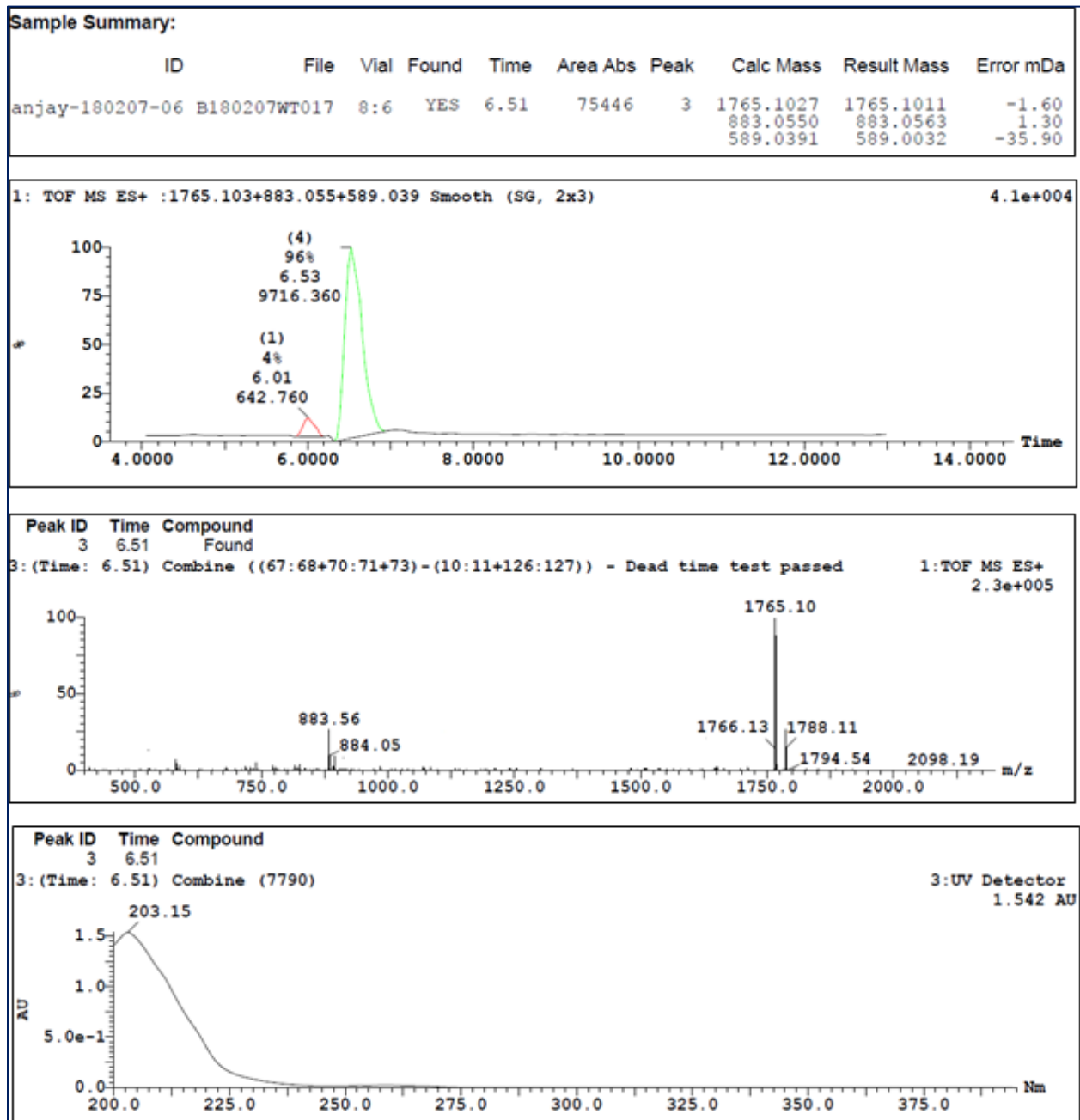


**Figure S57.** LC/TOF-ES-MS spectra of the synthesized peptide **4** (mass spectra in the positive mode), HPLC chromatogram with **4** and its purity determined by HPLC-DAD from 200-375 nm (96%). The peak at 6.51 min belongs to **4** ( $m/z = 1765$ ).

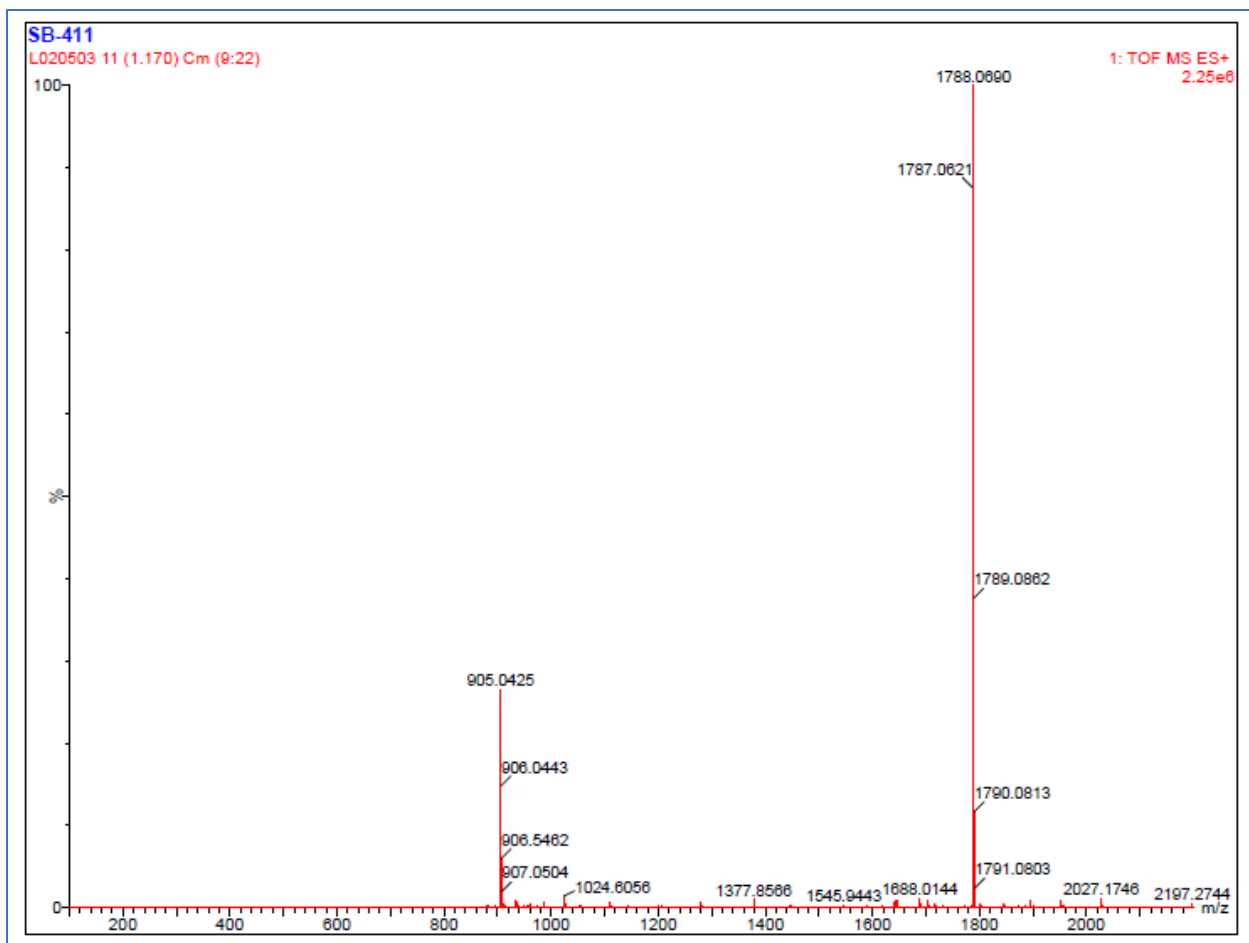


**Figure S58:** Section of HRMS (ESI):  $m/z$   $[M + Na]^+$  spectra for the synthesized peptide **4**. calcd for  $C_{91}H_{145}N_{17}O_{18}Na$ : 1787.0852; found: 1787.0621.

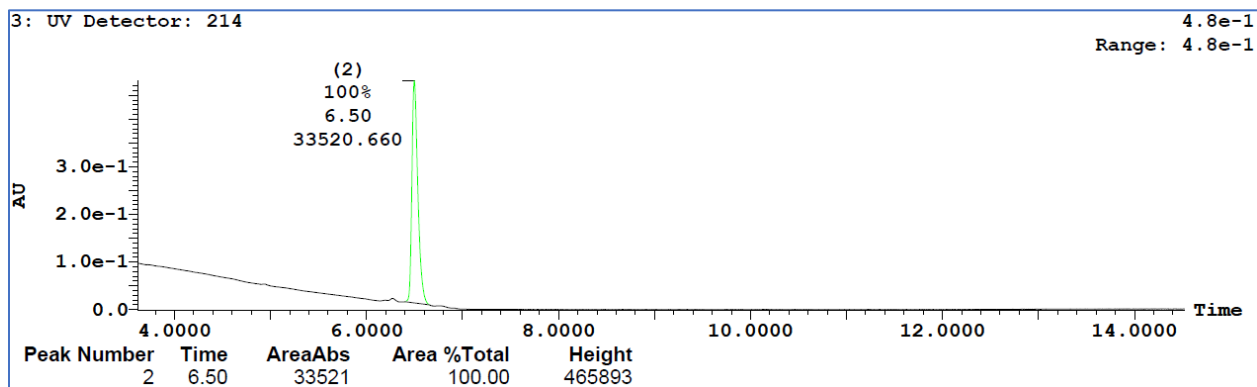


**Figure S59:** Purity of peptide **4** determined by HPLC-UV (214 nm)-ESI-MS and was found to be 100%.

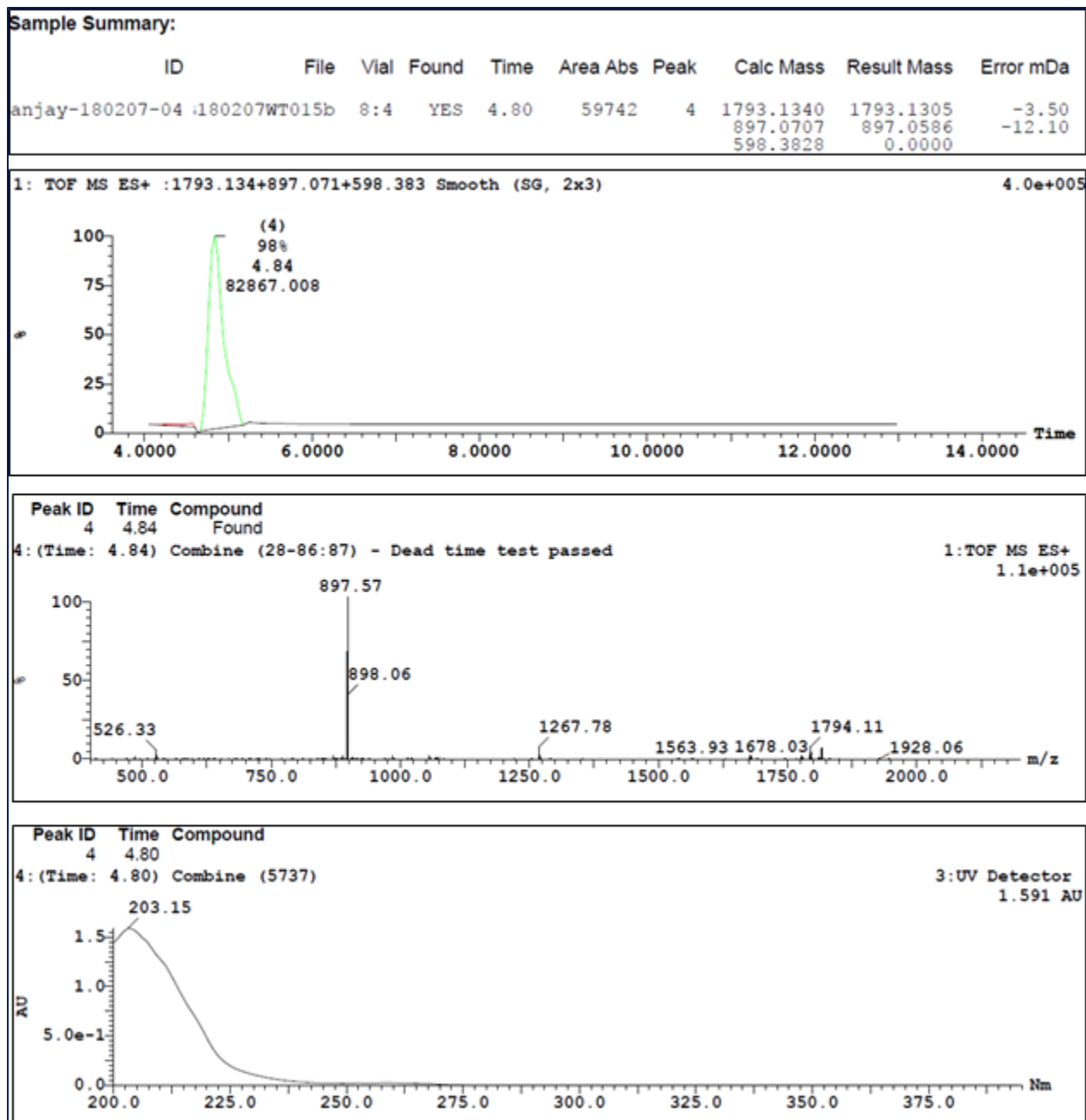


**Figure S60.** LC/TOF-ES-MS spectra of the synthesized peptide **5** (mass spectra in the positive mode), HPLC chromatogram with **5** and its purity determined by HPLC-DAD from 200-370 nm (98%). The peak at 4.84 min belongs to **5** ( $m/z = 1793$ ).

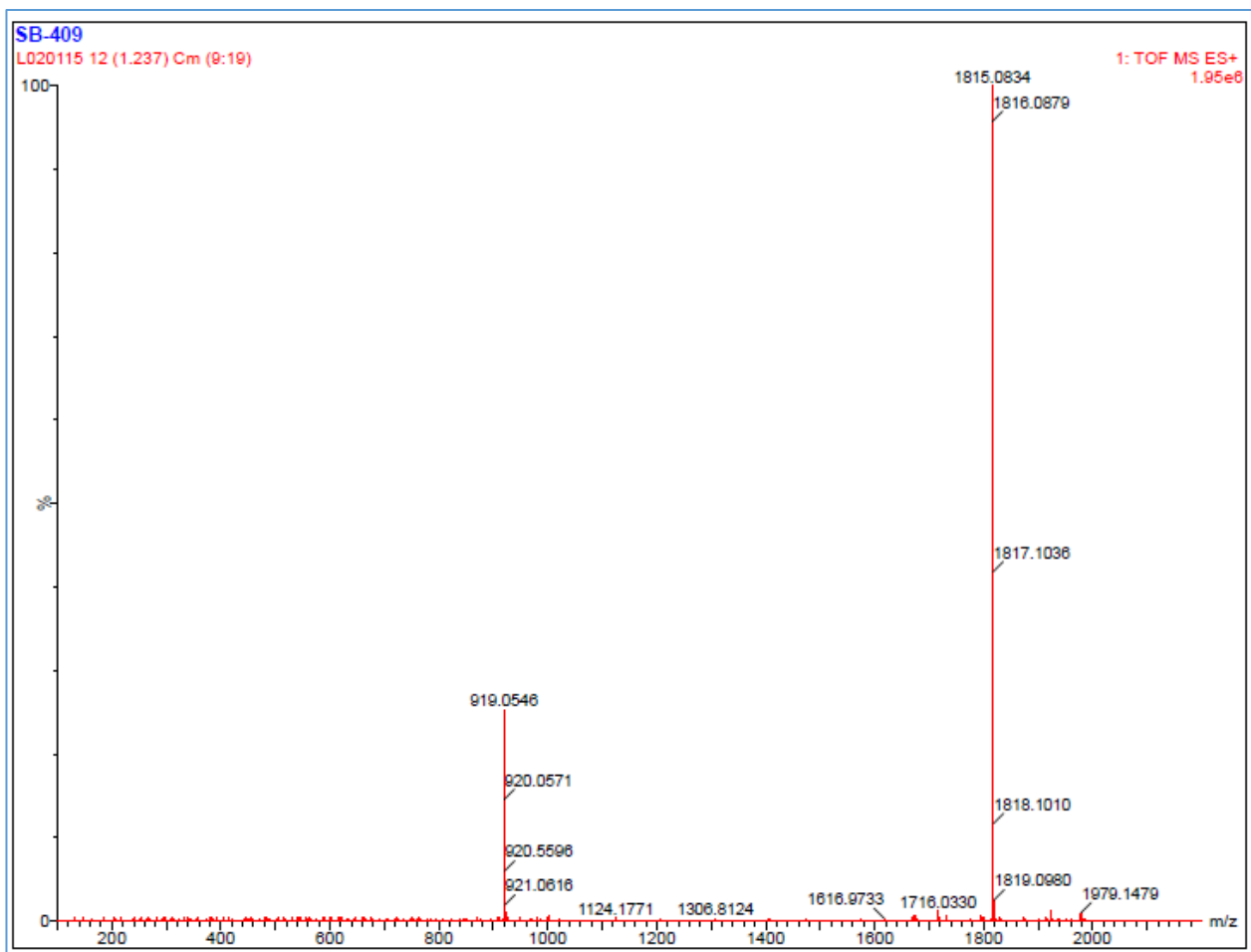


**Figure S61:** Section of HRMS (ESI):  $m/z$   $[M + H]^+$  spectra for the synthesized peptide **5**. calcd for  $C_{93}H_{149}N_{17}O_{18}$ : 1815.1165; found: 1815.0834.

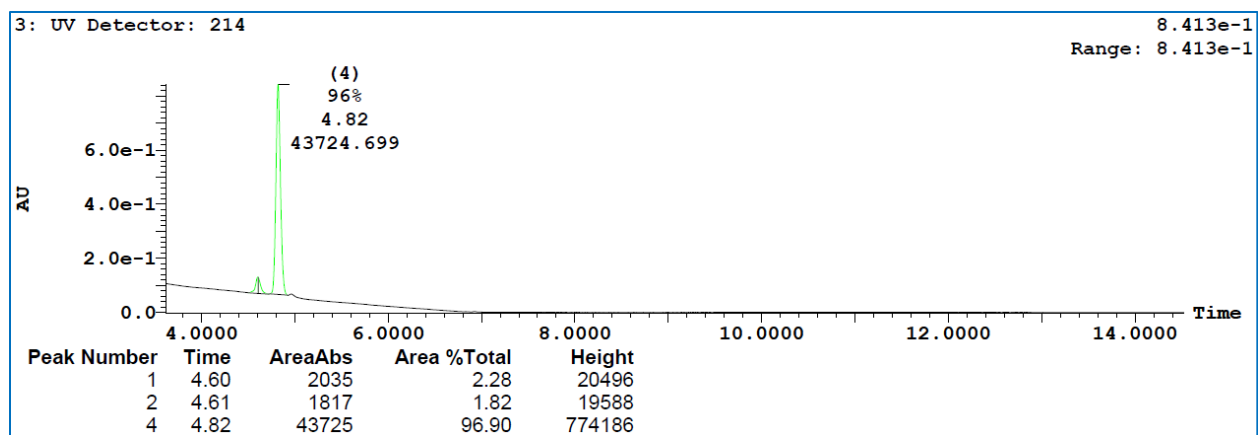


**Figure S62:** Purity of peptide **5** determined by HPLC-UV (214 nm)-ESI-MS and was found to be 96%.

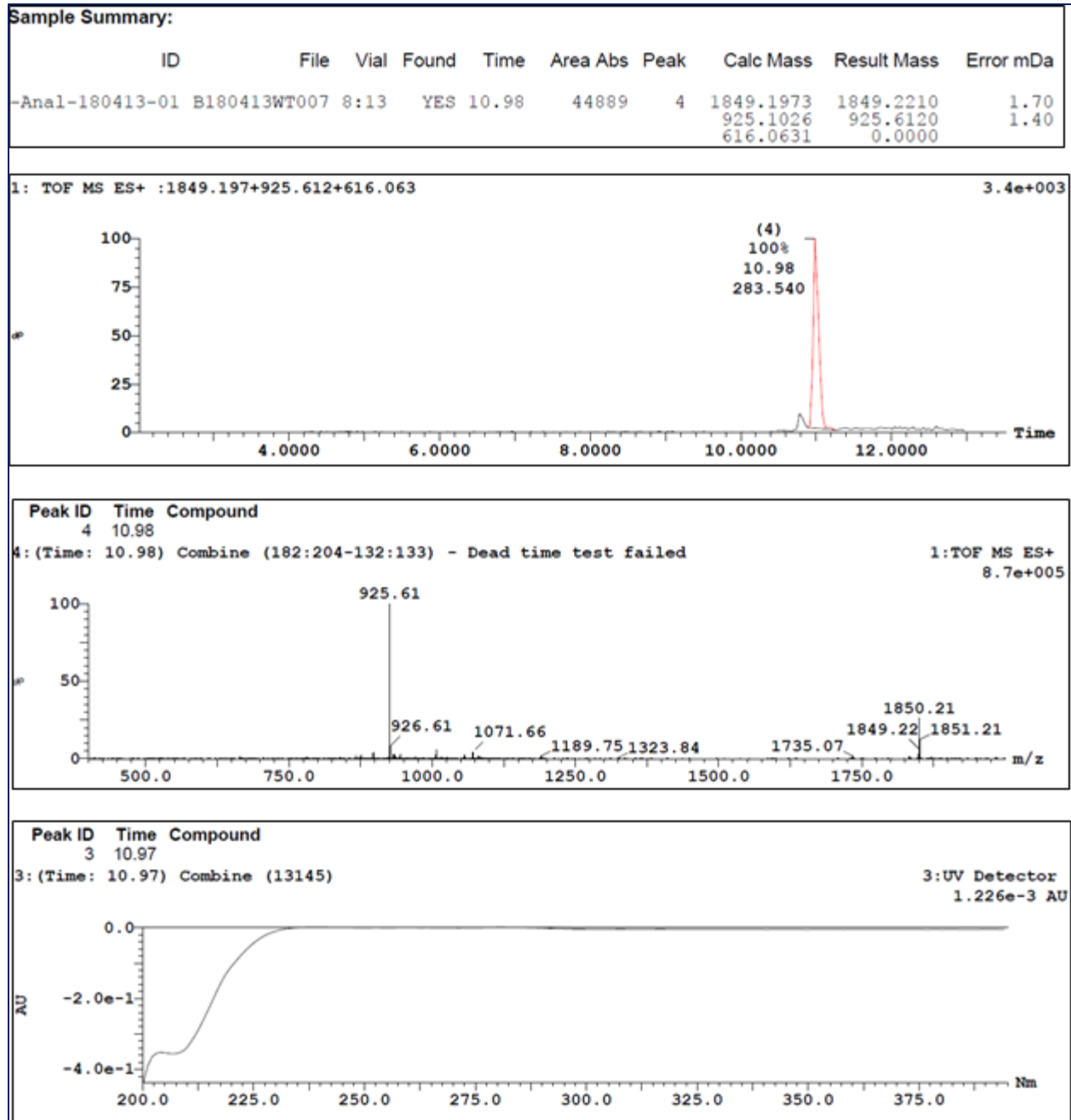


**Figure S63. LC/TOF-ES-MS spectra of the synthesized peptide 6** (mass spectra in the positive mode), HPLC chromatogram with **6** and its purity determined by HPLC-DAD from 200-375 nm (100%). The peak at 10.98 min belongs to **6** ( $m/z = 1849$ ).

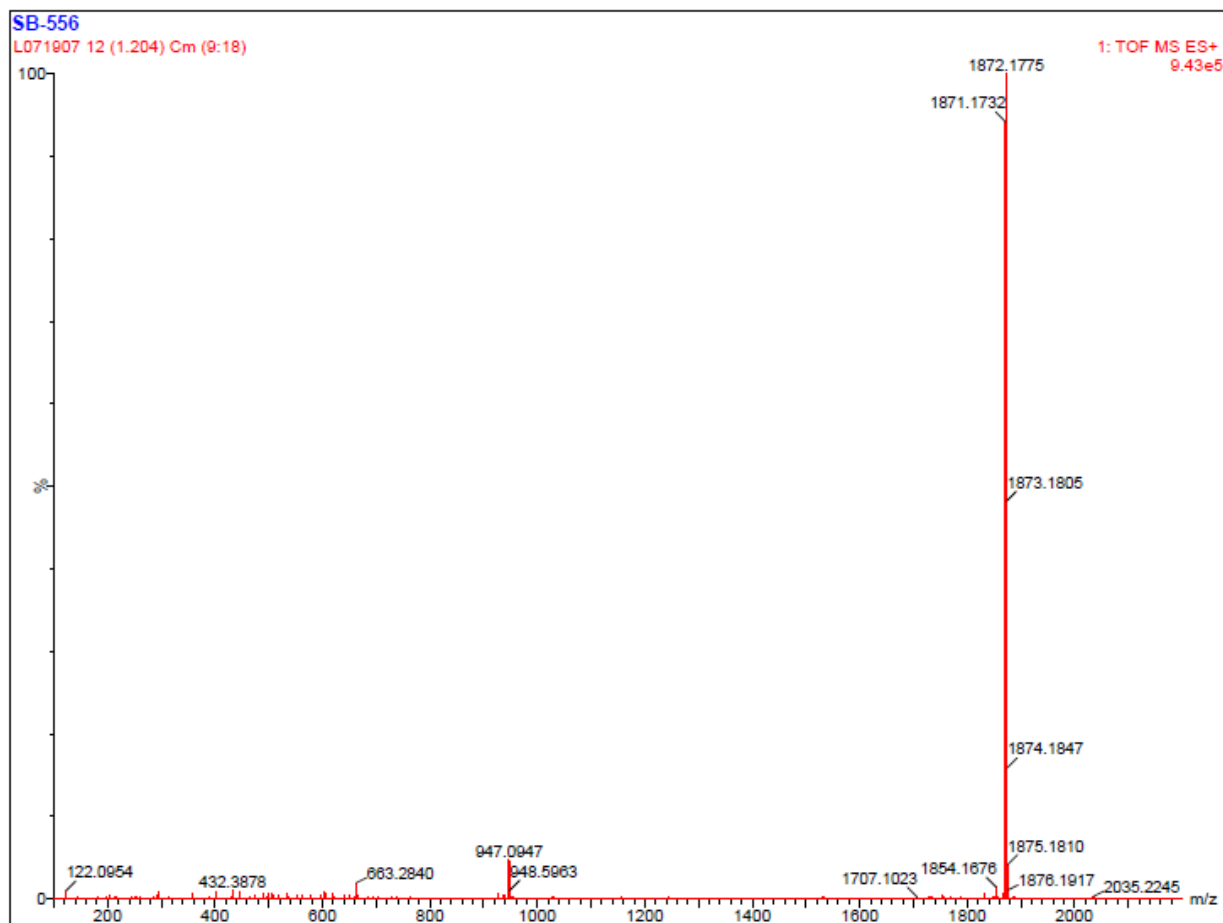


**Figure S64:** Section of HRMS (ESI):  $m/z$   $[M + Na]^+$  spectra for the synthesized peptide **6**. calcd for  $C_{97}H_{157}N_{17}O_{18}Na$ : 1871.1791; found: 1871.1732.

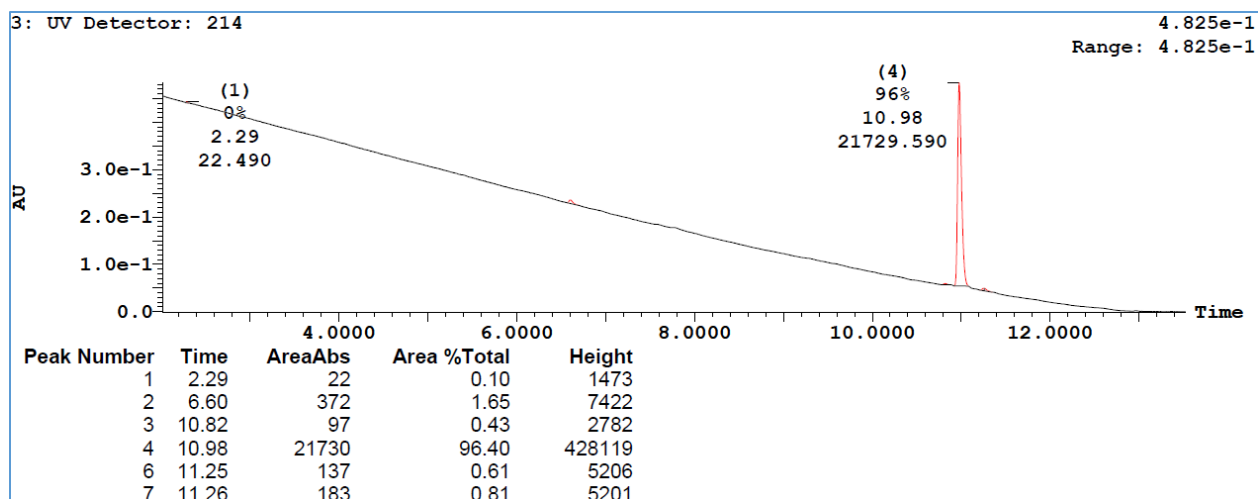


**Figure S65:** Purity of peptide **6** determined by HPLC-UV (214 nm)-ESI-MS and was found to be 96%.



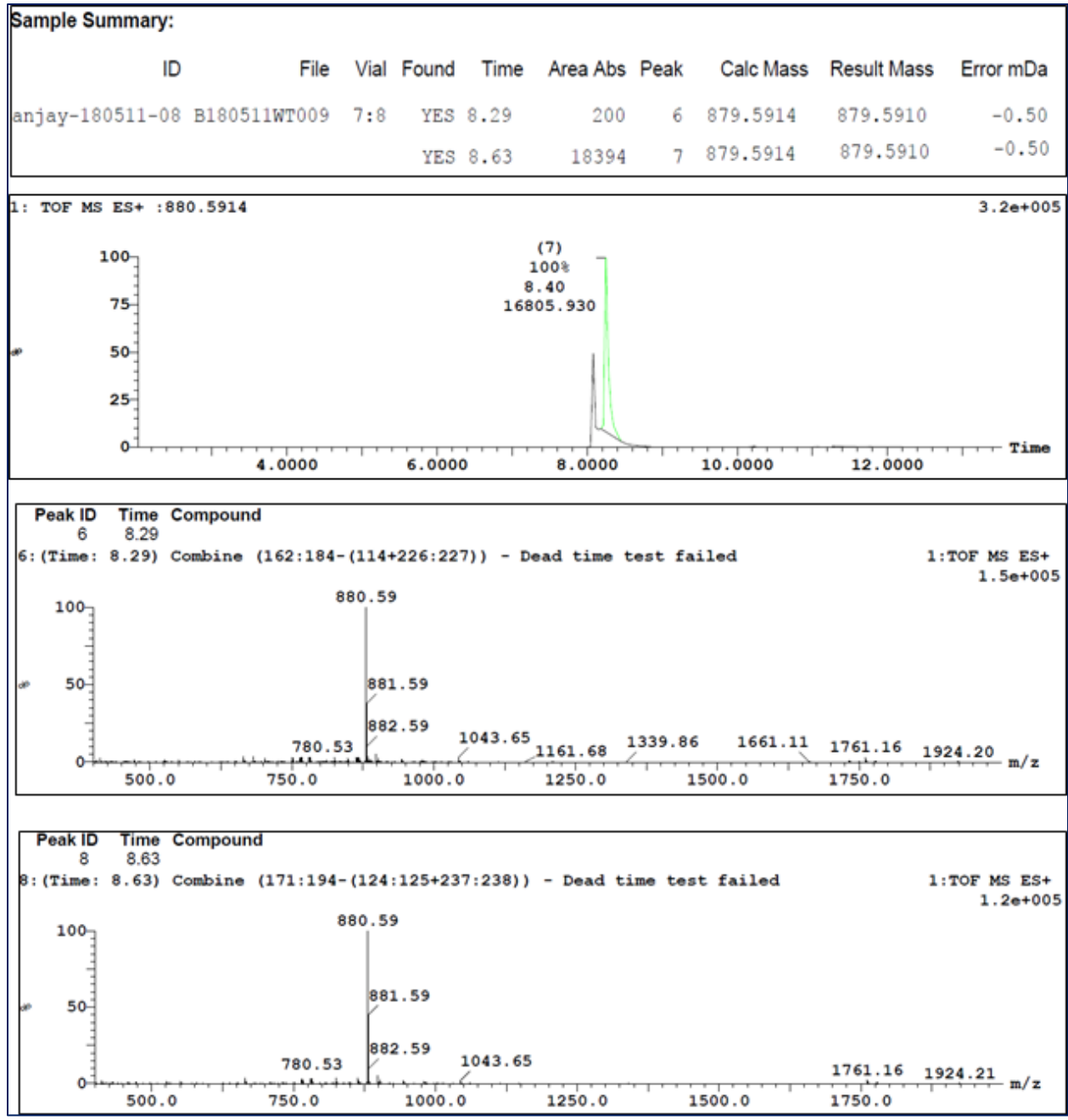


**Figure S66.** LC/TOF-ES-MS spectra of the synthesized peptide **7** (mass spectra in the positive mode), HPLC chromatogram with **7** and its purity determined by HPLC-DAD from 200-375 nm (100%). The peak at 8.40 min belongs to **7** ( $m/z = 880$ ).

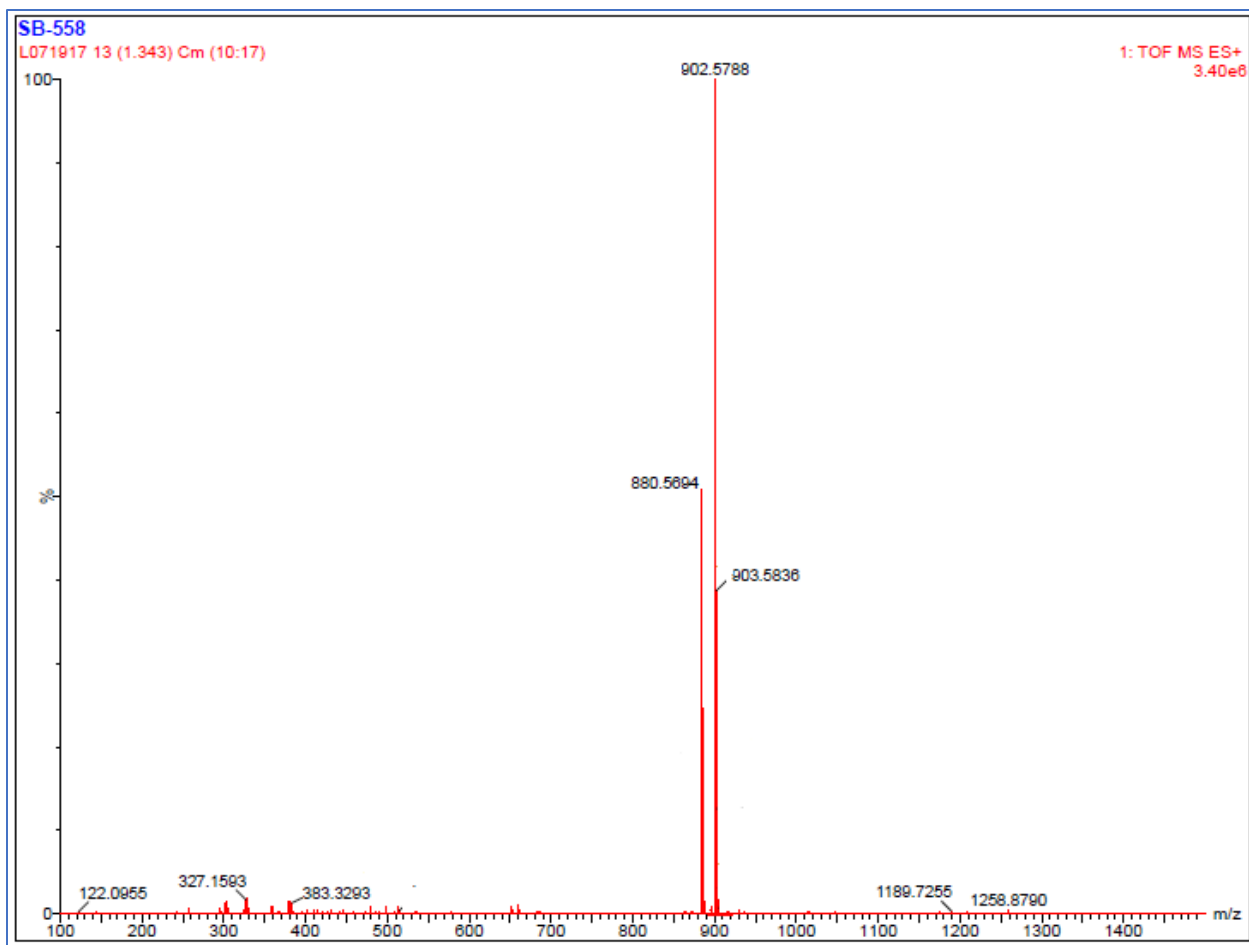


**Figure S67:** Section of HRMS (ESI):  $m/z$   $[M + H]^+$  spectra for the synthesized peptide **7**. calcd for  $C_{48}H_{77}N_7O_8$ : 880.5914; found: 880.5694.

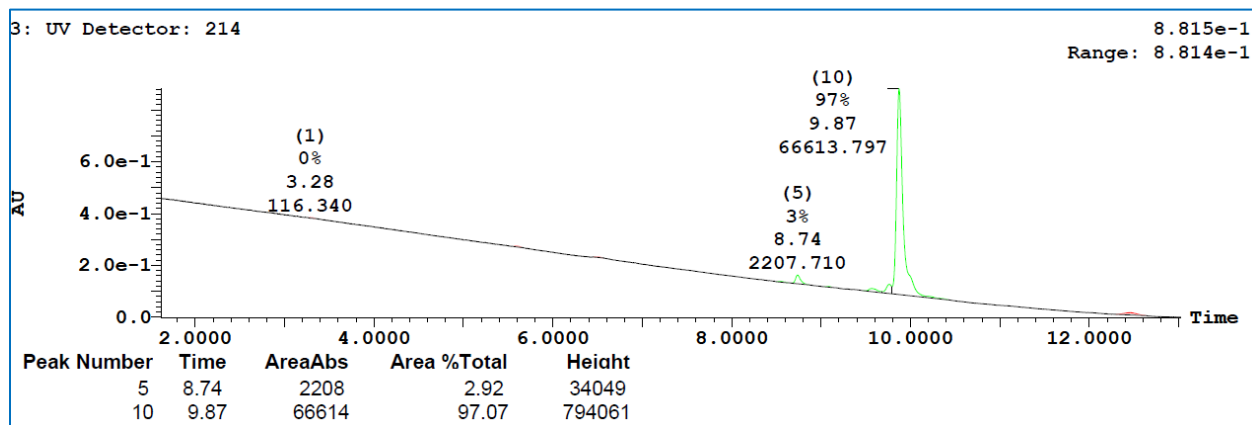


**Figure S68:** Purity of peptide **7** determined by HPLC-UV (214 nm)-ESI-MS and was found to be 97%.

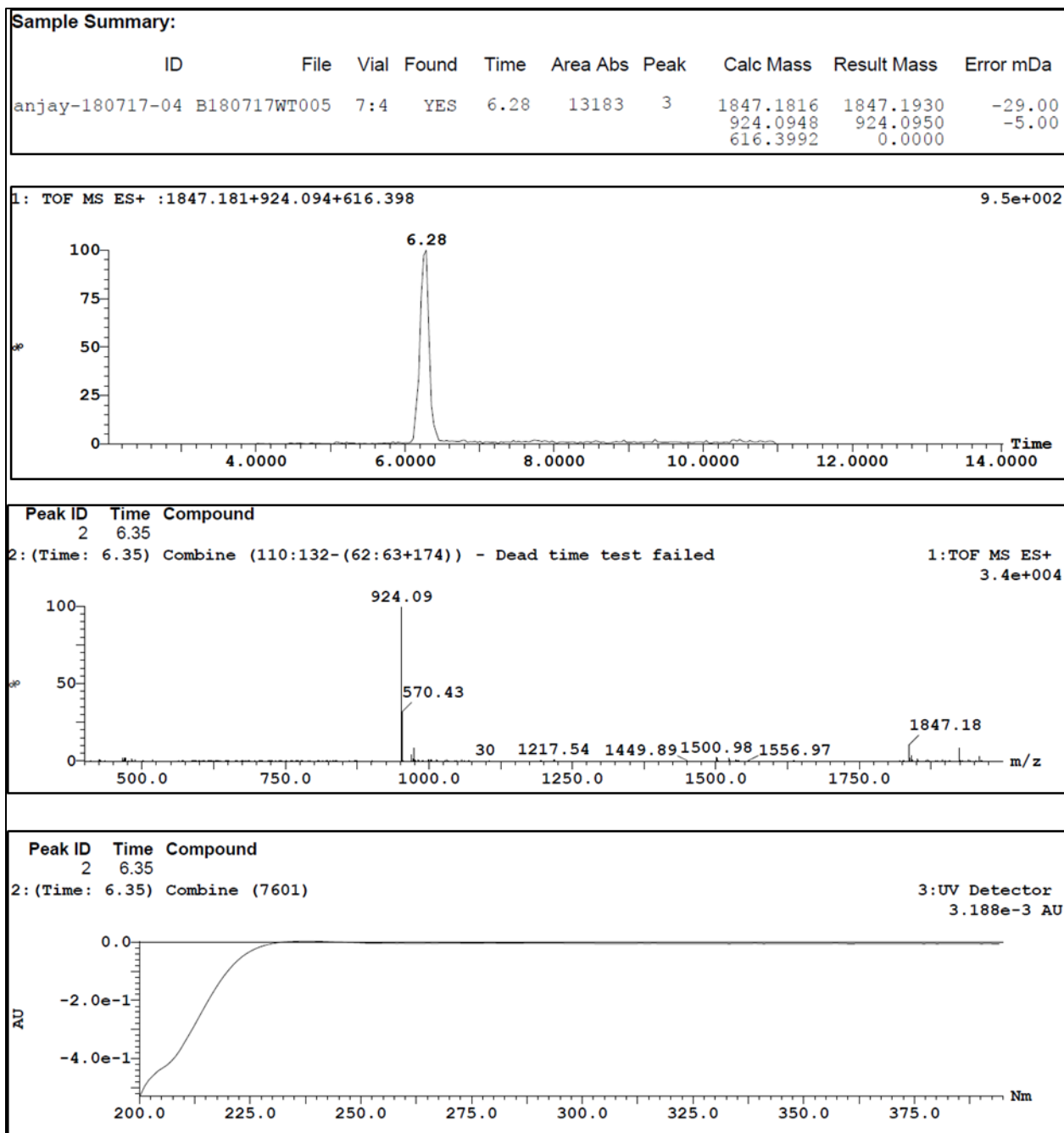


**Figure S69.** LC/TOF-ES-MS spectra of the synthesized peptide **8** (mass spectra in the positive mode), HPLC chromatogram with **8** and its purity determined by HPLC-DAD from 200-375 nm (100%). The peak at 6.28 min belongs to **8** ( $m/z = 1847$ ).

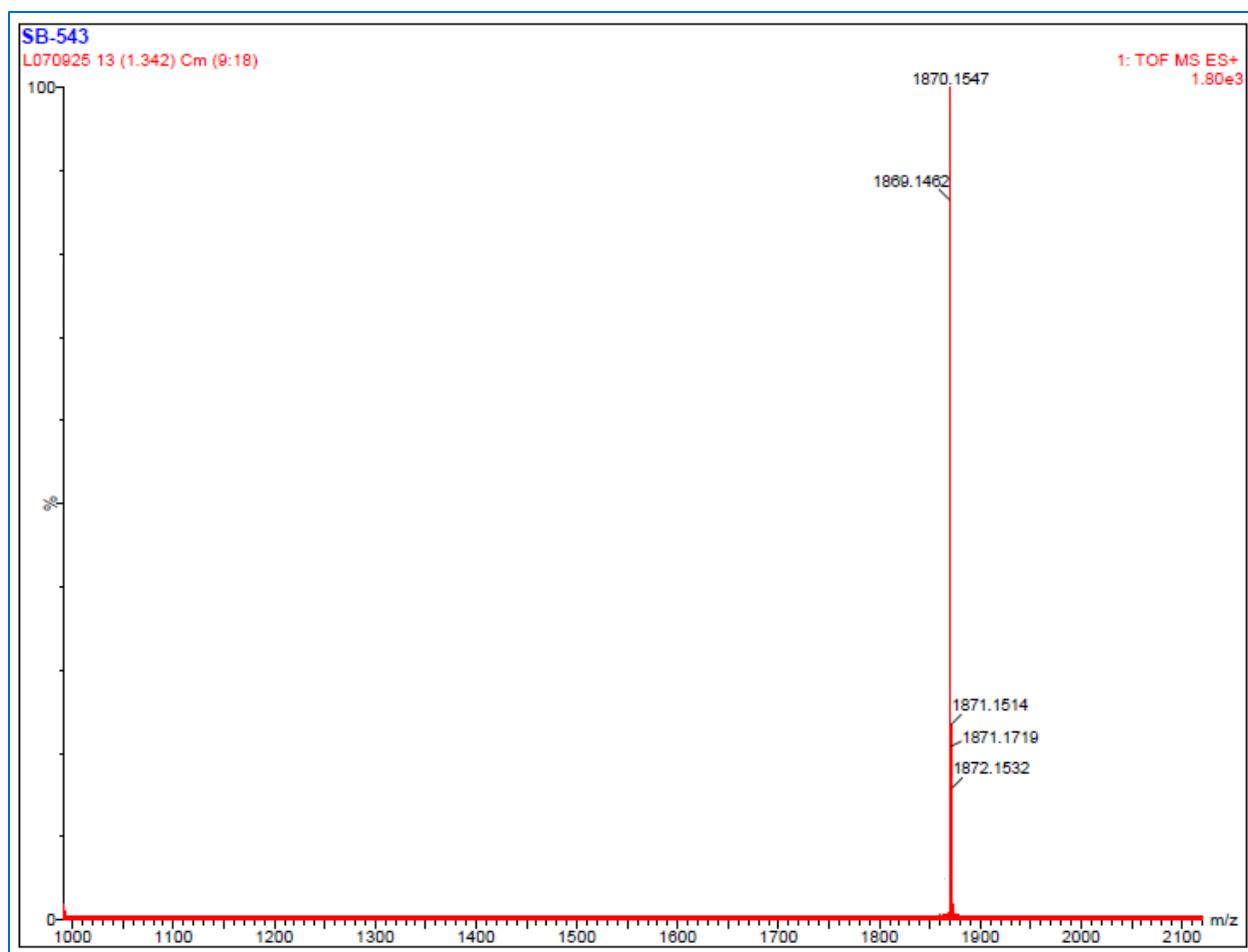


**Figure S70:** Section of HRMS (ESI):  $m/z$   $[M + Na]^+$  spectra for the synthesized peptide **8**. calcd for  $C_{97}H_{155}N_{17}O_{18}Na$ : 1869.1834; found: 1869.1462.

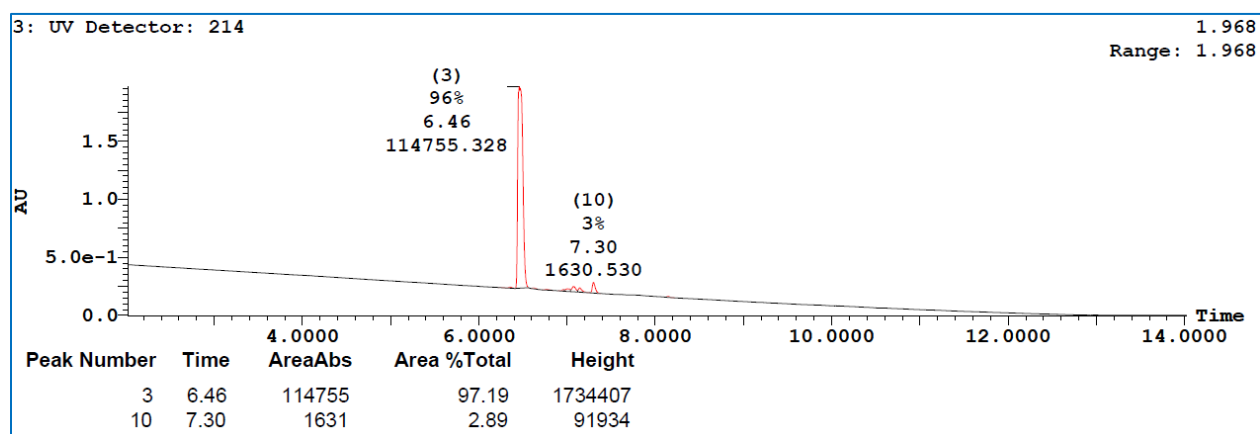


**Figure S71:** Purity of peptide **8** determined by HPLC-UV (214 nm)-ESI-MS and was found to be 96%.

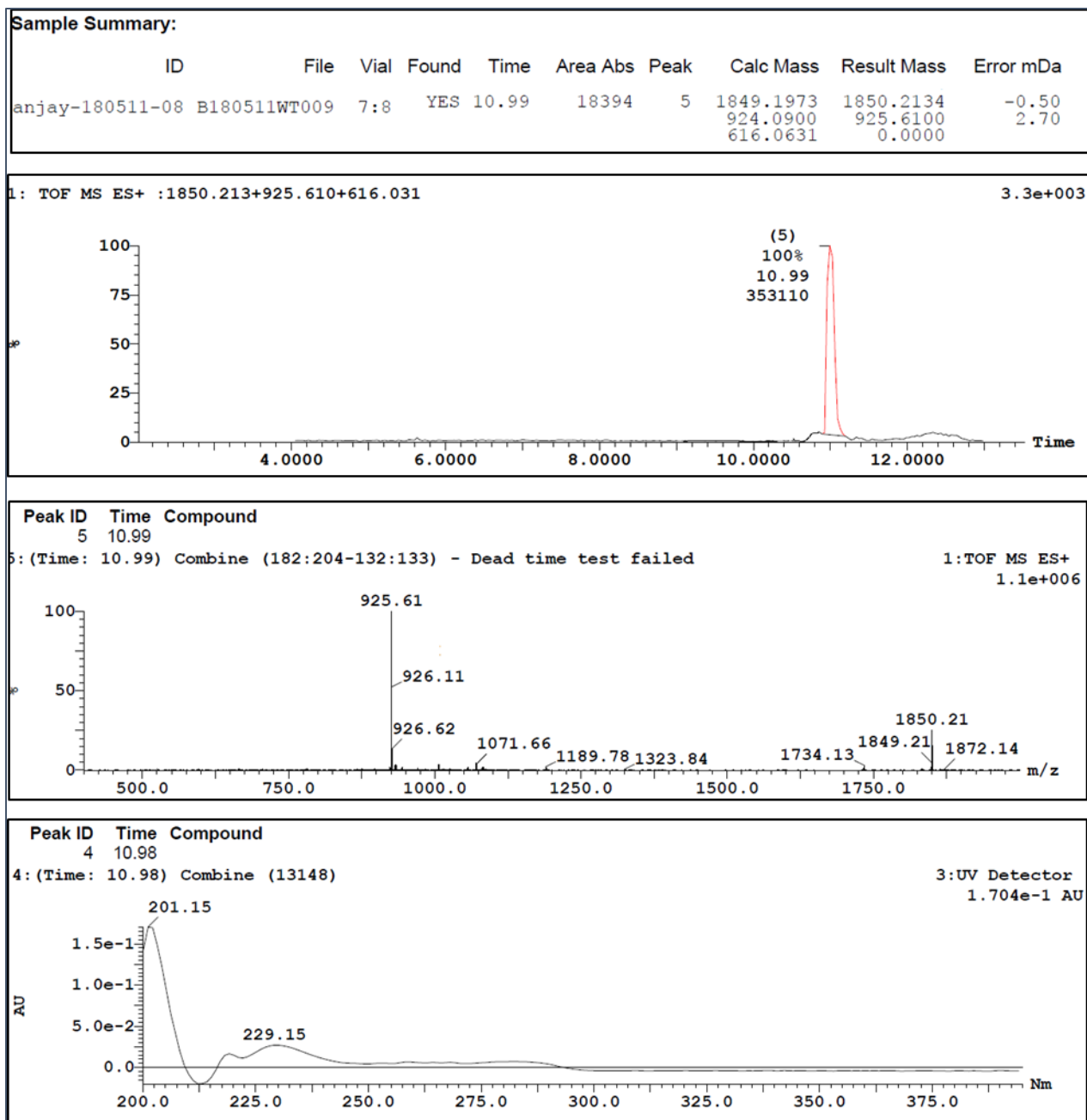


**Figure S72.** LC/TOF-ES-MS spectra of the synthesized peptide **9** (mass spectra in the positive mode), HPLC chromatogram with **9** and its purity determined by HPLC-DAD from 200-373 nm (100%). The peak at 10.98 min belongs to **9** ( $m/z = 1849$ ).

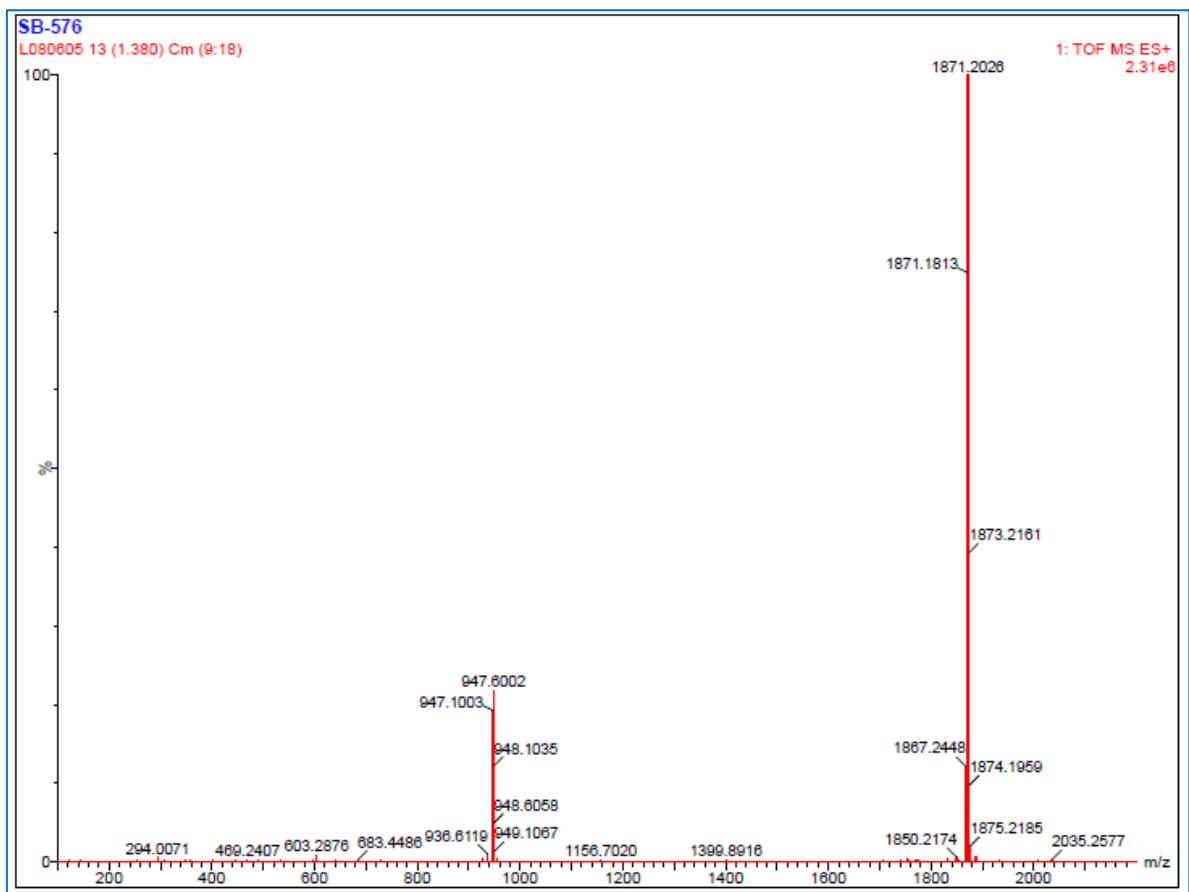


**Figure S73:** Section of HRMS (ESI):  $m/z$   $[M + Na]^+$  spectra for the synthesized peptide **9**. calcd for  $C_{97}H_{157}N_{17}O_{18}$ : 1871.1791; found: 1871.1813.

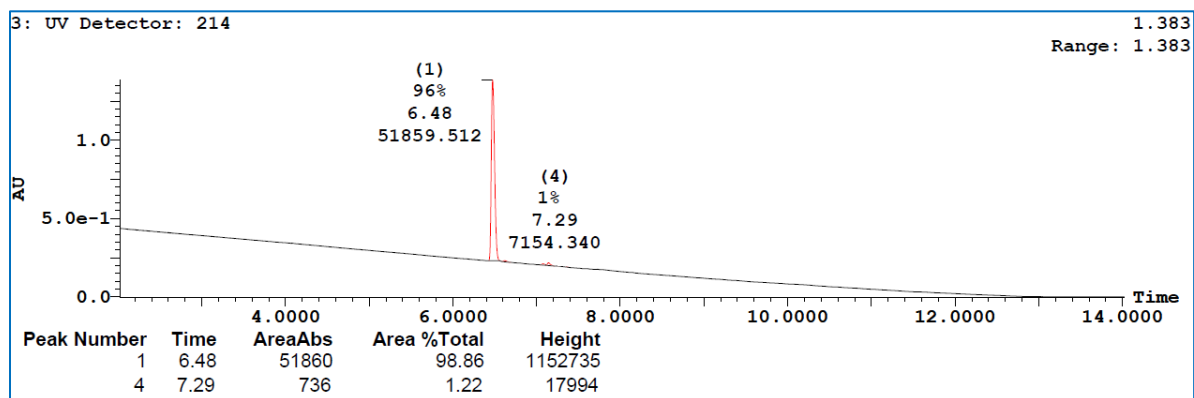


**Figure S74:** Purity of peptide **9** determined by HPLC-UV (214 nm)-ESI-MS and was found to be 96%.

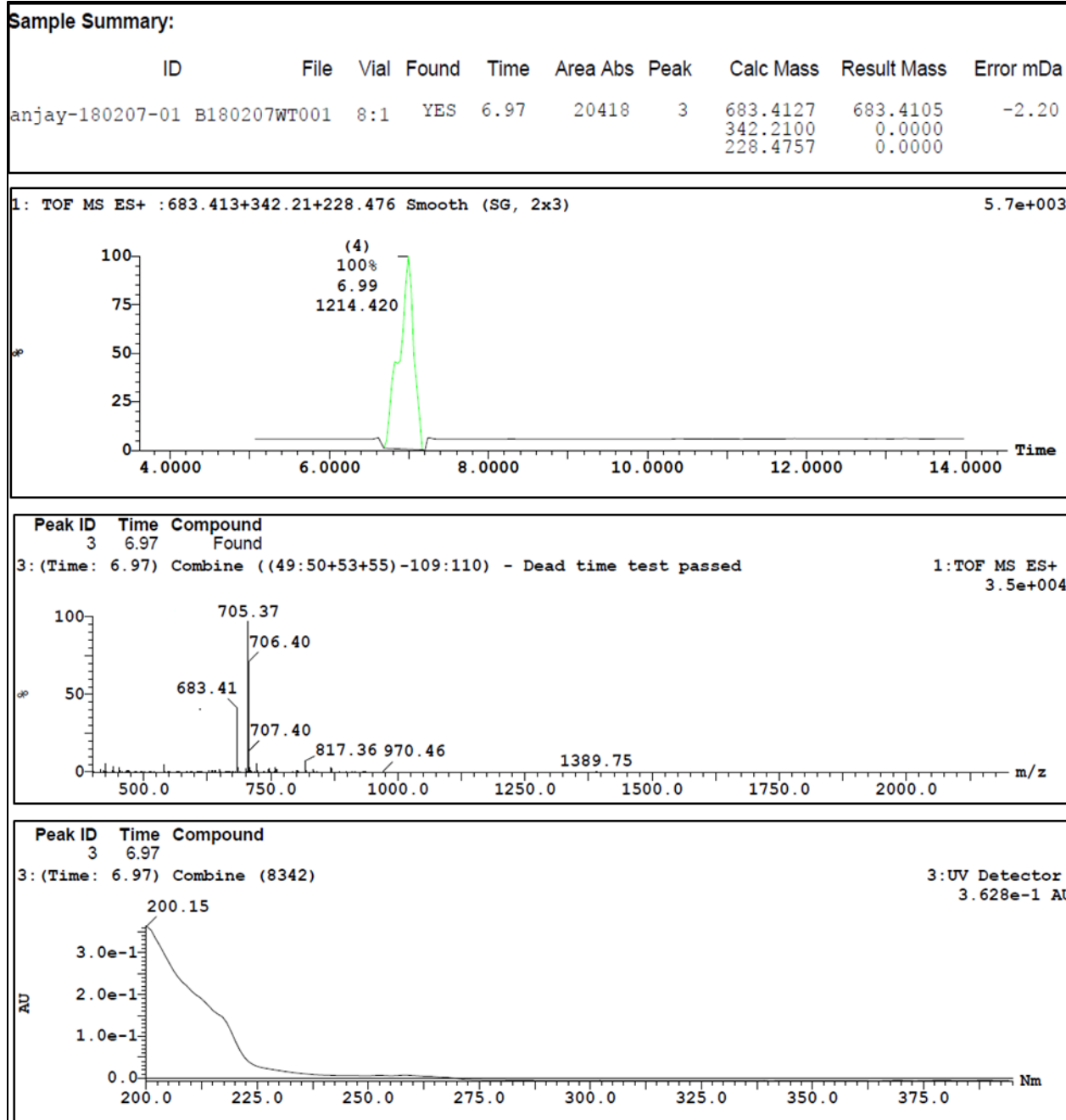


**Figure S75.** LC/TOF-ES-MS spectra of the synthesized peptide **10** (mass spectra in the positive mode), HPLC chromatogram with **10** and its purity determined by HPLC-DAD from 220-375 nm (100%). The peak at 6.99 min belongs to **10** ( $m/z = 683$ ).

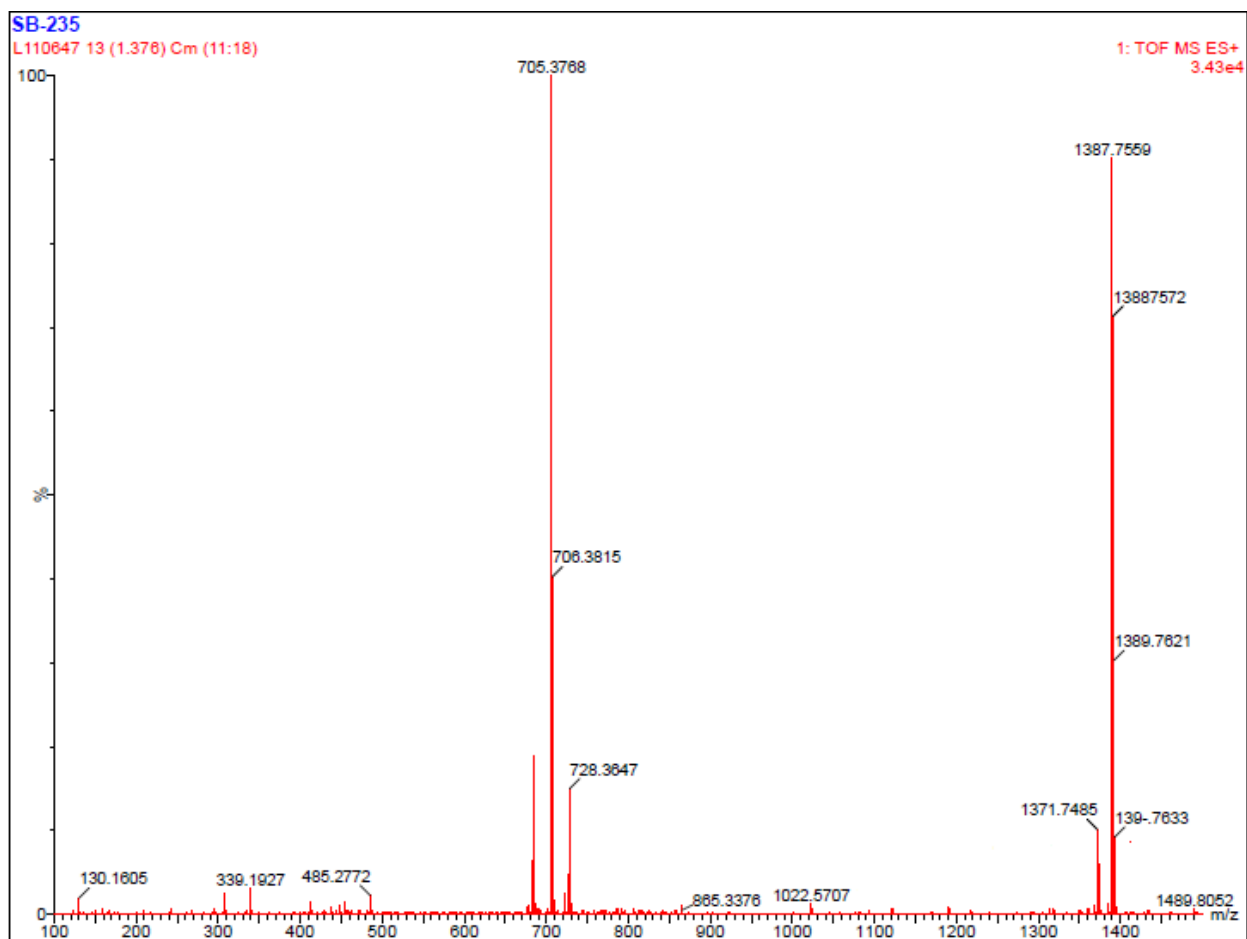


**Figure S76:** Section of HRMS (ESI):  $m/z$   $[M + H]^+$  spectra for the synthesized peptide **10**. calcd for  $C_{36}H_{54}N_6O_7$ : 705.3952; found: 705.3768.

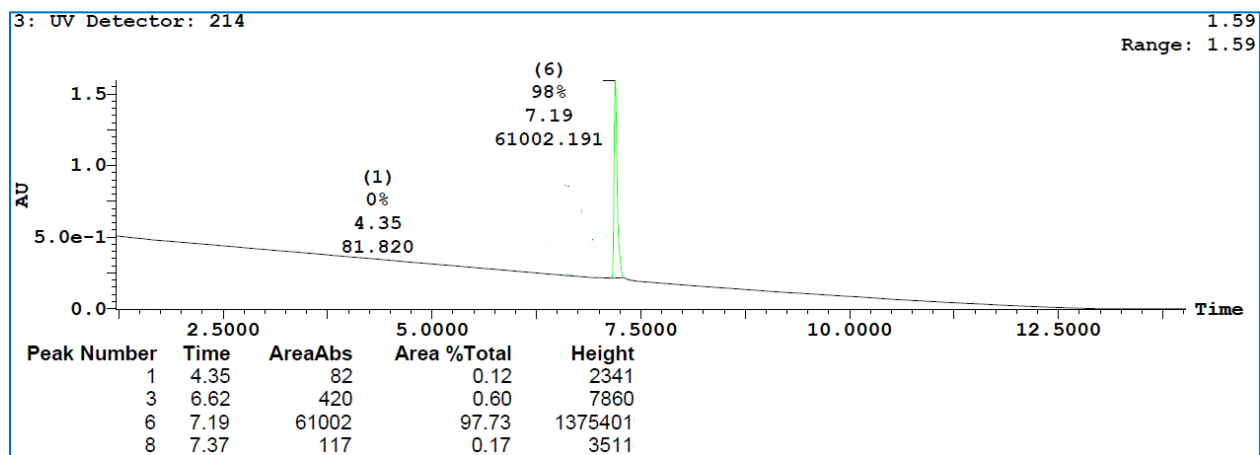


**Figure S77:** Purity of peptide **10** determined by HPLC-UV (214 nm)-ESI-MS and was found to be 98%.



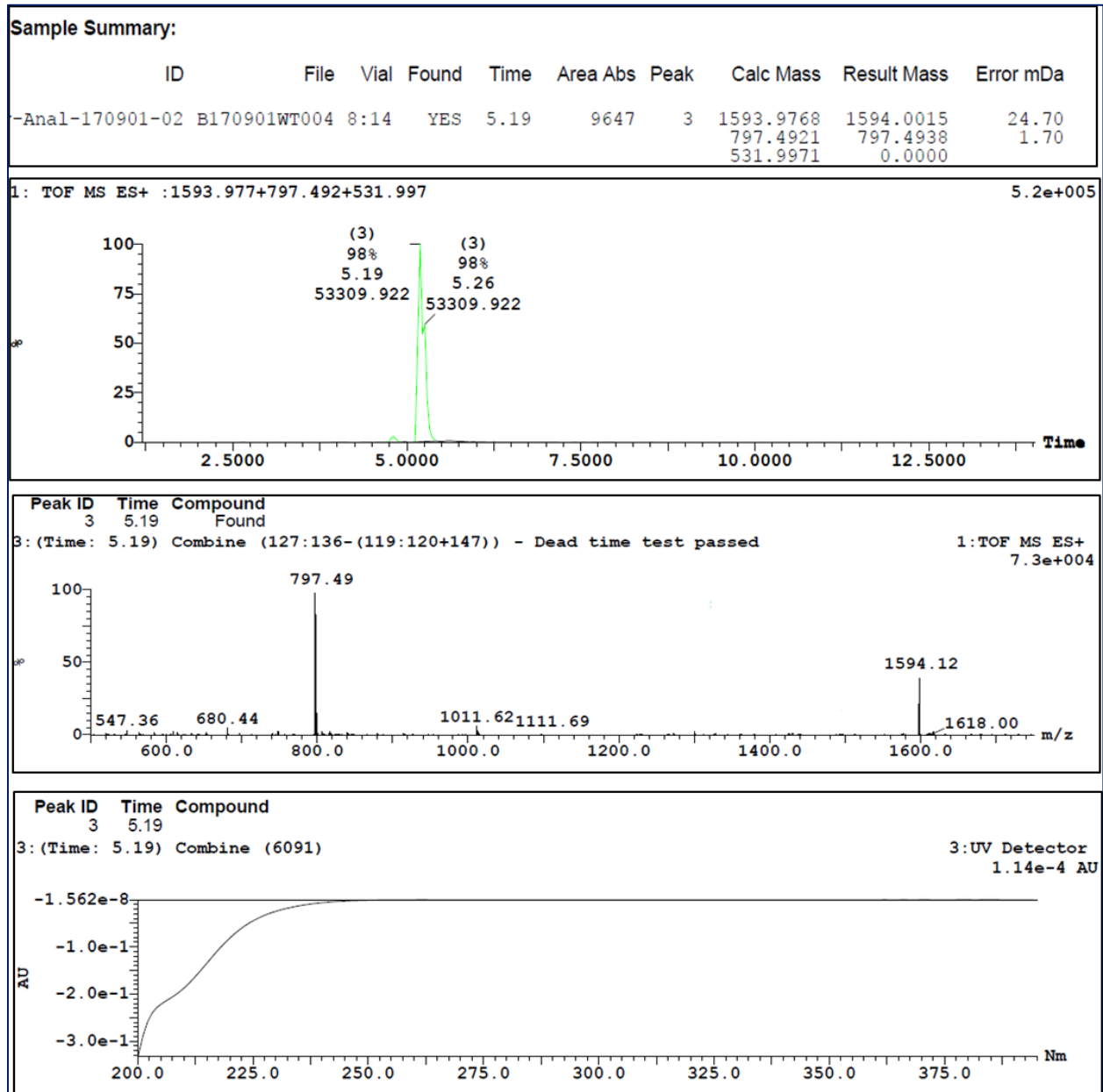


**Figure S80. LC/TOF-ES-MS spectra of the synthesized peptide 11** (mass spectra in the positive mode), HPLC chromatogram with **11** and its purity determined by HPLC-DAD from 200-375 nm (98%). The peak at 5.19 min belongs to **11** ( $m/z = 1594$ ).

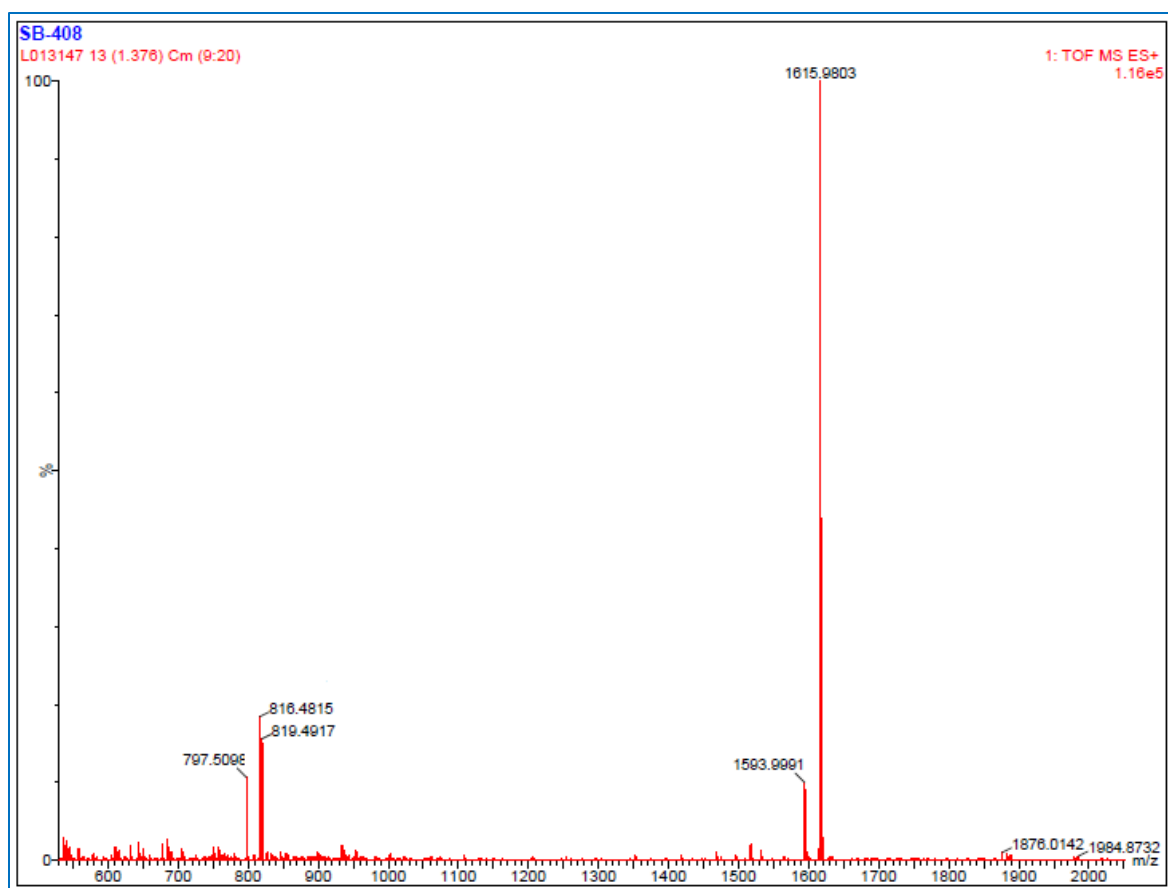


**Figure S81:** Section of HRMS (ESI):  $m/z$   $[M + H]^+$  spectra for the synthesized peptide **11**. calcd for  $C_{82}H_{128}N_{16}O_{16}$ : 1593.9774; found: 1593.9991.

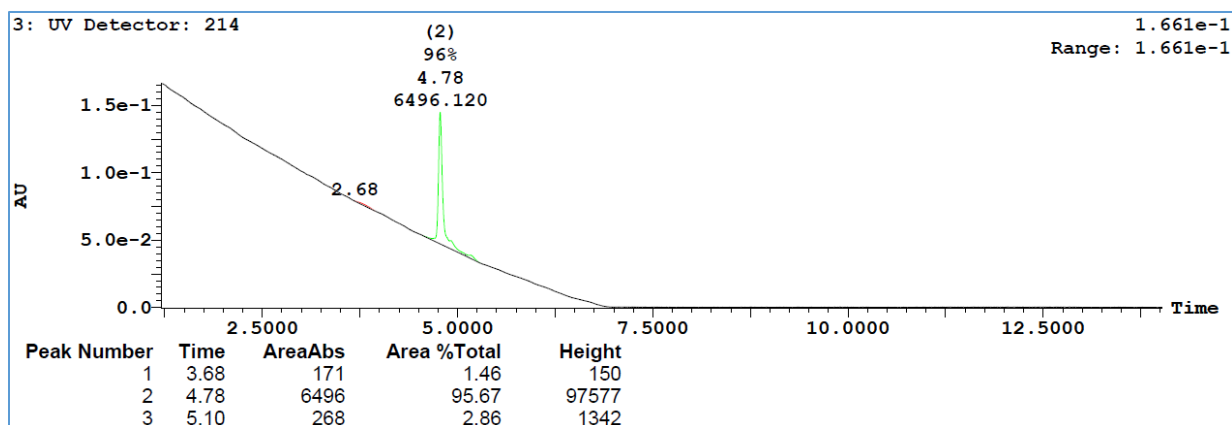


**Figure S82:** Purity of peptide **11** determined by HPLC-UV (214 nm)-ESI-MS and was found to be 96%.

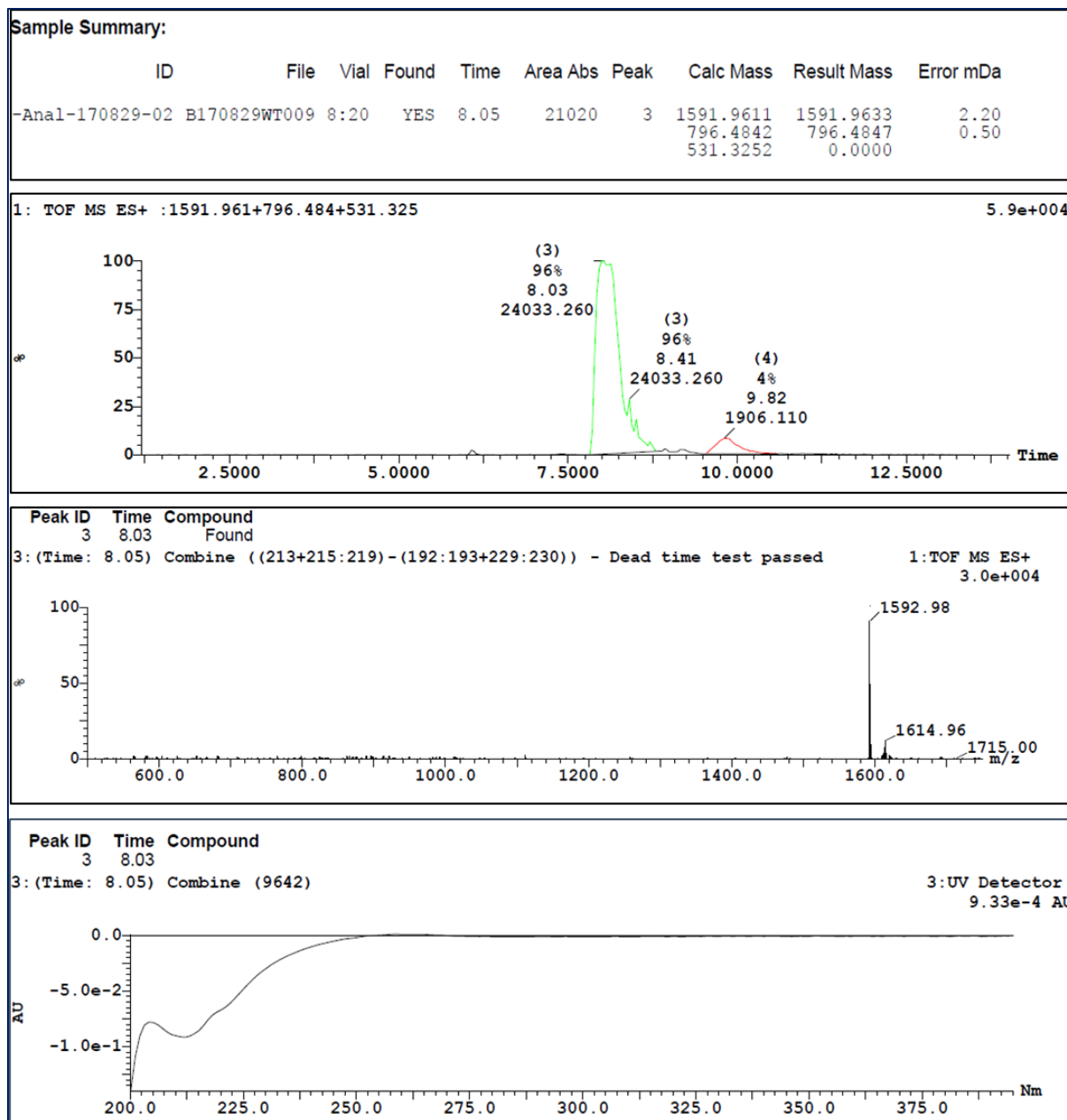


**Figure S83. LC/TOF-ES-MS spectra of the synthesized peptide 12** (mass spectra in the positive mode), HPLC chromatogram with **12** and its purity determined by HPLC-DAD from 200-375 nm (100%). The peak at 8.03 min belongs to **12** ( $m/z = 1591$ ).



**Figure S84:** Section of HRMS (ESI):  $m/z$   $[M + Na]^+$  spectra for the synthesized peptide **12**. calcd for  $C_{82}H_{126}N_{16}O_{16}Na$ : 1613.9436; found: 1613.9194.

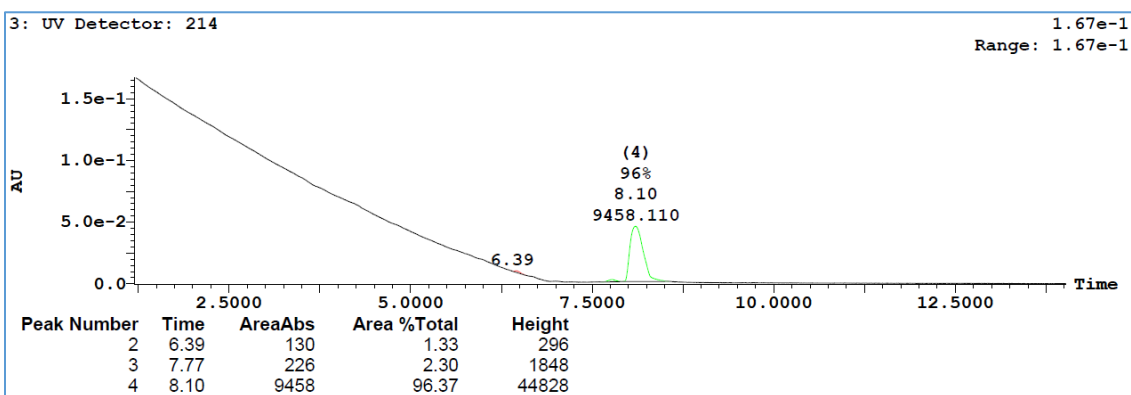


**Figure S85:** Purity of peptide **12** determined by HPLC-UV (214 nm)-ESI-MS and was found to be 96%.

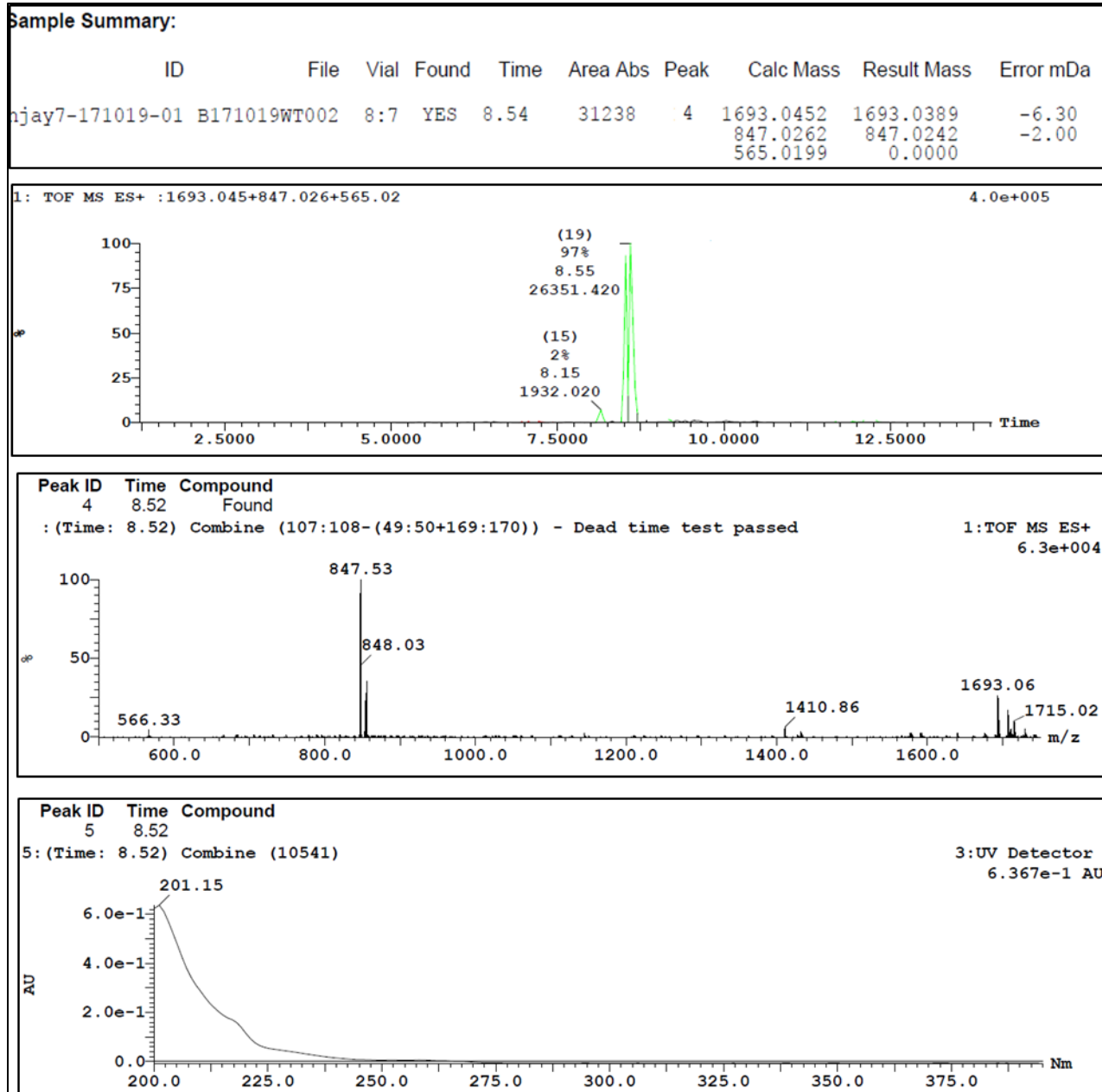


**Figure S86. LC/TOF-ES-MS spectra of the synthesized peptide 13** (mass spectra in the positive mode), HPLC chromatogram with **13** and its purity determined by HPLC-DAD from 200-375 nm (97%). The peak at 8.52 min belongs to **13** ( $m/z = 1693$ ).

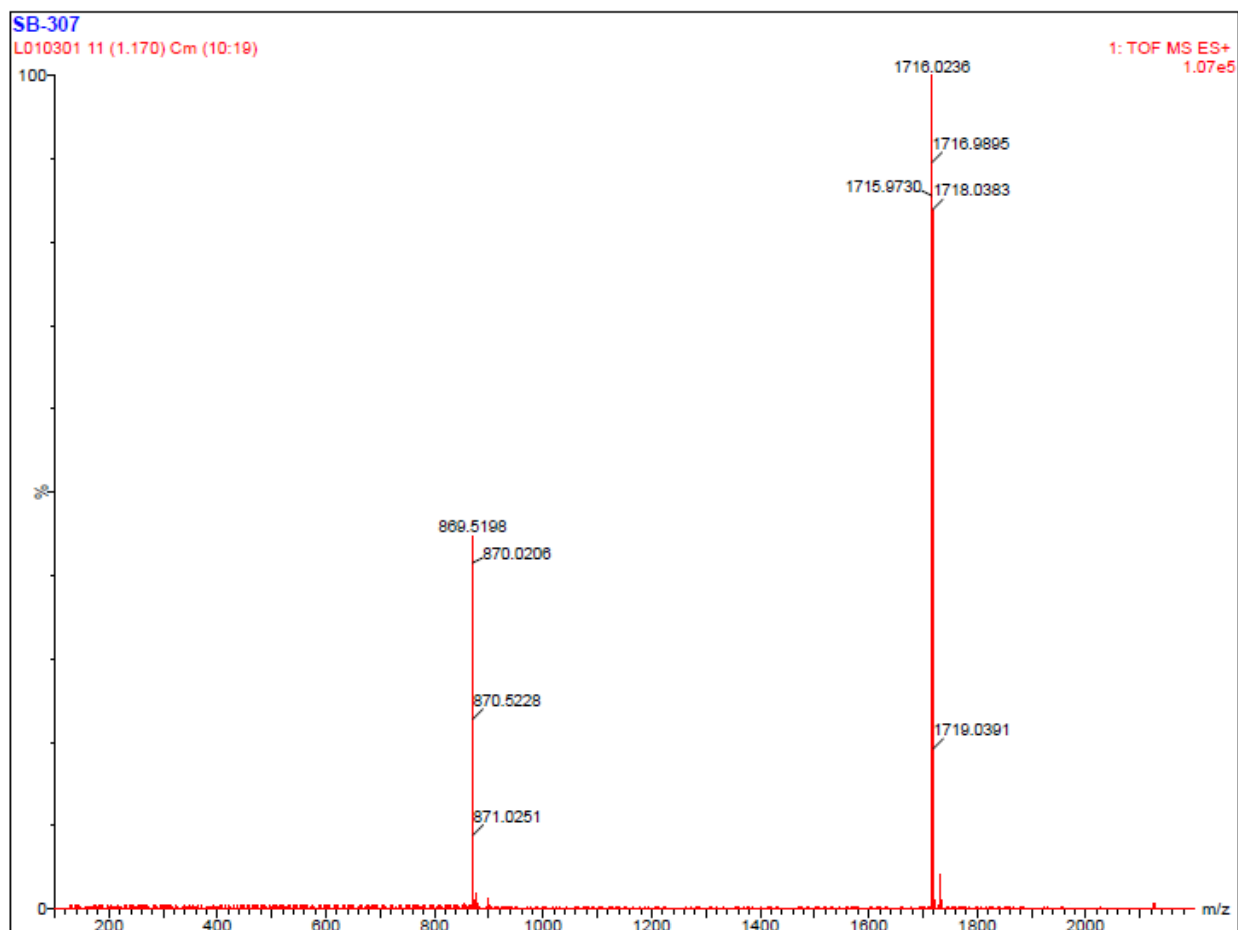


**Figure S87:** Section of HRMS (ESI):  $m/z$   $[M + Na]^+$  spectra for the synthesized peptide **13**. calcd for  $C_{87}H_{137}N_{17}O_{17}Na$ : 1715.0276; found: 1715.9730.

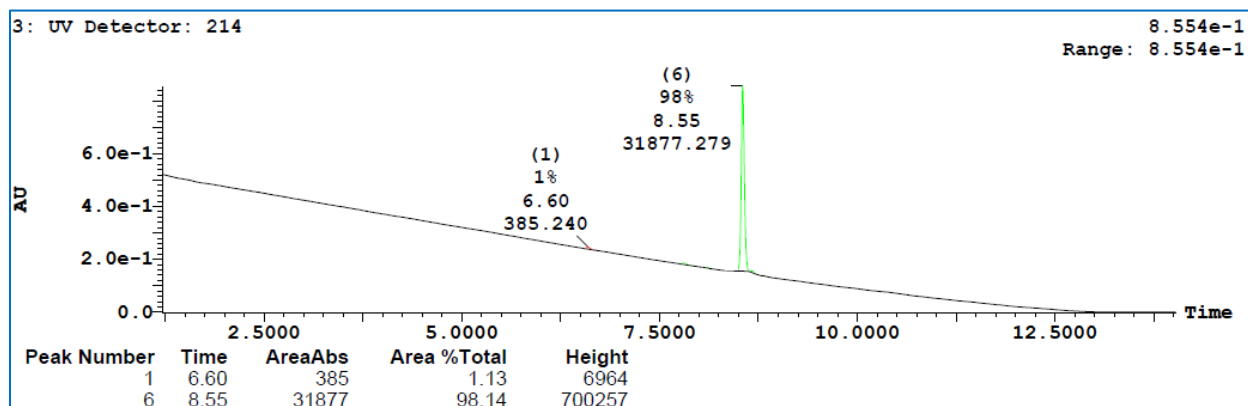


**Figure S88:** Purity of peptide **13** determined by HPLC-UV (214 nm)-ESI-MS and was found to be 98%.

Sample Summary:

ID	File	Vial	Found	Time	Area	Abs	Peak	Calc Mass	Result Mass	Error mDa
sanjay-180313-01	B180313WT007	8:25	YES	6.94	7047		6	1751.0870	1751.0575	-29.50
									876.0472	876.0500
			YES	7.14	132878		7	1751.0870	1751.0575	-29.50
								876.0472	876.0500	2.80
								584.3672	584.3373	-29.90

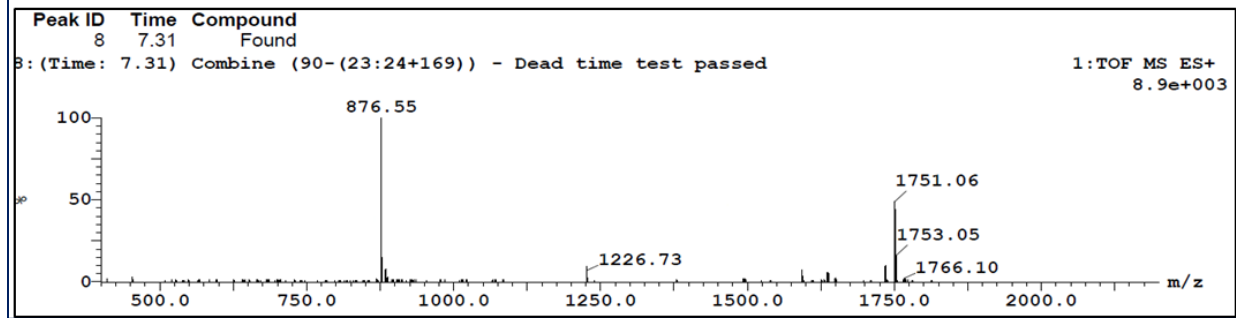
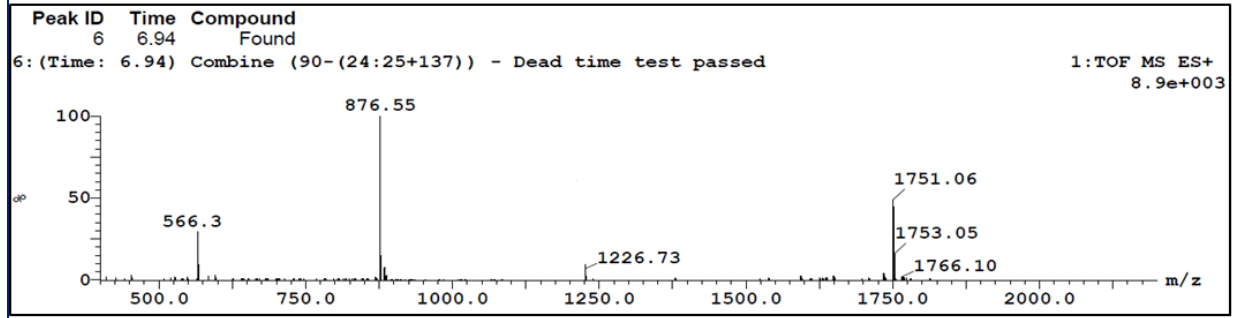
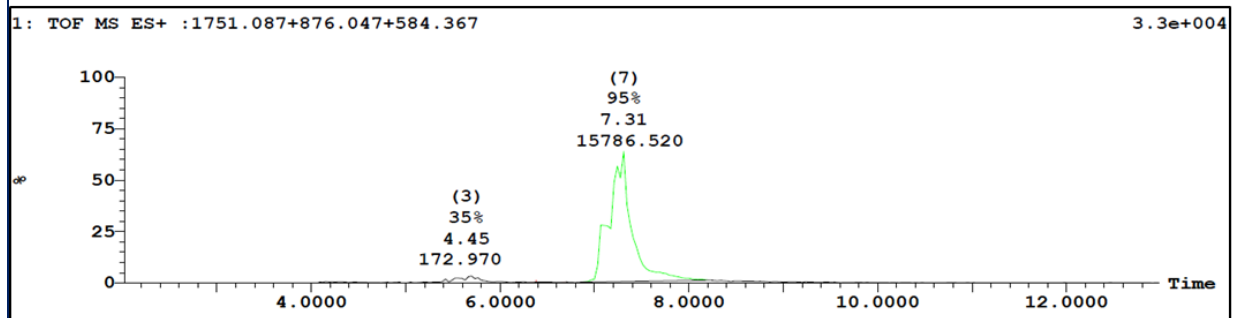
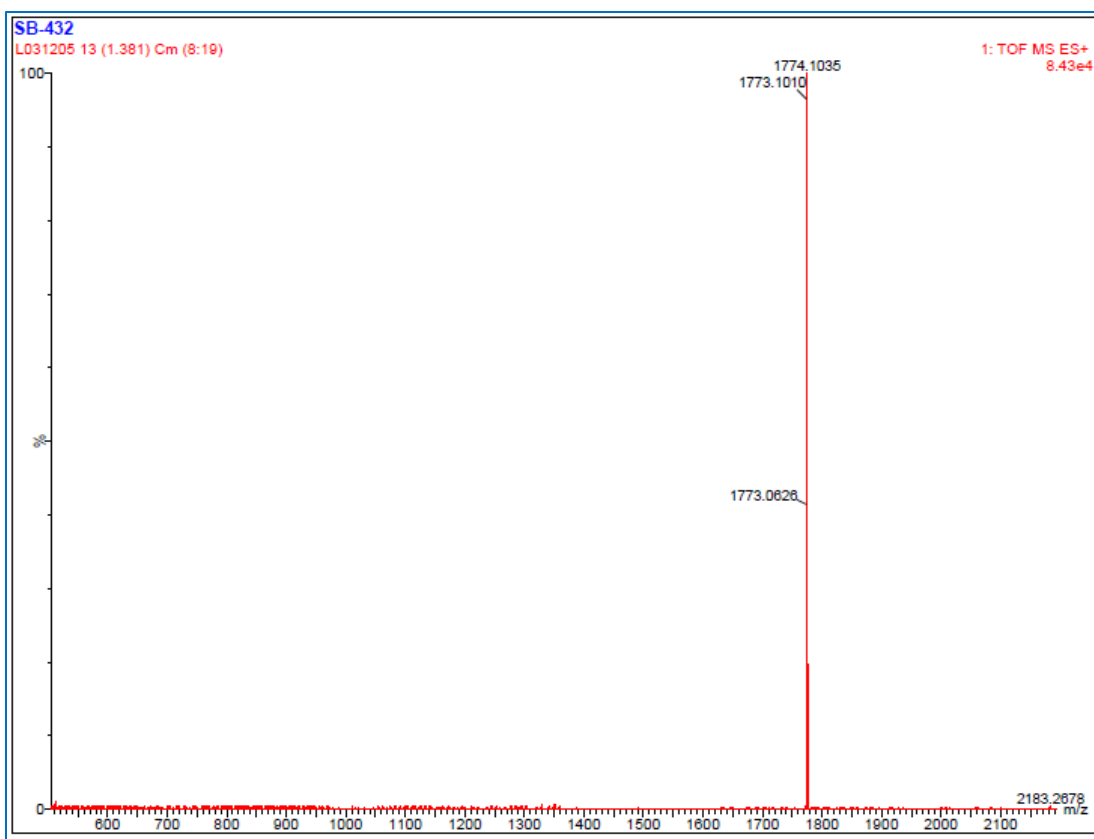
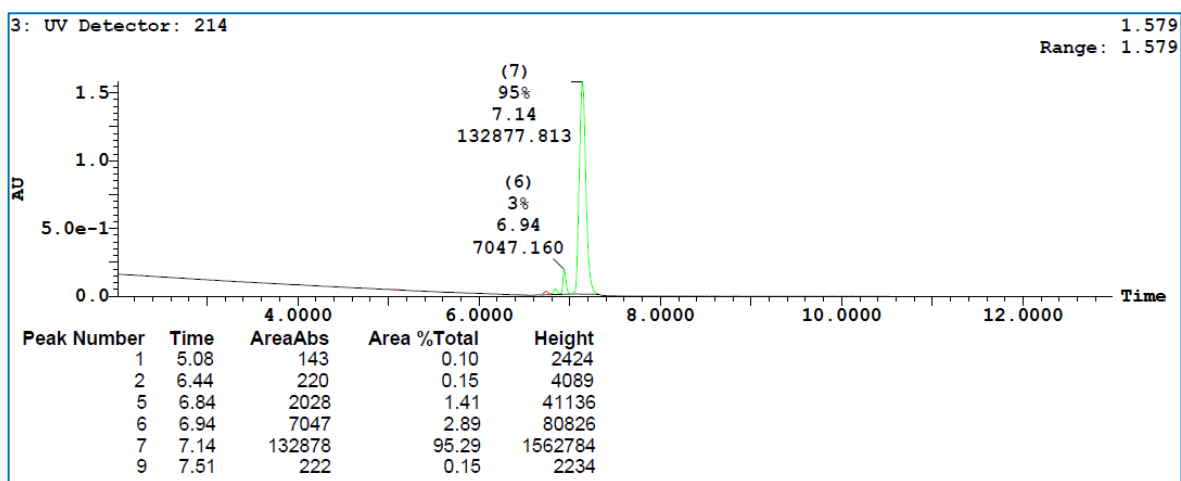


Figure S89. LC/TOF-ES-MS spectra of the synthesized peptide **14** (mass spectra in the positive mode), HPLC chromatogram with **14** and its purity determined by HPLC-DAD from 200-375 nm (95%). The peak at 8.52 min belongs to **14** ( $m/z = 1751$ ).



**Figure S90:** Section of HRMS (ESI):  $m/z$   $[M + Na]^+$  spectra for the synthesized peptide **14**. calcd for  $C_{90}H_{143}N_{17}O_{18}Na$ : 1773.0695; found: 1773.0626.



**Figure S91:** Purity of peptide **14** determined by HPLC-UV (214 nm)-ESI-MS and was found to be 95%.



Sample Summary:

ID	File	Vial	Found	Time	Area	Abs	Peak	Calc Mass	Result Mass	Error mDa
-Anal-180413-02	B180413WT008	8:14	YES	11.04	11662		8	1766.0867	1766.0887	2.00
								883.5470	883.5470	0.00
								589.3671	0.0000	
			YES	11.30	160		10	1766.0867	1766.0887	2.00
								883.5470	883.5470	0.00
								589.3671	0.0000	

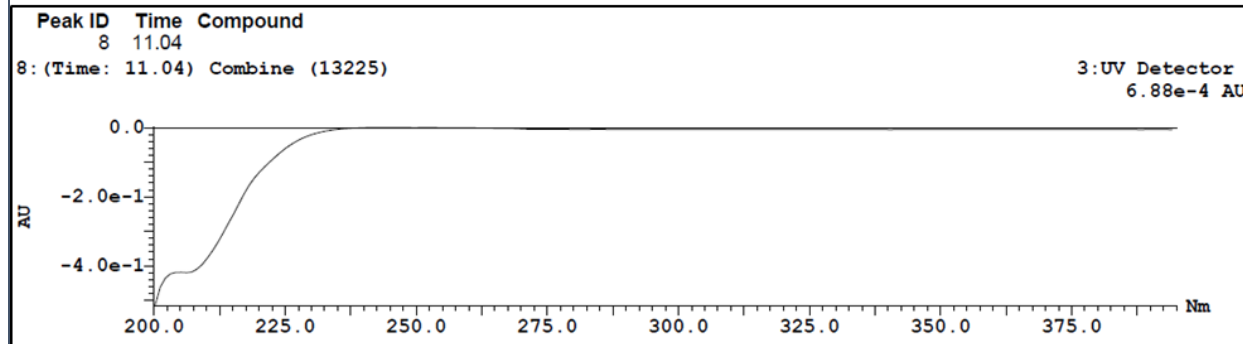
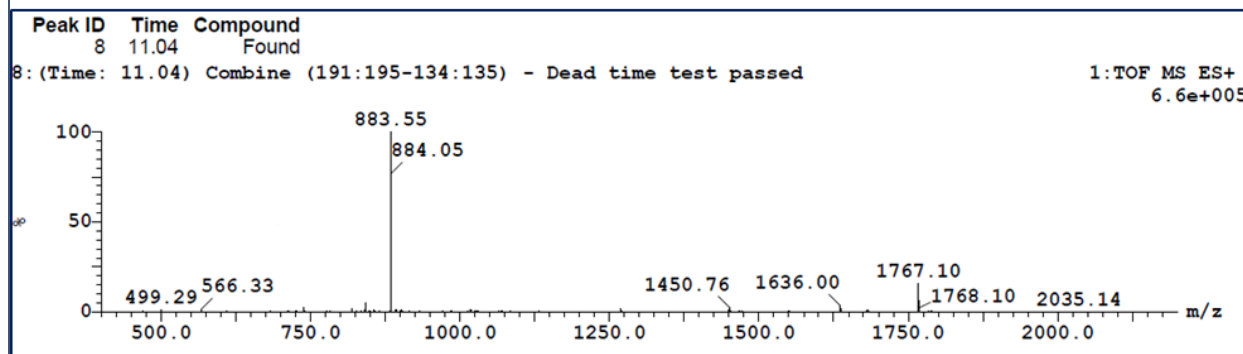
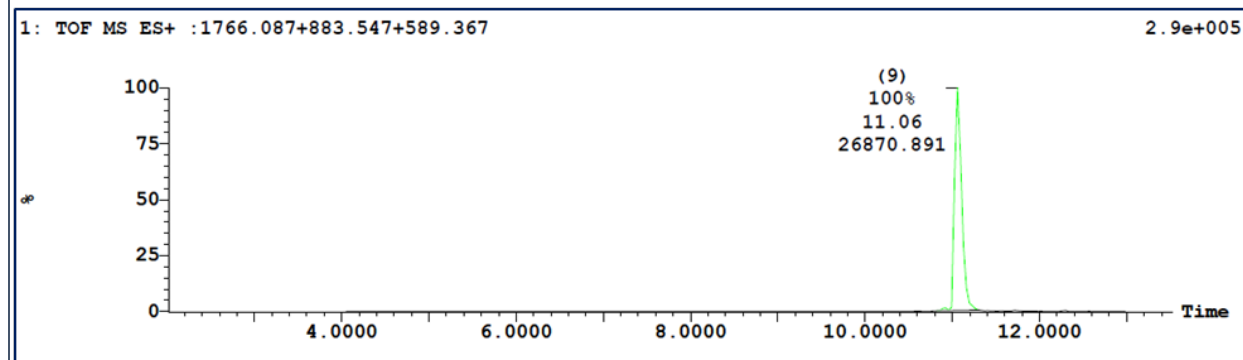


**Figure S92.** LC/TOF-ES-MS spectra of the synthesized peptide **15** (mass spectra in the positive mode), HPLC chromatogram with **15** and its purity determined by HPLC-DAD from 200-375 nm (100%). The peak at 11.04 min belongs to **15** ( $m/z = 1766$ ).

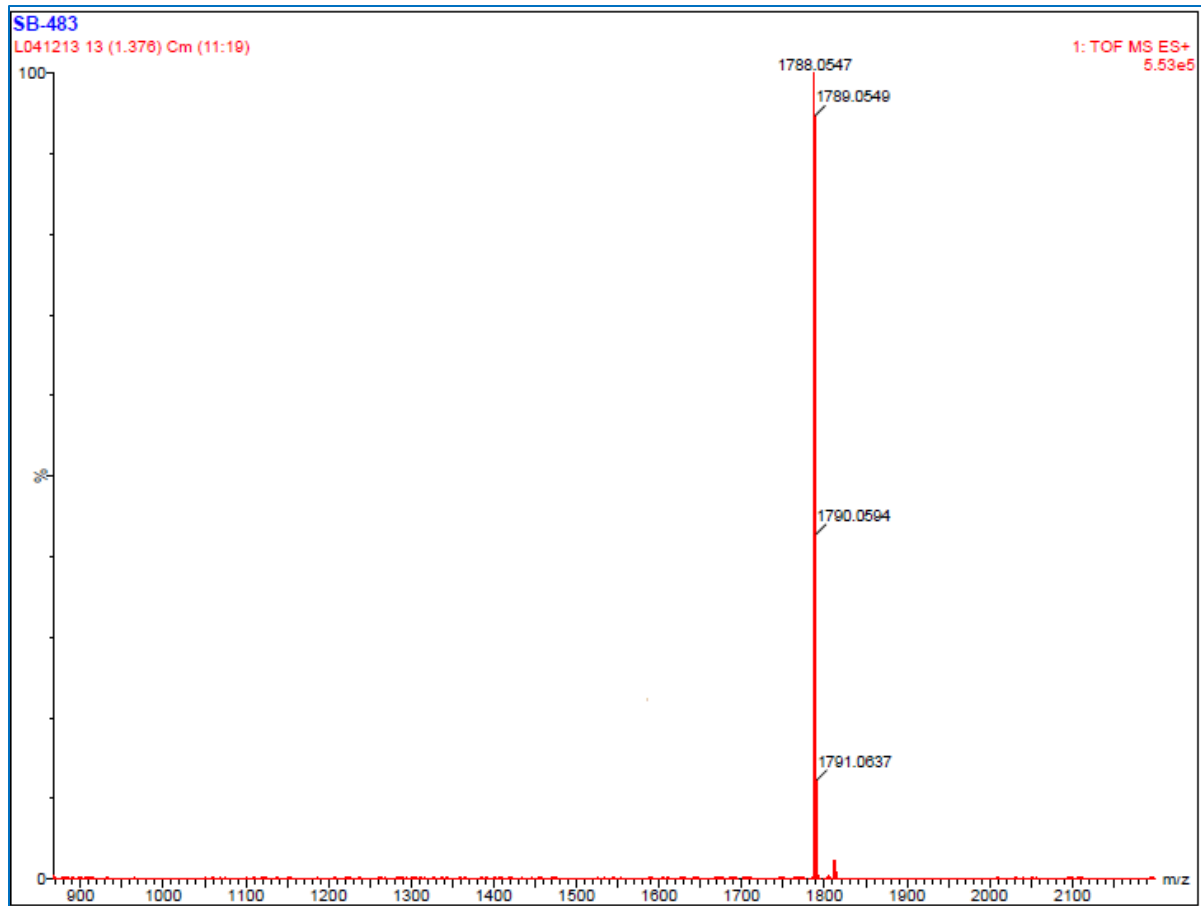


**Figure S93:** Section of HRMS (ESI):  $m/z$   $[M + Na]^+$  spectra for the synthesized peptide **15**. calcd for  $C_{91}H_{144}N_{16}O_{19}Na$ : 1788.0692; found: 1788.0547.

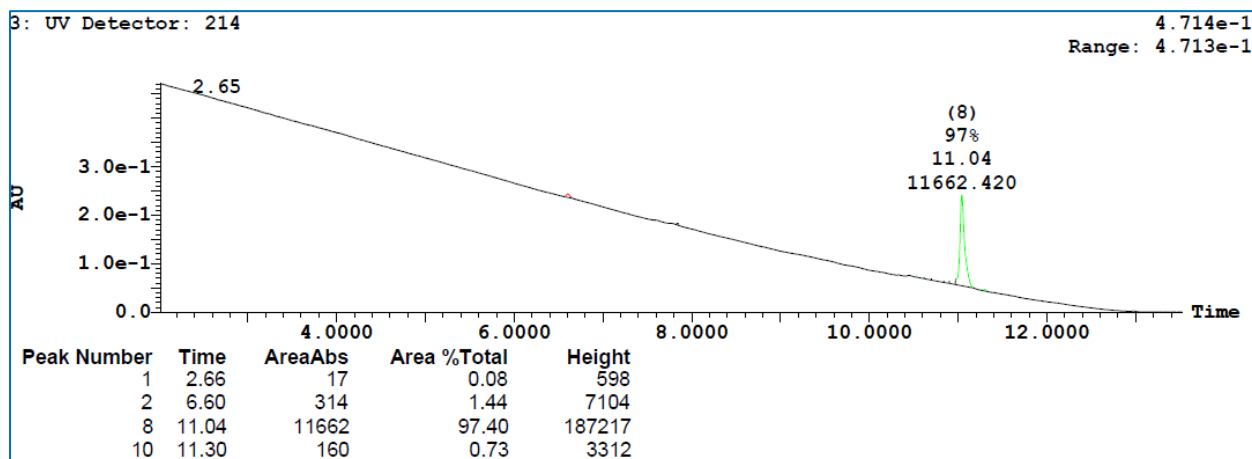


**Figure S94:** Purity of peptide **15** determined by HPLC-UV (214 nm)-ESI-MS and was found to be 97%.

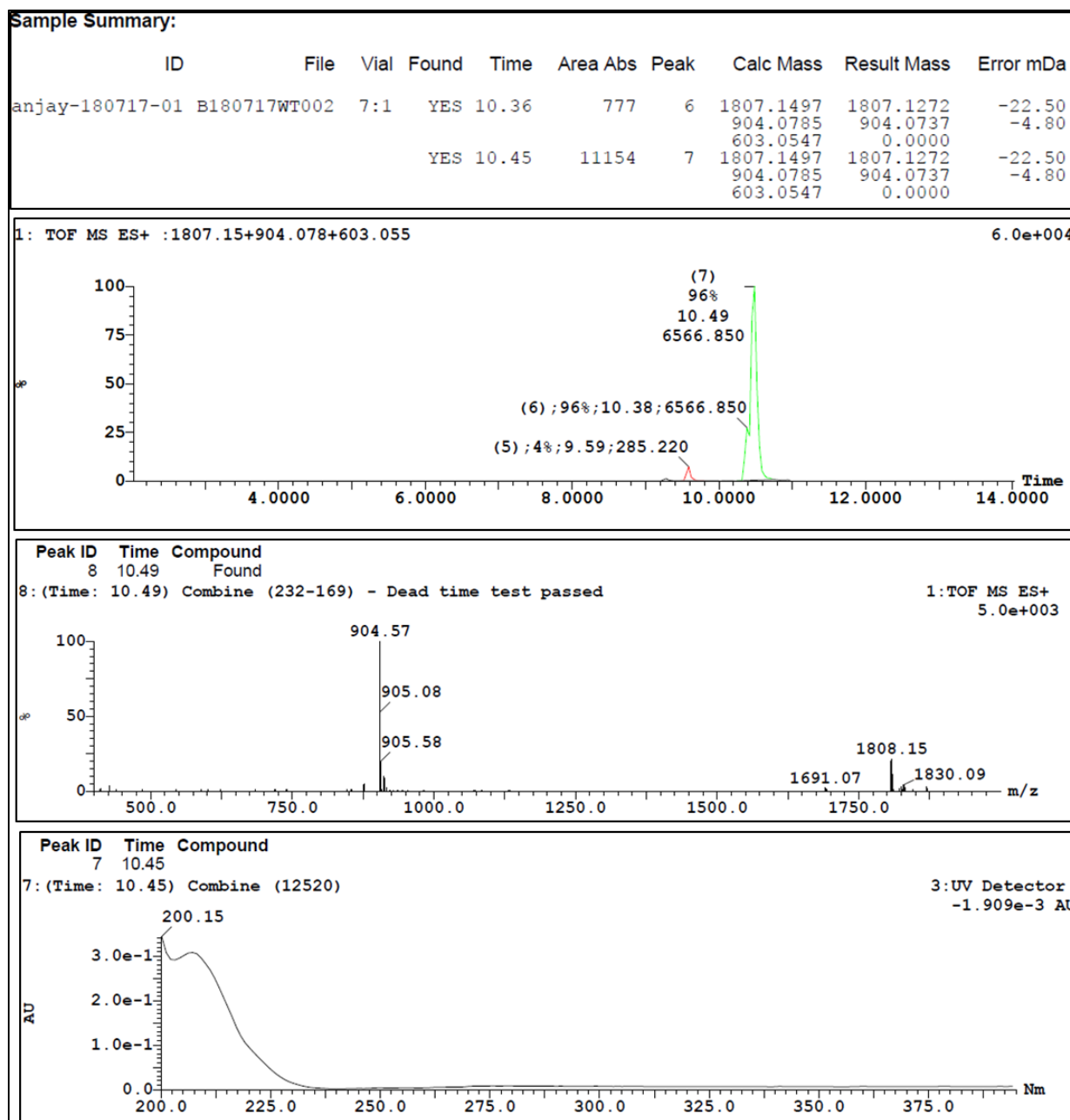


**Figure S95. LC/TOF-ES-MS spectra of the synthesized peptide 16** (mass spectra in the positive mode), HPLC chromatogram with **16** and its purity determined by HPLC-DAD from 200-375 nm (96%). The peak at 10.49 min belongs to **16** ( $m/z = 1807$ ).

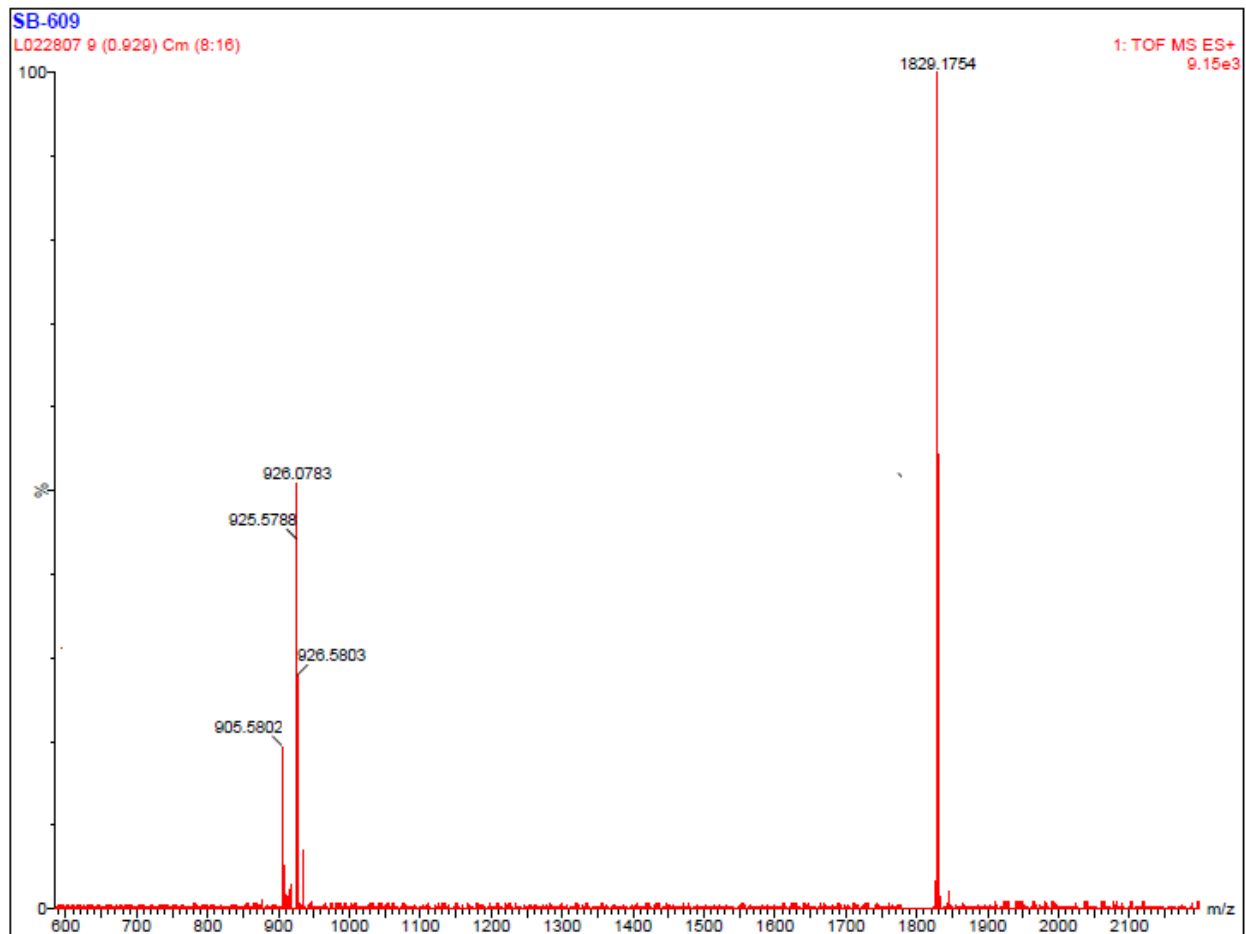


**Figure S96:** Section of HRMS (ESI):  $m/z$   $[M + H]^+$  spectra for the synthesized peptide **16**. calcd for  $C_{94}H_{151}N_{17}O_{18}$ : 1829.1321; found: 1829.1754.

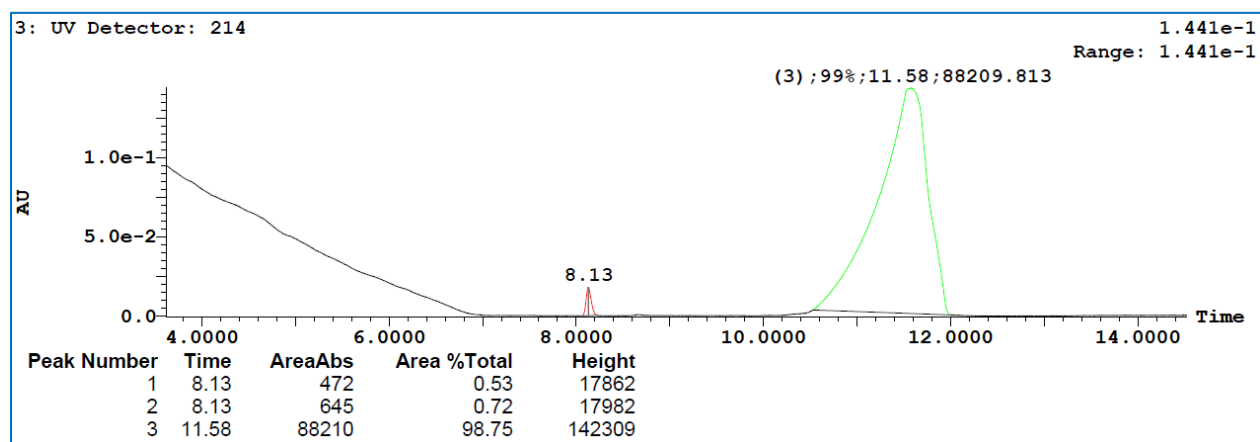


**Figure S97:** Purity of peptide **16** determined by HPLC-UV (214 nm)-ESI-MS and was found to be 99%.

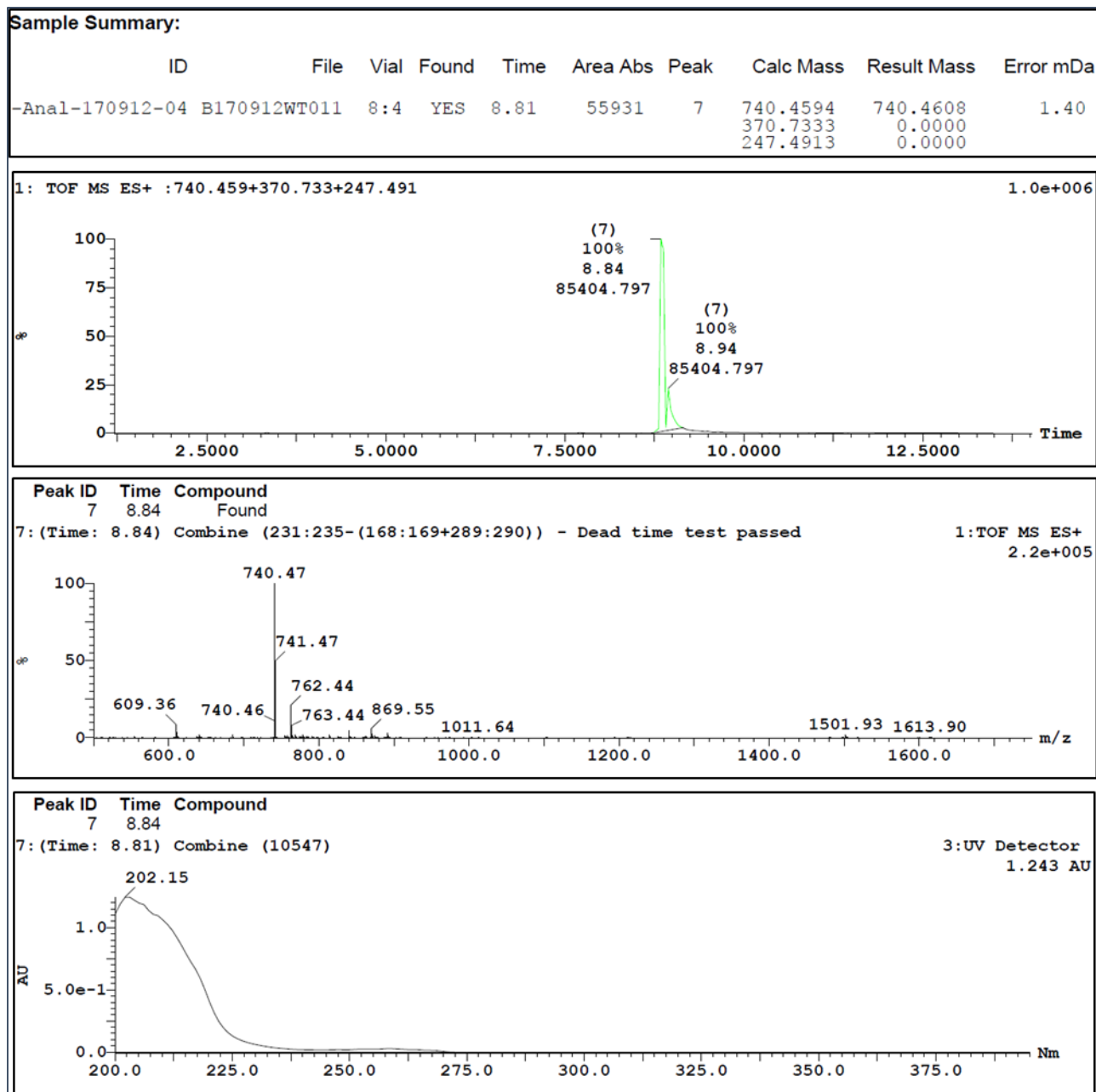


**Figure S98. LC/TOF-ES-MS spectra of the synthesized peptide 17** (mass spectra in the positive mode), HPLC chromatogram with **17** and its purity determined by HPLC-DAD from 200-375 nm (100%). The peak at 8.81 min belongs to **17** ( $m/z = 740$ ).

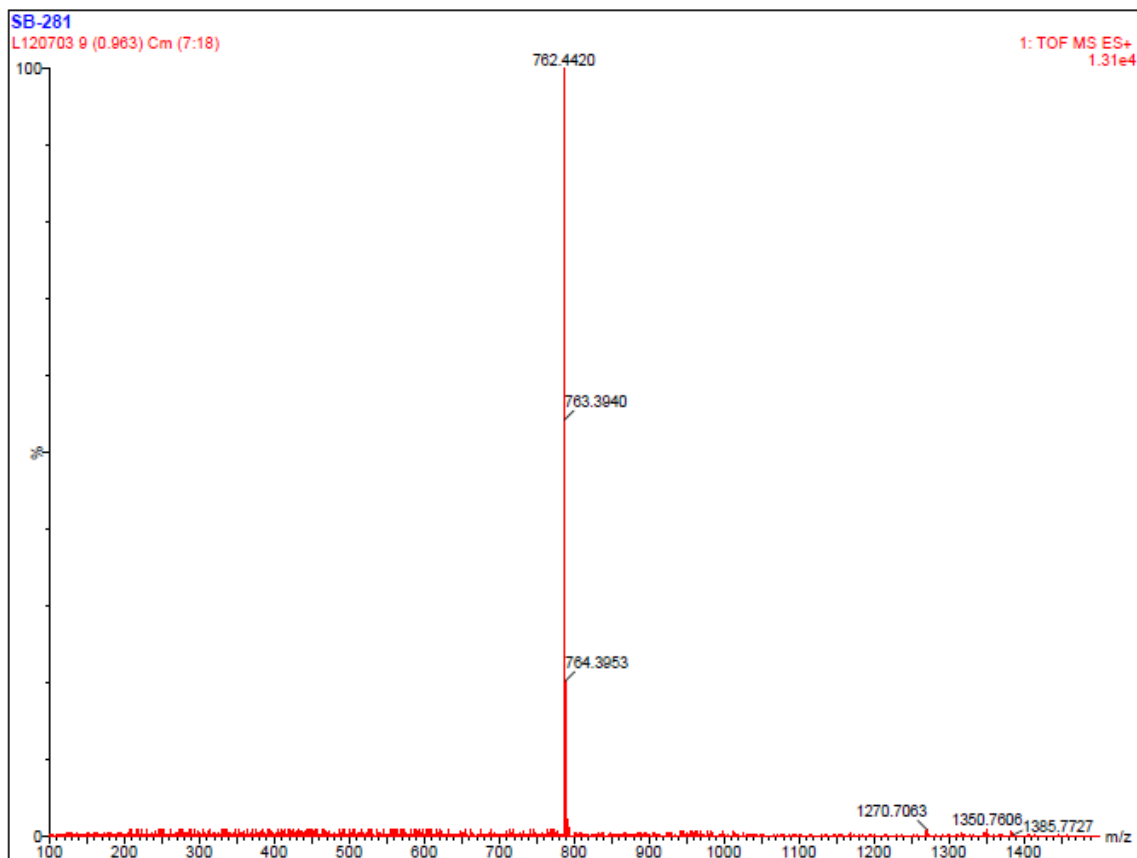


**Figure S99:** Section of HRMS (ESI):  $m/z$   $[M + H]^+$  spectra for the synthesized peptide **17**. calcd for  $C_{40}H_{61}N_5O_8$ : 762.4398; found: 762.4420.

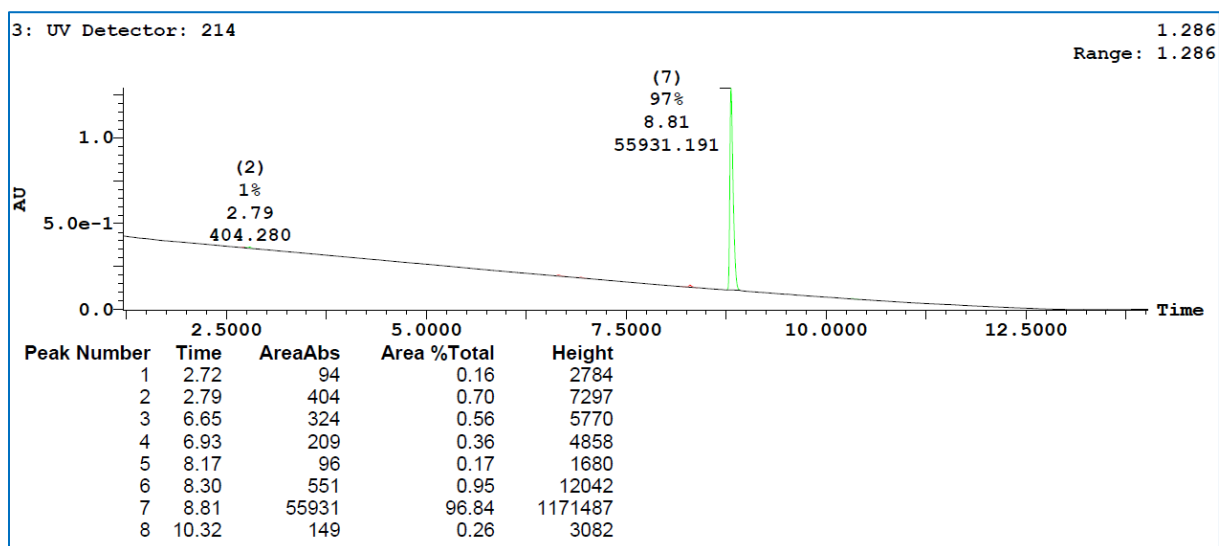


**Figure S100:** Purity of peptide **17** determined by HPLC-UV (214 nm)-ESI-MS and was found to be 97%.

## References

1. Bakshi, P.; Wolfe, M. S., Stereochemical analysis of (hydroxyethyl)urea peptidomimetic inhibitors of  $\gamma$ -secretase, *J Med Chem* **2004**, *47*, 6485-6489.
2. Tsai, J.; Takaoka, L.; Powell, N.; Nowick, J. Synthesis of amino acid ester isocyanates *Org. Synth.* **2002**, *78*, 220-224
3. Das, C.; Berezovska, O.; Diehl, T. S.; Genet, C.; Buldyrev, I.; Tsai, J. Y.; Hyman, B. T.; Wolfe, M. S., Designed helical peptides inhibit an intramembrane protease, *J Am Chem Soc* **2003**, *125*, 11794-11795.
4. Esler, W. P.; Das, C.; Wolfe, M. S., Probing pockets S2-S4' of the  $\gamma$ -secretase active site with (hydroxyethyl)urea peptidomimetics, *Bioorg Med Chem Lett* **2004**, *14*, 1935-1938.
5. Kornilova, A. Y.; Bihel, F.; Das, C.; Wolfe, M. S., The initial substrate-binding site of gamma-secretase is located on presenilin near the active site, *Proc Natl Acad Sci USA* **2005**, *102*, 3230-3235.
6. Bai, X. C.; Yan, C.; Yang, G.; Lu, P.; Ma, D.; Sun, L.; Zhou, R.; Scheres, S. H.; Shi, Y., An atomic structure of human  $\gamma$ -secretase, *Nature* **2015**, *525*, 212-217.
7. Bolduc, D. M.; Montagna, D. R.; Seghers, M. C.; Wolfe, M. S.; Selkoe, D. J., The amyloid- $\beta$ forming tripeptide cleavage mechanism of  $\gamma$ -secretase, *eLife* **2015**, *5*, pii: e17578.
8. Li, Y. M.; Lai, M. T.; Xu, M.; Huang, Q.; DiMuzio-Mower, J.; Sardana, M. K.; Shi, X. P.; Yin, K. C.; Shafer, J. A.; Gardell, S. J., Presenilin 1 is linked with  $\gamma$ -secretase activity in the detergent solubilized state, *Proc Natl Acad Sci USA* **2000**, *97*, 6138-6143.
9. Fraering, P. C.; Ye, W.; Strub, J. M.; Dolios, G.; LaVoie, M. J.; Ostaszewski, B. L.; Van Dorsselaer, A.; Wang, R.; Selkoe, D. J.; Wolfe, M. S., Purification and characterization of the human  $\gamma$ -secretase complex, *Biochemistry* **2004**, *43*, 9774-89.
10. Tian, G.; Sobotka-Briner, C. D.; Zysk, J.; Liu, X.; Birr, C.; Sylvester, M. A.; Edwards, P. D.; Scott, C. D.; Greenberg, B. D., Linear non-competitive inhibition of solubilized human gamma-secretase by pepstatin A methylester, L685458, sulfonamides, and benzodiazepines, *J Biol Chem* **2002**, *277*, 31499-31505.
11. Tian, G.; Ghanekar, S. V.; Aharony, D.; Shenvi, A. B.; Jacobs, R. T.; Liu, X.; Greenberg, B. D., The mechanism of  $\gamma$ -secretase: multiple inhibitor binding sites for transition state analogs and small molecule inhibitors, *J Biol Chem* **2003**, *278*, 28968-28975.
12. Delaglio, F.; Grzesiek, S.; Vuister, G. W.; Zhu, G.; Pfeifer, J.; Bax, A., NMRPipe: a multidimensional spectral processing system based on UNIX pipes *J Biomol NMR* **1995**, *6*, 277-293.
13. Vranken, W. F.; Boucher, W.; Stevens, T. J.; Fogh, R. H.; Pajon, A.; Llinas, M.; Ulrich, E. L.; Markley, J. L.; Ionides, J.; Laue, E. D., The CCPN data model for NMR spectroscopy: development of a software pipeline, *Proteins* **2005**, *59*, 687-96.
14. Maciejewski, M. W.; Schuyler, A. D.; Gryk, M. R.; Moraru, I. I.; Romero, P. R.; Ulrich, E. L.; Eghbalnia, H. R.; Livny, M.; Delaglio, F.; Hoch, J. C., NMRbox: A Resource for Biomolecular NMR Computation, *Biophys J.* **2017**, *112*, 1529-1534.
15. Schwieters, C. D.; Kuszewski, J.J.; Tjandra, N.; Clore, G. M., The Xplor-NIH NMR Molecular Structure Determination Package, *J. Magn. Res.* **2003**, *160*, 66-74.
16. Schüttelkopf, A. W.; van Aalten, D. M. F., PRODRG: a tool for high-throughput crystallography of protein-ligand complexes, *Acta Crystallogr.* **2004**, *D60*, 1355-1363.
17. Bermejo, G. A.; Schwieters, C. D., Protein Structure Elucidation from NMR Data with the Program Xplor-NIH, *Methods Mol Biol.* **2018**, *1688*, 311-340.